Spring 1986

ON THE SPECTRA OF GAMMA-RAY BURSTS AT HIGH ENERGIES

STEVEN MICHAEL MATZ
University of New Hampshire, Durham

INFORMATION TO USERS

This reproduction was made from a copy of a manuscript sent to us for publication and microfilming. While the most advanced technology has been used to photograph and reproduce this manuscript, the quality of the reproduction is heavily dependent upon the quality of the material submitted. Pages in any manuscript may have indistinct print. In all cases the best available copy has been filmed.

The following explanation of techniques is provided to help clarify notations which may appear on this reproduction.

1. Manuscripts may not always be complete. When it is not possible to obtain missing pages, a note appears to indicate this.

2. When copyrighted materials are removed from the manuscript, a note appears to indicate this.

3. Oversize materials (maps, drawings, and charts) are photographed by sectioning the original, beginning at the upper left hand corner and continuing from left to right in equal sections with small overlaps. Each oversize page is also filmed as one exposure and is available, for an additional charge, as a standard 35mm slide or in black and white paper format.*

4. Most photographs reproduce acceptably on positive microfilm or microfiche but lack clarity on xerographic copies made from the microfilm. For an additional charge, all photographs are available in black and white standard 35mm slide format.*

***For more information about black and white slides or enlarged paper reproductions, please contact the Dissertations Customer Services Department.**

U·M·I Dissertation Information Service

University Microfilms International
A Bell & Howell Information Company
300 N. Zeeb Road, Ann Arbor, Michigan 48106

Matz, Steven Michael

ON THE SPECTRA OF GAMMA-RAY BURSTS AT HIGH ENERGIES

University of New Hampshire PH.D. 1986

ON THE SPECTRA OF GAMMA-RAY BURSTS AT HIGH ENERGIES

BY

STEVEN MICHAEL MATZ
AB, University of Chicago, 1979

A DISSERTATION

Submitted to the University of New Hampshire
in Partial Fulfillment of
the Requirements for the Degree of

Doctor of Philosophy
in
Physics

May 1986

This dissertation has been examined and approved.

Edward L. Chupp
Professor of Physics

Roger L. Arnoldy
Professor of Physics

John F. Dawson
Professor of Physics

Robert E. Houston, Jr.
Professor of Physics

Lyman Mower
Professor of Physics

1986 March 15
Date

To my parents

ACKNOWLEDGEMENTS

I would like to express my thanks to my advisor, E. L. Chupp, for his support, especially in giving me access to the rich GRS data set and in allowing me to pursue my research with a great deal of independence. I also gratefully acknowledge my debt to Dave Forrest for much instruction in how to do real physics and for insight into the working of the instrument. I am also grateful to Tom Vestrand for useful discussions and seminal suggestions. I also thank Sherry Palmer for fast and professional drafting of the figures. This dissertation was printed by TEX on a QMS Lasergrafix800, courtesy of Prof. John Dawson and the Nuclear Physics Group at the University of New Hampshire. Finally, I thank the taxpayers of the United States, who supported this work under NASA contracts NAS5–23761 and NAS5–28609, and NASA research grant NGL30–002–021.

TABLE OF CONTENTS

LIST OF TABLES

LIST OF FIGURES

ABSTRACT

ON THE SPECTRA OF GAMMA-RAY BURSTS AT HIGH ENERGIES

by

Steven Michael Matz
University of New Hampshire, May, 1986

Between 1980 February and 1983 August the Gamma-Ray Spectrometer (GRS) on the Solar Maximum Mission satellite (SMM) observed 71 gamma-ray bursts. These events form a representative subset of the class of classical gamma-ray bursts. Since their discovery more than 15 years ago, hundreds of gamma-ray bursts have been detected; however, most observations have been limited to an energy range of roughly 30 keV–1MeV. The large sensitive area and spectral range of the GRS allow, for the first time, an investigation of the high-energy (> 1 MeV) behavior of a substantial number of gamma-ray bursts.

It is found that high-energy emission is seen in a large fraction of all events and that the data are consistent with all bursts emitting to at least 5 MeV with no cut-offs. Further, no burst spectrum measured by GRS has a clear high-energy cut-off. The high-energy emission can be a significant part of the total burst energy; on the average about 30% of the observed energy above 30 keV is contained in the > 1 MeV photons.

Tests of spectral models yield mixed results. Neither a power law nor a thermal model can adequately explain all of the observed spectra. Some GRS spectra show clear curvature and cannot be well-fit by a power law. However, a number of spectra are clearly power laws, and the power-law model is consistent with more events ($\sim 80\%$) than either thermal synchrotron or optically-thin thermal bremsstrahlung. In addition, the two thermal models are generally too soft to explain the observed high-energy emission.

The fact that the observations are consistent with the presence of high-energy emission in all events implies a limit on the *preferential* beaming of high-energy photons, from any mechanism. Single-photon pair-production in a strong magnetic field produces such beaming; assuming that the low-energy emission is isotropic, the data imply an upper limit of 1×10^{12} G on the *typical* magnetic field at burst radiation sites.

INTRODUCTION

Gamma-ray bursts were first discovered during a search for gamma-ray transients in the data from the Vela detectors (Klebesadel, Strong, and Olson 1973). The Vela instruments were designed to verify Soviet compliance with the 1963 Nuclear Test-Ban Treaty by monitoring for radiation (neutrons, X-rays, and gamma-rays) from nuclear explosions in the atmosphere or space. (Descriptions of the discovery can be found in Klebesadel and Strong (1976), and Strong and Klebesadel (1976).) These events aroused great interest for a number of reasons, including the relatively high luminosity of the sources, the short timescales for intensity variations, and the relatively hard observed spectra. The nature of the sources was unknown, and there were no obvious counterparts.

These transients have typical durations of seconds or tens of seconds, although much shorter events have been observed. While they last they are often the brightest source of gamma-rays in the sky. A typical burst, for example, may have a flux from 30 keV to 1 MeV of 10–100 times that of the Crab nebula in the same energy band. Several hundred events have been observed to date.

Most observations of gamma-ray bursts cover the range of photon energies from $\sim$ 30 keV to $\sim$ 1 MeV. At these energies the spectra can generally be described by an exponential-type spectrum of the form $dN/dE \propto E^{-1}\exp(-E/E_0)$, with an average E_0 being $\sim$ 300 keV (corresponding to a temperature of $\sim 3.5 \times 10^{9}$°K). Deviations from the smooth continuum have been seen in some cases and attributed to absorption or emission lines.

We present below the general observational characteristics of gamma-ray bursts as known pre-GRS, including the physical implications of those characteristics. In addition, the major theories of gamma-ray burst production will be briefly reviewed. This presentation is necessarily abbreviated; for more detailed information the reader is referred to the cited references, as well as to review articles such as Ruderman (1975), Hurley (1983), Lamb (1984a, b), and Teegarden (1982, 1984). The

discussion is organized around three basic questions: 1) What type of objects are the burst sources? 2) Where are they? Specifically, how far away are they: are they galactic, extragalactic, or local? 3) How are the bursts produced? In particular, what are the energy source, acceleration mechanism, and radiation mechanism?

These questions are closely related. For example, knowing what type of object the source is, we can infer what the physical conditions may be in the emission region (surface gravity, magnetic field, densities, etc.). These parameters strongly affect production theories, many of which require a neutron star as the source. Likewise, if the distance to the sources is not known, the total intrinsic luminosity of bursts cannot be estimated. This makes it impossible to determine if a theory is satisfactory by even the crudest standard (i.e., whether it can produce enough energy). As a final example, the type of object might be determined from known source locations, either by comparing the distribution of burst sources with distributions of possible source objects, or by observations of source positions at other wavelengths.

Two types of events are excluded from the following discussion and analysis. The first is the very intense event of 1979 March 5, and subsequent bursts from the same source (Mazets *et al.* 1979; Cline *et al.* 1980; Evans *et al.* 1980; Mazets *et al.* 1982b). For a number of reasons (time-history, spectrum, etc.) this is generally considered a unique source, not connected with the "classical" gamma-ray bursts (Cline 1982; Cline 1980; Barat *et al.* 1984b). The second excluded class are the so-called "Jacobson events" (Jacobson *et al.* 1978; Ling *et al.* 1982). There is one member of this class, detected during a balloon flight in 1974. This transient lasted $\sim$ 20 min, much longer than any detected gamma-ray burst. In addition, the spectrum consisted entirely of high-energy lines, with no continuum radiation. In this case the only similarity with the bursts we are discussing is the energy range of emission.

CHARACTERISTICS OF THE SOURCE OBJECT

What can be determined about the environment at the burst site from the observed characteristics (spectral and temporal) of burst emission? Do the characteristics so determined imply a specific type of object as the source of gamma-ray bursts? There are several discrete features that have been used to make deductions about the source object: 1) The relatively brief timescales of gamma-ray bursts indicate that the source is compact. 2) High-energy features, if interpreted as redshifted positron annihilation lines, imply a source with high surface gravity. 3) Low-energy features, if produced by cyclotron absorption and emission, imply very high magnetic field strengths. 4) Finally, observations of source locations by optical instruments show that quiescent burst sources are extremely dim.

If all these arguments are taken at face value, bursts must be produced on or near dark, compact, dense objects with very strong fields; these constraints can only be satisfied by neutron stars. However, these conclusions are far from proven. The evidence for these four points is briefly reviewed below, and some of the associated problems and ambiguities are indicated.

Burst Timescales and Source Size

Durations of detected gamma-ray bursts range from ~0.1 s to ~100 s. Minimum measured rise and fall times of peaks are on the order of 1 ms (Barat *et al.* 1984b) and the smallest observed peak widths are $\leq$ 5 ms (Laros *et al.* 1985b). Spectral evolution has been seen at the finest available time resolution, 0.25 s (Golenetskii *et al.* 1983; Mitrofanov *et al.* 1984).

The observed burst timescales can provide an upper limit on the source size, based on causality: the speed of light limits the size of the source of a pulse to less than $c\Delta t$, where c is the speed of light and Δt is a characteristic burst timescale, such as the rise time. Thus the events with the most rapid rise times ($\sim$ 1 ms) must be from sources smaller than $\sim 3 \times 10^7$ cm; others (with longer rise and fall times) may be correspondingly larger. Thus a fairly compact emission region is required.

These timescales may also be compared to characteristic timescales for different compact objects (Lamb, Lamb, and Pines 1973). We note specifically the values for neutron stars: free-fall time from the magnetosphere ~0.1–1.0 s; dynamical

time scale at surface $\sim 10^{-3}$–10^{-4} s. These are roughly consistent with the fastest durations and rise times observed.

The indications are then that the sources are compact, with timescales consistent with those of neutron stars. However, one must be careful not to make too much of these arguments. Even the smallest upper limit to the size of the emission region is still large compared to the typical radii ($\sim 10^6$ cm) of neutron stars. In addition, there may be multiple emission regions (e.g., one for each pulse) and therefore a larger *total* source size. Relativistic effects may also modify this limit (Ruderman 1975).

Further, the timescales of transient events are actually limited by the size of the emission region, which may be larger or smaller than the source object. Thus, the characteristic timescales of the source object may not always determine the event timescales; consider, for example, the case of solar flares. Kiplinger *et al.* (1983) reported fast spikes in solar flares detected by the Hard X-Ray Burst Spectrometer (HXRBS) on SMM. These spikes had minimum rise and decay times of 20 ms, spike FWHM of 45 ms. Fast spikes were observed in about 10% of flares which were above the estimated threshold to detect such features. While there have been some questions about the significance of this result (Brown, Loran, and MacKinnon 1985), it is clear that short-duration peaks (~100 ms) *are* observed. These timescales are much shorter than would be predicted based on the size of the sun, which has a radius of about 2 light-seconds. Since events with fast time structure can be produced by non-compact objects, strong conclusions about the size of the source object cannot be drawn from observed timescales. Note however that *characteristic* flare timescales are longer than typical burst timescales, though the distributions overlap significantly.

Surface Gravity

In a small number of events line-like emission features have been seen in the energy range 400–500 keV. If these are redshifted positron annihilation lines it would imply that the burst sources have high surface gravity, consistent with neutron stars or black holes.

Observations. Mazets *et al.* (1980, 1981d) reported the observation of both low-

and high-energy features in the spectra of some gamma-ray bursts detected by the KONUS experiments on Venera 11 and 12. The low-energy lines are discussed below. The high-energy lines had peak energies of ~400–460 keV and were generally quite broad. About 5% (7/150) of all events showed significant evidence of such features. The lines tended to appear early in the events (e.g., at or prior to peak intensity). Additional observations of such features have been reported from the KONUS instruments on Venera 13 and 14 (Mazets *et al.* 1983). The Signe instruments on Venera 11 and 12 have also observed features in this energy range for GRB781104 (Barat *et al.* 1984d, 1984e) and GRB781119 (Barat 1983).

An additional observation of interest in this class was made by ISEE-3 in the burst of 1978 November 19 (Teegarden and Cline 1980). A line of marginal significance was found at ~740 keV. The authors suggested that this might be a redshifted 847 keV line from the decay of the first excited state of ^{56}Fe. There were also indications of a very weak, broad feature at ~420 keV.

Interpretation. The usual interpretation of these features is that they are redshifted (two-photon) positron annihilation lines. In this case the redshifts inferred are $z = E_{emitted}/E_{observed} - 1 \doteq 0.11$–$0.28$. The value derived from the Teegarden and Cline (1980) measurement of the ~740 kev feature is $z \doteq 0.14$, assuming that this is a redshifted 847 keV line. The gravitational redshift z is related to the mass (M) and the radius (R) of the source by

$$z = (1 - 2GM/Rc^2)^{-1/2} - 1$$

(Lang 1980, eq. 2-235). The range of observed redshifts implies $(M'/R_6) \doteq 1.32$–0.64, with M' in units of the solar mass and $R_6 = (R/10^6 \text{ cm})$. The only objects that can satisfy this are neutron stars and black holes. (Typical values expected for neutron stars are $M' = 1.4$ and $R_6 = 1$.) Since the observed z depends on the location of the emission region, and not on the radius of the source object, the measurements actually provide lower limits on the source M/R.

Therefore, if the features are gravitationally redshifted annihilation lines, the sources must be neutron stars or black holes. If gamma-ray bursts form a single class of phenomena this conclusion would apply by extension to all sources, not just

those producing detectable lines. However, there are alternative explanations, and some experimental problems associated with these measurements.

Experimental questions. Based on the reported fluences and error bars, the KONUS line detections range in significance from less than 3σ to more than 10σ. However, as Fenimore *et al.* (1982a) have shown, the derived strength of the line depends on the continuum shape assumed to lie beneath it. In particular, for the event of 1978 November 4, the KONUS experiment measured a line of about 6σ significance at 400 ± 50 keV, assuming an underlying continuum of optically-thin thermal bremsstrahlung. Fenimore *et al.* (1982a) found that an inverse Compton continuum fitted the entire spectrum well without the need to add a line. In this case the "bump" in the spectrum corresponded to the Wien peak of the inverse Compton continuum. However, as Fenimore *et al.* point out, the *narrow* observed features cannot be explained by this mechanism.

Further questions are raised by two results from SMM/GRS. In one case the spectral data of 60 GRS gamma-ray bursts were searched over a broad energy range for narrow lines (Nolan *et al.* 1983). None were found; however, as Nolan *et al.* noted, there is no direct conflict because this search was for narrow lines, and the previously observed lines were broad. In the second case, GRS spectra were compared to published KONUS spectra for a burst for which line emission was claimed (Nolan *et al.* 1984a). Though the GRS should have been able to see the line, no feature was observed. The source of this discrepancy has not been determined.

Magnetic Field

A second class of spectral features at lower energies have been attributed to cyclotron absorption and emission in or above the burst radiation site. Under this interpretation it is possible to derive the strength of the magnetic field in the line formation region.

The observations of these features is also primarily due to the various KONUS instruments. Most are absorption lines, with energies in the range of ~30–70 keV and equivalent widths of ~3–30 keV (Mazets *et al.* 1981d). Absorption features were found in ~13% (20/150) of all events, or ~20% of the strong bursts (Mazets *et*

al. 1980). Four of these are events with wide absorption bands at low energies. The same type of features have also been seen by the more recent KONUS experiments (Mazets *et al.* 1983). A narrow absorption line at 55 ± 5 keV was detected by the HEAO-A4 instruments in the spectrum of the 1978 March 25 burst (Hueter 1984).

These features are commonly interpreted as the result of cyclotron absorption and emission in a strong magnetic field. The field strengths implied are in the range $(2\text{–}6)\times 10^{12}$ G, if no correction is made for possible redshift. If the fields are this strong the source object must almost certainly be a neutron star. Such a field will strongly affect particle dynamics and radiation.

Section IV of this work contains a more complete discussion of the interpretation of these features, and the associated experimental and theoretical problems. To summarize: experimental problems exist which call into question the existence of at least some of the reported lines; more seriously, however, there are theoretical problems with the interpretation of the features as cyclotron lines, and alternative hypotheses which can explain them without requiring strong fields.

Source Luminosity at Other Wavelengths

Once the position of the burst source has been determined (see below), attempts to detect the quiescent object at other wavelengths can be made. Such observations may provide much useful information; in particular, if an identifiable counterpart is found it may lead to a determination of the nature of the source object or of the distance to the source. This same procedure was used to discover the nature of the discrete radio sources (see, for example, Shklovsky 1960; Minkowski 1975).

Early attempts at making this type of correlation met with a notable lack of success, indicating the difficulty of the problem. For example, in searches of six fairly large gamma-ray burst error boxes, Cline *et al.* (1979a, b) found no cataloged sources consistent with a burst location. Thus, it seemed that deep observations of burst error regions would be necessary to identify the source object. For this kind of investigation the error box around the burst position must be quite small, since a large area will produce a high probability of chance associations. As of 1984 there were nine well-localized source positions (including the 1979 March 5 event source), typically with errors of less than 1 arcmin. Observations of these locations at a

variety of wavelengths have yielded some interesting results and useful constraints, but no pattern of association with any class of known objects. The data pertaining to this subject have been recently reviewed by Hurley (1982).

Quiescent optical. Stringent limits have been placed on the quiescent optical luminosity of gamma-ray burst sources (and possible companions) by observations of the positions of GB790406 (Laros *et al.* 1981) and GB781119 (Pizzichini *et al.* 1981). Laros *et al.* found no sources in the error box down to $m_v \approx 22.3$. They point out that if the burst source is galactic, this limit means that the source object and any companion must be an M star or something less luminous (e.g., a white dwarf, neutron star, or black hole). In addition, the error region contained no cataloged object or any known radio, X-ray, infrared, or gamma-ray source. Pizzichini *et al.* found two objects with $m_v \approx 20$ consistent with the 1978 November 19 position. Again, if the source is within the galaxy it must be an M star or less luminous.

Cline *et al.* (1981) and Fishman, Duthie, and Dufour (1981) reported an optical survey of the location of the 1978 November 19 burst revealed only "extremely faint stars" in the error box. Hjellming and Ewald (1981) found no optical counterparts for the radio sources (see below) in this same region, to about $m_v = 21$. Cline *et al.* (1984) reported no cataloged objects in three other source fields.

In three cases there is evidence that optical transients have occurred in the past at positions consistent with those of recent gamma-ray bursts (Schaefer 1981; Schaefer *et al.* 1984). Because the optical burst positions are known very precisely, deep searches can be made for quiescent counterparts. This assumes, as seems likely, that the optical transients are real and from the same source as the gamma-ray burst. At least two candidate objects were found; both are very dim ($m_R > 23$) and apparently variable (Schaefer, Seitzer, and Bradt 1983; Pedersen *et al.* 1983).

If these results are representative of gamma-ray burst sources, the source objects must belong to a fairly restricted class of under-luminous objects. This same constraint applies to any companion object (e.g., an accretion disk, or a star in a neutron star binary). These limits can be avoided if the sources are at great distances, but even then it is not obvious what type of object would be appropriate.

Radio. VLA observations were made of the source region of the 1978 November

19 gamma-ray burst at two frequencies by Hjellming and Ewald (1981). A total of 17 sources were found, with three inside the burst error box. The authors point out that there are a number of similarities between a set of three radio sources (two inside, one outside the burst region) and the arrangement of three radio sources associated with Sco X-1. If this association is correct, and the source is the same size as Sco X-1, Hjellming and Ewald calculate that the distance to the emitter is $\sim$ 100 pc. However, this conclusion involves not only the assumption that the three sources form a Sco X-1 type triple, but that they are the source of the gamma-ray burst. As the authors note, the burst might originate from any one of the radio sources individually, or from none of them. It is not possible to reach a conclusion from the available data.

X-ray counterparts. Observations of three burst locations in the 0.15–3.0 keV range were carried out by Pizzichini *et al.* (1981) using the Einstein X-ray Observatory. For two of the positions only upper limits were obtained. In the error box of the 1978 November 19 burst there was evidence for a quiescent source at the 3.5σ level. The position was apparently consistent with at least one of the radio sources (B) found by Hjellming and Ewald (1981) and with the location of an optical transient recorded in 1928 (Grindlay *et al.* 1982).

Infrared. There have also been searches for infrared emission from quiescent burst sources. Apparao and Allen (1982) made observations of sources of 1978 November 19 and 1979 April 6 bursts. Nothing was found for the second event; a very weak source was seen at radio source B (Hjellming and Ewald 1981) for 1978 November 19. They reported that this source was not like a star but more like an extragalactic object. Schaefer and Cline (1985b) have searched IRAS data for 23 burst positions. Three additional regions were observed with a ground-based instrument. With the exception of the GB790305 position, no IR source was found.

Conclusions. It was hoped that observations of burst source positions at other frequencies would find clear counterparts, and thus reveal the nature of the source objects; this hope has not been realized. On the contrary, the data show that there is no known type of object generally associated with gamma-ray burst locations. When not bursting the sources are apparently very dim at infrared, optical, and

X-ray wavelengths. This information does provide useful constraints on the nature of the source and any companion. Other valuable limits can also be deduced (e.g., on accretion; Ventura 1983).

The best observed location is that of GB781119. There are positive observations of a quiescent source in radio, infrared, and X-ray bands. These data, however, while inspiring interesting hypotheses, do not make up a clear and coherent picture.

WHERE ARE THEY?

There are two approaches to determining the spatial positions and distribution of the burst sources. In one, the actual positions of individual burst sources are determined; in the other, the statistical properties of the set of gamma-ray bursts are used to deduce the distribution of burst sources.

Statistical Treatment (logN-logS)

The statistical approach relies on the measured relation between the rate of events with total fluence greater than S ($N(>S)$), and S. Since the data are plotted on log scales, this type of analysis is referred to as *logN-logS*. This technique was used with some success in radio astronomy, leading to the identification of two classes of sources, one of galactic, the other of extragalactic oriin (see Shklovsky's (1960) description of the results of Mills (1952)).

The way that this information relates to the spatial distribution of sources can be illustrated by the simplest case, in which all bursts have the same intrinsic luminosity (L), and the observed variations result only from the varying distances to the sources. We also assume a constant density (ρ_0) of sources everywhere. Then the observed flux S depends only on the distance to the source (d),

$$S = L/(4\pi d^2),$$

and

$$\begin{aligned} N(>S) = N(<d) &= 4\pi\rho_0 d^3/3 \\ &= \frac{4\pi}{3}\rho_0\left(\frac{L}{4\pi}\right)^{3/2}(S^{-1/2})^3 \\ &\propto S^{-3/2} \end{aligned}$$

For a finite spherical distribution of radius R, this relationship holds to $S = L/(4\pi R^2)$; for smaller S (larger d), $N(> S)$ is constant. In the case of a slab distribution of thickness h, $N(> S) \propto S^{-3/2}$ for $d \ll h$, but for $d \gg h$, $N(> S) \propto S^{-1}$. Modifications with a spectrum of luminosities have been calculated by several authors (e.g., Fishman 1979; Jennings 1982, 1984).

Thus it may be possible, based on the measured logN-logS relation, to deduce the geometry of the burst source distribution. By comparing this to the known mass distributions for different distance scales (e.g., disk shaped for galactic) the characteristic distances to the sources might be determined, and therefore the intrinsic energies of bursts. A comparison with the distributions of different types of known objects (e.g., pulsars) might help to identify the type of source.

In practice there are a number of difficulties that make it hard to carry out this program. Most burst instruments do not record and transmit data continuously; instead, data are stored only when some trigger criterion is met. The criterion is typically an increase above the background in some particular energy band on some fairly short timescale. Because the instruments do not trigger on total integrated fluence (S) but on another characteristic of the burst, the sample will be incomplete with respect to S unless all bursts have the same time profile and spectral shape. In particular, long, low-intensity events may have a fluence nominally above threshold, yet not trigger the detector because the flux at any instant is too low. Additionally, an event with a hard spectrum may have S above threshold but a low intensity in the trigger energy range. Bias as a result of differing time profiles has been treated by Barat *et al.* (1982) and Jennings (1985); incomplete sampling due to spectral effects by Higdon and Lingenfelter (1985) and Jennings (1985). Because of these problems Jennings (1985) has concluded that the largest body of data (from the KONUS instruments) cannot be used to deduce position information from log$N$-log$S$.

In addition to sampling problems, there are apparently difficulties in determining S from the data once a burst has been detected. For example, for the very short ($\sim$ 48 ms duration) event of 1979 June 13, the total fluence determined by Barat *et al.* (1984a) from the measurements of four different instruments was approximately

an order of magnitude higher than the fluence determined by Mazets *et al.* (1981b). Klebesadel, Fenimore, and Laros (1984) report that, on some individual events, the measured fluences from the PVO and KONUS experiments differ by as much as a factor of 40. It should also be noted that the calculation of S from the data requires extrapolation to energies above those observed by the instrument. Therefore the derived value of S depends to some extent on the spectral model assumed in the extrapolation.

The consensus is that the high-fluence data (above $\sim 10^{-4}$ ergs-cm^{-2}) are consistent with (but do not require) $N(>S) \propto S^{-3/2}$ (Klebesadel, Fenimore, and Laros 1984). At the lower fluences the distribution seems to flatten, indicating a departure from isotropy or homogeneity, possibly a limit to the source distribution. Specific upper limits at low fluences have been reported by Meegan, Fishman, and Wilson (1984) and Helfand and Vrtilek (1983), among others; recent Los Alamos work using data from multiple satellites may provide positive measurements at low values of S (Fikani and Laros 1984).

Some of the problems with logN-logS can be avoided, or at least minimized, by analyzing *logN-logP*, where P is the peak flux observed. The triggering threshold is generally closely related to P, so that the sampling is more complete with respect to P than to S. However, it is even more difficult with logN-logP analysis to compare or combine data from two experiments. It is Jennings' (1985) contention that the KONUS logN-logP data are inconsistent with either a disk model or an outwardly unbounded, homogeneous, and isotropic source distribution, regardless of the intrinsic luminosity function assumed.

Individual Source Locations

In addition to the statistical treatment described above, it is possible in some cases to deduce the direction to an *individual* source. If these locations coincide with those of otherwise interesting objects (supernova remnants, quasars, known neutron star binaries, etc.), the type of object producing the bursts might be discovered. This in turn might also lead to an accurate estimate of the distance to the source. Even if no counterpart object is found, a statistical analysis of the positions can be used to test whether the spatial distribution of burst sources is consistent with

that of any known population of objects. In addition, the sources can be monitored at various wavelengths in their quiescent state. Finally, the set of derived locations can be used to place limits on the time for burst recurrence from a single source (e.g., Schaefer and Cline 1985a). The usefulness of precise source locations leads many researchers to feel that they are the key to understanding gamma-ray bursts.

Two techniques have been used to derive precise source locations from burst data. The first method requires observations of the burst by a number of widely separated spacecraft. The difference in the observed time of the burst at two different locations can be used to determine the direction of the event wavefront (Giacconi 1972; Bisnovaty-Kogan *et al.* 1981); from this the source location can be narrowed down to a circle (or annulus) in the sky. Observations by three spacecraft allow the construction of two circles, with the source constrained to be at one of the two intersections. With the proper additional data the position can be unambiguously fixed.

In practice there are a number of difficulties with carrying out this procedure: 1) the burst must be observed by several widely separated instruments; 2) the absolute timing of the data from the different experiments must be determined to accuracies $\leq$ 10 ms; and 3) the time shift must be deduced precisely from the data. Fulfilling the first condition is a matter of chance since it depends on having a number of operating detectors at appropriate locations. See Hurley (1983b) for a discussion of factors affecting localization accuracy.

The second technique uses the known anisotropic response of a burst instrument to determine the source direction. An application of this method (described by Mazets and Golenetskii 1981) to the KONUS data has produced a large number of position determinations (Mazets *et al.* 1981a, b, c). The KONUS instruments consist of six separate detectors, one facing each side of an imaginary cube, i.e., in the positive and negative directions along the three Cartesian axes. With three-axis stabilization of the spacecraft, a comparison of the responses of the different detectors can produce a measure of the source position. This is less precise than the first technique when many observations are available.

Results. There are currently more than 80 known source positions, mostly from

KONUS (Mazets *et al.* 1981a, b, c) and the interplanetary network (Atteia *et al.* 1985; Klebesadel *et al.* 1982). These data are summarized in Atteia *et al.* (1985). There is no evidence for a concentration of sources in the galactic disk, as would be expected if the sources were distributed as the matter in the galaxy. There is some indication of a north-south asymmetry in the KONUS data (Vedrenne 1981; Pizzichini 1982), but this is not seen in the positions from the interplanetary network, which were consistent with isotropy (Atteia *et al.* 1985). However, a distribution with 42% in the northern and 58% in the southern hemisphere is consistent with both data sets, with probability > 0.1 (Atteia *et al.* 1985).

As with logN-logS, statistical treatments of positions require a consideration of sampling biases. If the instrument response is not isotropic and the detectors do not view all parts of the sky for the same amount of time, corrections have to be made for unequal sampling. Questions of this type have been raised about the KONUS distribution (Laros *et al.* 1982, 1983; Mazets and Golenetskii 1982). In particular, the north-south asymmetry may be caused by this (Laros *et al.* 1983).

To summarize the main results: there is no indication of a galactic distribution of sources because there is no observed concentration of burst locations in the galactic plane, and no significant center-anticenter asymmetry (Jennings 1982). Nor do the positions seem to be correlated to any extragalactic mass distributions (galaxies, superclusters, etc.) (Jennings 1984).

Summary of Conclusions

By using a combination of logN-logP and position analysis Jennings (1984) concluded that sources are probably in a large-scale ($D \sim 100$ kpc) galactic halo. If this is the case the sources correspond to no known population of object, although there is independent dynamical evidence for some type of massive halo. Others claim that intrinsic intensity distributions and selection effects are sufficient to make the data consistent with a local origin (Higdon and Lingenfelter 1985; Yamagami and Nishimura 1985).

THEORIES OF GAMMA-RAY BURSTS

The question of how bursts are actually produced is intimately connected to the issues discussed in the preceding sections. However, while the theories of burst production are inspired by the observations, implications of the available data are vague enough to provide few strong constraints.

A complete gamma-ray burst theory would describe the entire burst process from energy release, to particle heating/acceleration, to radiation and the observed gamma-ray spectrum. This is obviously a problem of daunting complexity, especially when little or nothing is known about the nature of the burst source. In the physically comparable but much better observed case of solar flares no such theory exists. Instead of seeking to produce a complete theory, then, theoretical treatments of bursts have generally addressed two parts of the problem independently: first, the energy source/release mechanism and second, the radiation production mechanism. One attempt at a complete theory, from energy release to observed spectra, is Hameury *et al.* (1985).

The major constraints which any energy production theory must satisfy are 1) total energy content of $\sim 10^{39}(d/1kpc)^2$ ergs, where d is a typical distance to a source; 2) short timescales for energy release (< 0.1 s); and 3) total duration, that is, the energy release mechanism must produce, in some fairly natural way, bursts of the observed durations ($\sim$ 0.1–100 s). The complex nature of burst time histories is presently only a minor constraint, since it is generally thought to be easy to add complexity.

The acceleration and radiation mechanisms are constrained by the observed spectra which are the result of energetic particle interactions. The spectra thus yield coupled information on the energetic particle distribution and the interaction which produces the observed radiation. Additional constraints arise from the measured time histories, especially from the comparison of intensities in different energy bands over the course of the burst.

Theories of Energy Production and Release

A wide variety of models have been proposed for the production of gamma-ray bursts, some of them quite exotic. However, the source of energy in the different

models is generally one of two types: thermonuclear or gravitational/kinetic. Thermonuclear models involve the thermonuclear explosion of matter accreted on the surface of a neutron star. Theories differ on the composition of the accreted matter, the rates of accretion, and other details; extensive calculations have been made (e.g., Woosley and Wallace 1982; Hameury *et al.* 1984). The total energy available is limited by the basic nuclear physics to roughly 9 MeV/nucleon. The total amount of accreted matter required is then typically $\sim 10^{20}(d/1kpc)^2$ g. Whether this amount of matter can be accreted from the interstellar medium, or whether a companion is required depends on a number of factors, including the repetition rate (Ventura 1983). These models usually need a strong magnetic field to channel accretion to a limited area (at the poles).

The second set of models is more varied, but most involve radiation from rapidly accreted matter. The matter may be in the form of a solid body (a comet or asteroid: see, e.g., Newman and Cox 1980; Colgate and Petschek 1981), or material dumped by instabilities from an accretion disk (e.g., Kafka and Meyer 1984; Michel 1985; Epstein 1985b). Accretion onto the surface of a neutron star can provide up to $\sim$ 180 MeV/nucleon; it is thus much more efficient (per gram) than thermonuclear processes. Other theories get their energy from shifts of dense matter in the neutron star (e.g., Fabian, Icke, and Pringle 1976; Ramaty *et al.* 1980).

Gravitational accretion and nuclear burning are accepted as explanations of different types of X-ray bursts. However, there are two important problems with using these energy sources to power gamma-ray bursts. The first is, since they are so much like X-ray burst theories, why do they produce gamma-ray bursts instead? The usual answer is that the difference is the very strong magnetic field at gamma-ray burst sites (see, e.g., Woosley 1984). The second problem is, as several authors have noted (e.g., Katz 1983; Colgate and Petschek 1985; Epstein 1985a), that both of these mechanisms by their natures produce their radiation under a large amount of material, and therefore at very great optical depth. The resulting spectrum should then be very soft, with a characteristic temperature of a few keV; however, the observed spectra are much harder, and, indeed, non-thermal.

A third class of theories is loosely termed non-thermal. Included in this cate-

gory are the "flare models," based on the obvious similarities between bursts and solar flares, and proposing acceleration by magnetic field reconnection. The original source of the required field stress might be accretion or movement of the neutron star material itself (Liang and Antiochos 1984). Other theories which might be classed as non-thermal are modifications of the thermal models above in light of the optical depth problem. The fundamental energy source is the same as in those models discussed above (i.e., thermonuclear or accretion), but the radiation producing process is not the heating which takes place at the explosion or accretion. The thermal energy must be gotten out of the optically-thick region where it is produced to an optically-thin region where it can be used to produce hard photons. Two mechanisms which have been proposed to accomplish this are a strong, radiatively driven wind (Woosley 1984) and short-scale magnetic field reconnection (Hameury *et al.* 1985). In both cases the result is a stream of high-energy electrons along the field lines which then boost low-energy photons to high energies by inverse Compton collisions.

Radiation Mechanisms

Three different radiation mechanisms have been proposed: 1) electron bremsstrahlung in a hot plasma, 2) synchrotron radiation of electrons in a strong magnetic field, and 3) inverse Compton emission from a hot plasma overlying a soft X-ray source. Which radiation mode is dominant depends on the environment at the emission site (magnetic field strength, particle density, etc.), so that a spectral model assumes a set of conditions at the radiation region. Therefore, any measurement of physical parameters at the radiation site is also, indirectly, a test of the emission mechanism. The radiation mechanism itself can be tested by comparison with the observed spectral shape. The physics of the different radiation mechanisms and tests of the spectral models are discussed in detail in Section III.

SUMMARY

It may be useful to summarize the tentative consensus in the field about the nature of gamma-ray bursts and burst sources. This is not meant to imply unanimity among investigators, nor endorsement by this author.

The common belief is that gamma-ray bursts come from neutron stars with very strong magnetic fields. The data supporting this view, as detailed above, are: 1) short burst timescales indicate a compact source; 2) high-energy features imply a high surface gravity; 3) low-energy features imply a strong magnetic field; and 4) optical searches of error boxes imply low (quiescent) luminosity sources. In addition, neutron stars are thought to be a natural possibilty for gamma-ray bursts since they are the sources of X-ray bursts. Finally, the energy available in compact sources with high magnetic fields make it easier to produce very energetic phenomena. Because strong fields are thought to be present synchrotron radiation is expected to be dominant. There is no real consensus about the nature of the energy source or the typical distance to the sources.

As above, arguments based solely on GB790305 have been excluded as it is fairly well-established as a special case, a member of a different class of events than classical gamma-ray bursts.

The sum of the evidence does not produce a compelling case for the consensus view of burst sources. Perhaps the strongest argument for a neutron star origin comes from the optical observations which establish the very low quiescent luminosity of the sources. The evidence provided by the observation of low- and high-energy features is weaker. As we have seen, the mere existence of these features is controversial; even if they are real, the interpretation is ambiguous. Event timescales consistent with most bursts have been observed from the sun, which is not a neutron star.

So none of these arguments is convincing alone. However, it is of interest that all the arguments seem to point (albeit vaguely) to the same conclusion. The only data that points away from the neutron star hypothesis is that of the source locations and distributions, which are not consistent with the known populations. These data are not consistent with *any* known population, however. Therefore,

while it cannot be proven that neutron stars are the sources of gamma-ray bursts, that they *are* the sources is a reasonable working hypothesis. It should not be forgotten that it is only a hypothesis, and is far from proven.

In the body of this work a few of the questions raised above will be considered in light of the GRS data:

In Section II, general questions about the high-energy (> 1 MeV) emission in gamma-ray bursts will be addressed. First, is a significant amount of such emission observed? If so, is it present in all bursts or only in some particular subset? Second, how is the emitted energy distributed; in particular, how important is the energy in > 1 Mev photons compared to the total burst energy? This bears on all the questions of burst production (energy source, acceleration mechanism, and radiation mechanism).

In Section III, the various radiation mechanisms which have been proposed to explain gamma-ray burst spectra are discussed, and some of these models are tested against the GRS data. This again relates directly to questions of production, since the observed spectrum is the result of an energetic particle distribution (produced by some acceleration/heating process) losing energy by radiation. Which radiation mechanism is dominant depends on the source magnetic field strength, which is treated in detail in the following section. Particular emphasis is placed on tests at high energies because it is only above 1 MeV that the models diverge and can be easily distinguished.

In Section IV, the data and theory which indicate that burst sources may have very strong magnetic fields ($> 10^{12}$ G) are examined. The presence of high fields is one argument supporting the neutron star origin of bursts. In addition, the magnetic field strongly affects the production of radiation. The high-energy emission observed by GRS is used to place a limit on the magnetic field strength at the source, independent of the controversial low-energy features.

I. SMM/GRS GAMMA-RAY BURSTS

THE SMM GAMMA-RAY SPECTROMETER

The Gamma-Ray Spectrometer (GRS) is one of seven instruments on the Solar Maximum Mission satellite (SMM) launched on 1980 February 14. The purpose of the mission was to make coordinated measurements of solar flares and related activity over a wide range of wavelengths. As a dedicated solar instrument the satellite was kept actively oriented to face the sun, even during spacecraft night. A failure of the attitude control system about nine months after launch prevented the experiments requiring precise pointing from collecting useful data; however, the crude pointing which was still available was adequate to keep the sun within the wide field-of-view of the GRS. In April of 1984 the crew of the Space Shuttle retrieved, repaired, and redeployed the SMM satellite.

The GRS (Fig. I-1) was designed to make detailed, high sensitivity measurements of solar flare gamma-ray spectra from 0.3 to 9 MeV (Forrest *et al.* 1980). The main detector consists of seven 3 in. by 3 in. cylindrical NaI(Tl) crystals. The detector is actively shielded against gamma-rays by a 1 in. thick side shield and a 3 in. thick back plate, both made of crushed CsI. The entire instrument is surrounded by two plastic scintillators in anticoincidence with the main detector to reduce energetic particle background. Two auxiliary X-ray detectors cover the energy range $\sim$ 13–190 keV with four spectral channels each. The combination of the main detectors and back CsI shield allow crude spectroscopy from $\sim$ 10 to $\sim$ 100 MeV.

The total analog signal from all of the NaI detectors is summed and fed into a 476 channel PHA. The resulting count is stored in one of two memories, depending upon whether the photon interacted in one or several detectors. One spectrum is accumulated every 16.384 s. The channel number (n) to energy conversion is approximately quadratic ($n^2 = E$) so that the channel width increases roughly with the resolution ($\sigma \propto E^{1/2}$).

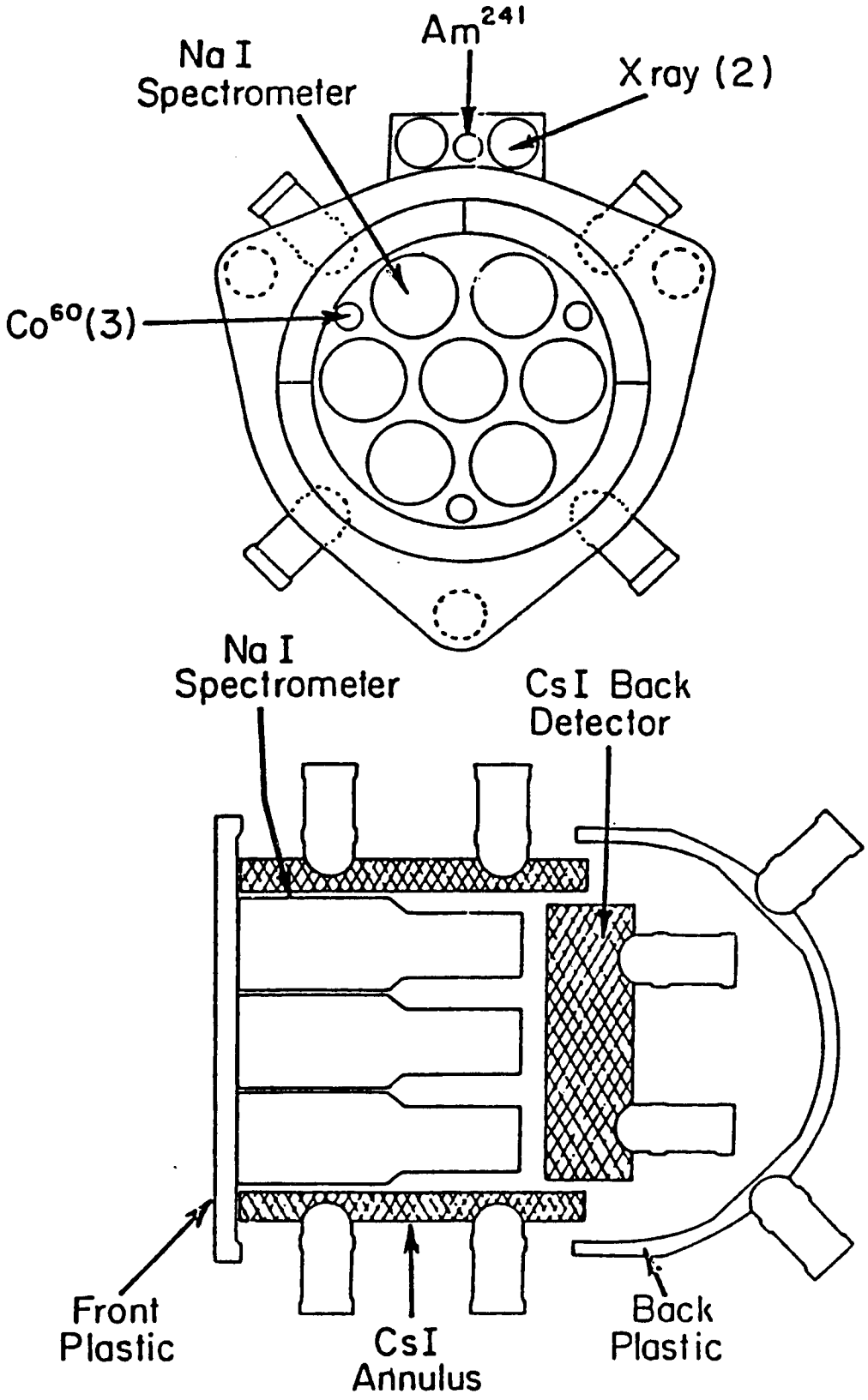

Fig. I-1: Diagram of the Gamma-Ray Spectrometer, front and side views.

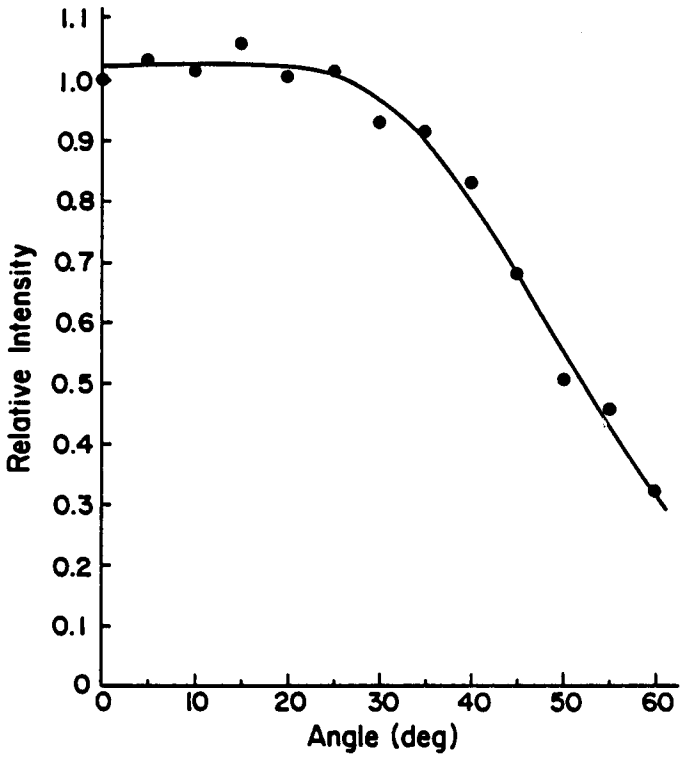

Fig. I-2: Relative sensitivity of the LGT as a function of angle, measured at 511 keV and normalized to 1 at $\theta = 0$. The line is an indication of the general behavior of the data, but it is not a formal fit. The data were provided by P. P. Dunphy, from his measurements.

Because of the detector arrangement in the GRS, and the active shielding on the sides and in back, the instrument sensitivity and response depend on the angle of the source with respect to the detector axis. However, a source in the wide forward field-of-view (half-angle $\sim 50°$) will suffer little or no attenuation from the shields. While this effect was not actually measured for the GRS, the angular response of the LGT (the balloon-borne prototype of the GRS) was determined. Figure I-2 shows the relative flux (at 511 keV) detected by the LGT as a function of angle.

Gain Stabilization System

Each of the detectors is individually and continuously gain stabilized (Forrest *et al.* 1980; Gleske and Forrest 1980). Three ^{60}Co sources embedded in plastic scintillator material are placed around the outside of the cluster of main detector

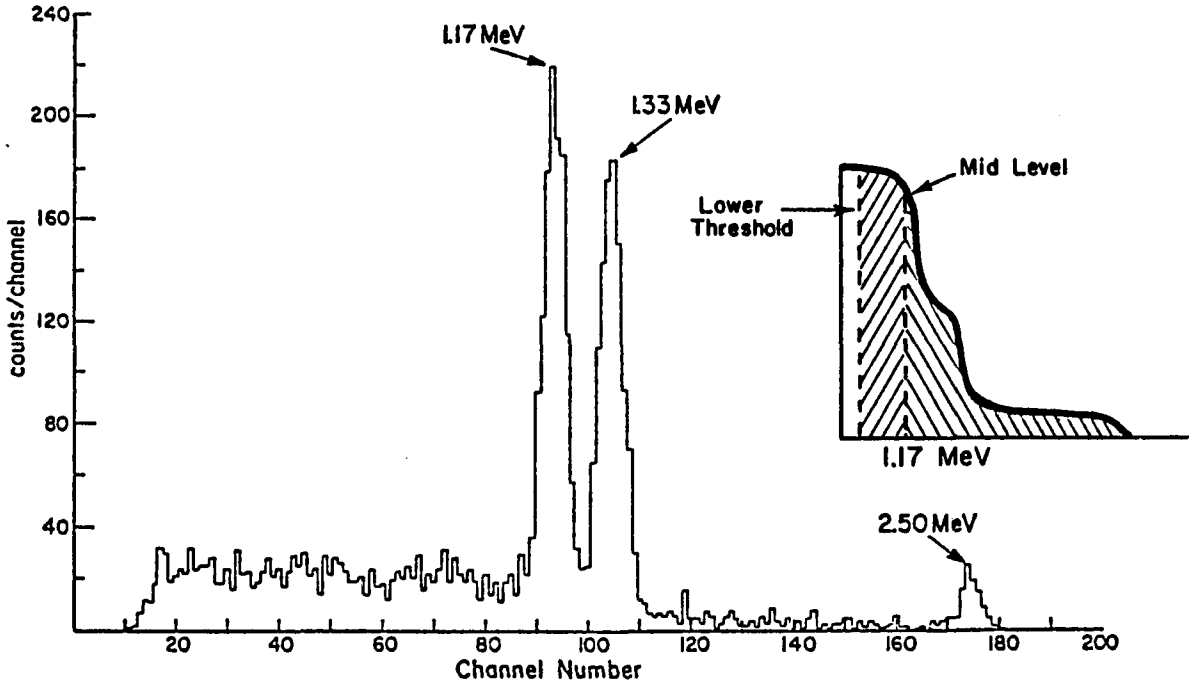

Fig. I-3: Calibration spectrum for the GRS showing the threshold for the automatic gain stabilization system. Inset is the integral counts spectrum indicating the threshold set at the 50% point.

crystals. The primary (> 99%) decay mode of ^{60}Co is by electron emission to an excited state of ^{60}Ni, which decays by the emission of a 1.17, then a 1.33, MeV gamma-ray. The electron is detected in the plastic scintillator, providing a coincidence signal and tagging the gamma-rays as calibration events. Each detected coincident gamma-ray event above (below) the threshold value of 1.17 MeV causes the high voltage on the relevant phototube to fall (rise) by a small amount (50 mV, corresponding to 0.4%). The threshold is set near the calibration peaks in such a way that at normal gain there will be as many counts above as below threshold, thus keeping each detector at the proper gain. Fig. I-3 shows the calibration spectrum in the main detector with the position of the threshold indicated. Also shown is the integral spectrum of calibration events, indicating the threshold set at the 50% point.

Calibration events which are not tagged (due to an undetected decay electron)

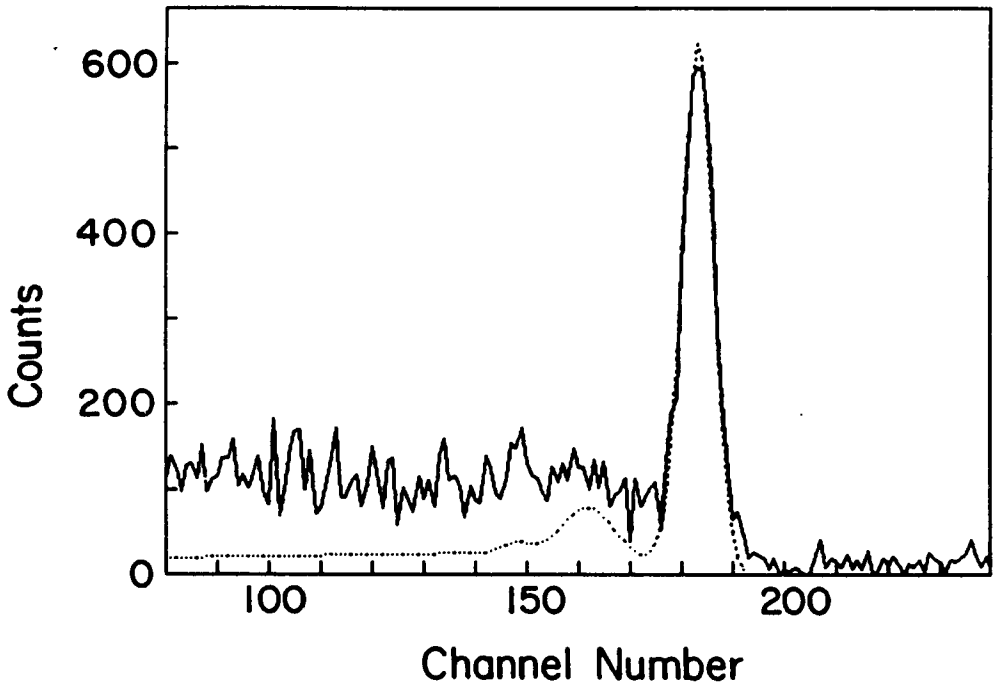

Fig. I-4: A comparison of the predicted and observed instrument response to a line at 2.223 MeV. The observed line was produced in the sun by neutron capture on hydrogen, after a large flare. The flare occurred on 1982 June 3, more than 2 years after launch.

appear in the normal data as "leakage" peaks. This effectively increases the background slightly in a small part of the spectrum, while providing a known background line for a check of calibration during data collection. Calibration spectra from each detector are accumulated and transmitted once each orbit, during spacecraft night.

The effectiveness of this system and the overall stability of the instrument are demonstrated by Fig. I-4 which shows a comparison of the 2.223 MeV deuterium formation line measured after a large solar flare with the predicted instrument response (see Appendix A). Although this flare occurred more than two years after launch, the peak channel shows no shift from that expected based on preflight calibration. Note also that there is no apparent degradation of instrument resolution. The higher-than-expected Compton continuum is due at least partly to scattering of 2.223 MeV photons in the solar atmosphere.

The GRS as a Gamma-Ray Burst Detector

Despite the fact that the GRS was not designed for the observation of cosmic sources, it is in some ways superior to dedicated burst instruments. It has a very large effective area (photopeak effective area $\sim$ 160cm^2 at 300 keV) and a large spectral range with good high-energy coverage. Because of the continuous data transmission of SMM, GRS data is not memory-limited or dependent on burst triggers. The high telemetry rate also allows a relatively large number of spectral channels. The instrument was extensively calibrated on the ground, with the gain continuously maintained by the system described above. Observations of solar flares have provided verification of the instrumental stability and cross-calibrations with other experiments. The detector is well shielded, reducing background. Fast time channels are available at a wide range of energies ($\sim$13–190 keV, $\sim$300–350 keV, $\sim$4.1–6.4 MeV, and $\sim$10–100 Mev).

The GRS has disadvantages for burst work that result from its being designed primarily to observe solar flare gamma-rays. In particular, its side and back shielding give it a strongly anisotropic response. This shielding also reduces its field-of-view, and thus the number of bursts detected. Its spectral accumulation time is long compared to gamma-ray burst timescales (where spectral variations have been observed down to 0.25 s). Finally, the lower energy threshold (300 keV) is too high for burst work: it limits the number of bursts detected and prevents measurements of the low-energy spectra.

Based on this discussion of the instrument properties some generalizations can be made about the kind of questions which the GRS data can best address. Because of the detector's anisotropic response and the fact that most burst source locations are not known, theories that depend sensitively on spectral shape or absolute sensitivity are difficult to test in general. The long spectral accumulation time usually rules out measurements of spectral variation, at least between the fast time channels (e.g., between 300 keV and 4 MeV). The GRS is best at measuring integrated or average properties of bursts. Most importantly, the GRS has provided unique data on the high-energy emission in gamma-ray bursts, data which allow tests of spectral theories and searches for the effects of pair-production processes.

GAMMA-RAY BURSTS IN THE GRS DATA SET

This section contains a discussion of the search techniques which have been used to find gamma-ray bursts in the SMM/GRS data, and the procedures used to identify them as cosmic. The actual work of search and identification was carried out at the Naval Research Laboratory (NRL) and the Max-Planck Institut (MPI). Finally, the relationship between the SMM/GRS data set and "classical" gamma-ray bursts is treated.

Detection of Events

Systematic searches of the GRS data for gamma-ray transients are carried out under the supervision of two co-investigators, G. Share at NRL and E. Rieger at MPI. NRL conducts an automated search for short time-scale (16 s) transient increases $\geq 4\sigma$ in the main-channel counting rate in the 350–800 keV band. The vast majority of events have been found this way. A separate test for long-duration transients is made by attempting to fit a polynomial to the time-history of the counting rates in this same energy band. This procedure is restricted to data taken while the magnetic rigidity is in a limited range and the background is well-behaved. If no acceptable fit can be made, the data are examined for transients. At MPI a visual examination of the counting rates in the low-energy main-channel data (approximately 280–350 keV) is performed. Again, the integration time is 16.384 s. In addition, GRS data are searched for events which have been detected by other experiments. The fact that some of the GRS events were found by this last method means that there was not a uniform selection criterion for all events.

The limitations of the search techniques should be noted. Because only a few particular energy ranges have been examined, classes of events with significant emission only at other energies will be missed. For example, there are probably a substantial number of events from off-axis sources which are strongly attenuated at low energies but still have significant counts either at higher energies or in the shields. Events near the beginning or end of data collection intervals may not be detected due to insufficient information about the background (G. H. Share 1985, private communication). In addition, some weak, soft events may be detectable in the auxilliary X-ray detectors but not at the higher energies searched for events.

Finally, there may be a class of events (Jacobson *et al.* 1978; Ling *et al.* 1982) with emission confined to high-energy lines.

These limitations have little effect on the study of classical gamma-ray bursts. "Jacobson events" are not classical gamma-ray bursts. The low-energy threshold of 300 keV means that detectability depends on flux at higher photon energies than in other burst detectors and is insensitive to spectral shape fluctuations at low energies. It is argued below that this does not significantly bias the GRS data set. The shield attenuation produces an angle-dependent threshold so that in most cases detected events will come from sources within the forward field-of-view. Since the detector FOV scans through the sky during the year, following the Sun, and the burst source distribution is at least roughly isotropic, this should cause no overall bias in the data set. However, at any particular time there is a strong bias toward sources in the forward direction.

The long (compared to gamma-ray burst timescales) integration time is also a limitation. For events significantly shorter than 16 s the threshold depends on the total integrated flux and varies with the background. For longer events, the threshold increases with the duration. Very short events, which would be detectable at shorter integration times, can be washed out by the large integrated background. One example of this is GB811231 at 0738 UT, an event with a peak FWHM of approximately 0.128 s. This burst was missed by the search routines but was found in the data at higher time resolution after detection was reported by the ISEE-3 experiment (Norris *et al.* 1984). There is no useful spectral data on this event, so it is not included in subsequent analyses.

In general, the long integration time means many very short bursts may be missed. Events with durations less than $\sim$ 0.1 s may be a different type of phenomenon, distinct from the classical gamma-ray bursts. There is currently some controversy about whether short events actually form a separate class (Mazets *et al.* 1982b; Norris *et al.* 1984; Barat *et al.* 1984b; Jennings 1985); if there is such a class as described by Mazets and Golenetskii (1981), they comprise only a small fraction (10–15%) of bursts observed by the KONUS instruments. This fraction depends on the detector and the trigger criteria; see Norris *et al.* (1984) for other

estimates. Assuming an extrapolation of the KONUS low-energy spectra, most such events would be below the GRS fluence threshold. A second type of event which may be missed is a long burst with low peak flux. Such an event might conceivably have significant integrated fluence, yet not be detected by the search routines.

It should be noted that the limitations of the search technique are sensibly related to the instrument characteristics. In most cases, for useful analysis to be performed the burst must produce significant counts in the main detector. For an event with a falling spectrum (steeper than $\sim E^{-15}$) this implies that there must be significant counts at the low end of the spectral range (about 300 keV) over the length of the spectral integration time of 16.384 s. These are exactly the type of events the above techniques were designed to find. What biases do exist are mitigated by including events found through comparison with other instruments. This, however, means that the data set no longer consists only of bursts meeting a single uniform standard.

In summary, the data set, like any data set from a finite instrument, is biased. None of the known biases, however, appear to be particularly important *a priori*. An argument is made below that the data are consistent with the GRS events being an unbiased subset of the normally detected classical gamma-ray bursts.

Identification of Gamma-Ray Bursts

After an event is detected by one of the search procedures it is necessary to determine whether or not it is of cosmic origin. The only unambiguous way to do this is by localizing the source position based on multiple spacecraft observations. If a position can be consistently determined by widely-separated spacecraft the source cannot be local; if the position so determined is significantly distant from the Sun the burst was not a solar flare. This process of finding source positions is difficult at best, and is impossible when an insufficient number of coincident observations exist. The result is that there are only two GRS events with source positions published at this time (Katoh *et al.* 1984; Yoshimori *et al.* 1984), one of which is ambiguous.

In the absence of such information, less definitive tests must be used to sort out the *cosmic* gamma-ray bursts. Comparison with unpublished event lists may show a coincident observation by another spacecraft, reducing the possibility of

local origin (in or near the spacecraft) or instrument malfunction. In many cases preliminary work by other experimenters has provided *tentative* identification of some events as "confirmed cosmic" or "unconfirmed cosmic." This information is available in an unpublished list (K. Hurley 1985, private communication). Of the 71 events analyzed in this work, 31 are listed as confirmed cosmic.

When positional information is not available indirect methods must be used to identify cosmic bursts. In particular, special care has been taken to eliminate events which may have been produced by non-cosmic sources. The techniques are not foolproof: real events may be excluded, and some spurious bursts included. The two primary sources of non-cosmic bursts are geomagnetic particle precipitations and solar flares.

Large transient increases in the energetic charged particle flux toward the earth ("particle precipitation") can cause a corresponding increase in the low-energy channels of the GRS main detector. Some of these events occur on a short enough timescale to mimic gamma-ray bursts. They differ significantly from actual gamma-ray events, however. The plastic anticoincidence shield is highly sensitive to charged particles and relatively insensitive to photons; therefore, the difference in the relative counting rates of the main detector and the plastic scintillators can serve to identify the charged particle events. In addition, such transients typically have longer timescales than gamma-ray bursts ($\sim$ 5 min. duration) and a flat X-ray spectrum (G. H. Share 1985, private communication). They usually occur at low rigidity, with profiles following the changes in rigidity. Fig. I-5 shows a comparison of the shield and detector responses to a gamma-ray burst and a particle event.

Eliminating solar flares is a more difficult task since they are actual gamma-ray transients from an astrophysical source. Flares and cosmic bursts are differentiated primarily by their spectral and temporal characteristics at roughly 10 keV, as measured by the GRS X-ray detectors. The typical flare observed by the GRS shows strong thermal emission in the 13–20 keV X-ray channel, persisting long after the $>$ 300 keV emission. Fig. I-6 shows 13–20 keV and 300–350 keV time histories for both a solar flare and a cosmic gamma-ray burst. The ratio of 13–20 kev to 300–350 keV flux indicates that the X-ray spectrum of the burst is much flatter than that

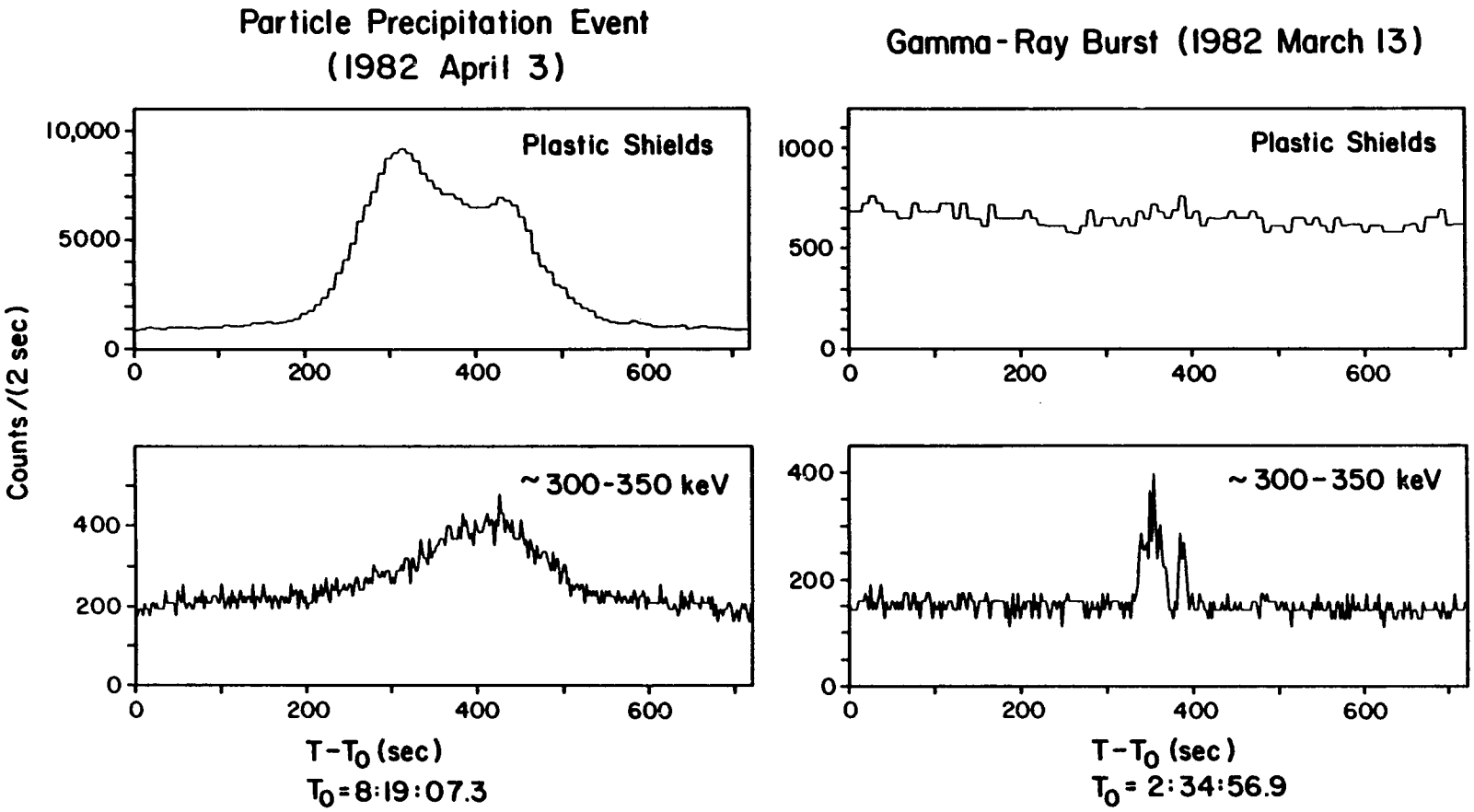

Fig. I-5: A comparison of the main detector and plastic shield response to a particle precipitation event and a gamma-ray burst. A large signal in the plastic anti-coincidence shields is the signature of a particle precipitation event.

of the flare. The intense extended thermal emission of the flare is absent from the burst. Indeed, many bursts show no detectable flux at all in the low-energy X-ray channels. This results from the intrinsically flat X-ray spectrum of bursts and the fact that the X-ray detector field-of-view is much narrower than that of the main spectrometer.

No event identified as cosmic has flare-like low-energy X-ray emission. At least one event (GB800419) *is* coincident with some extended 10 keV flux (which may or may not be solar). However, the inferred X-ray spectrum is still much flatter than that of a flare.

A secondary check has been made by searching for solar activity coincident with events thought to be bursts. The two measures of solar flare activity used are soft X-rays as detected by the GOES instruments and hard X-rays observed by the Hard X-Ray Burst Spectrometer (HXRBS) on SMM. While both the GOES and HXRBS can detect non-solar events, their fields-of-view are much smaller than that of the GRS and are centered on the sun. The GOES instruments scan in the equatorial plane, but their FOV perpendicular to the plane is roughly 13° FWHM in the 0.5–4 Å channel (Donnelly, Grubb, and Cowley 1977). The HXRBS FOV is $\sim$ 40° FWHM, or 0.38 sr (Orwig, Frost, and Dennis 1980), compared to $\sim$ 100° (2.24 sr) for GRS. GOES and HXRBS should thus have a much lower ratio of non-solar to solar events. In addition, X-ray spectra of bursts are much flatter than those of flares, making flares much more detectable by GOES. So *non-detection* by GOES and HXRBS is a strong indication of non-solar origin.

The rates of activity at these two wavelengths for GRS cosmic bursts can be compared to those for known solar flares. First, note that $\sim$ 18% (13/71) of GRS cosmic events occur during spacecraft night and so cannot be of solar origin. Of the remaining bursts, $\sim$ 24% (14/58) are coincident with a HXRBS event (Dennis *et al.* 1983) and $\sim$ 16% (9/58) start during a GOES event. Only 2 of 71 bursts are detected during spacecraft day and are coincident with both HXRBS and GOES events. In contrast, the solar flare data (D. J. Forrest 1985, private communication) show $>$ 85% (109/127) of flares in 1980–1982 were coincident with HXRBS events, and $>$ 99% (126/127) coincident with GOES. This comparison indicates that the

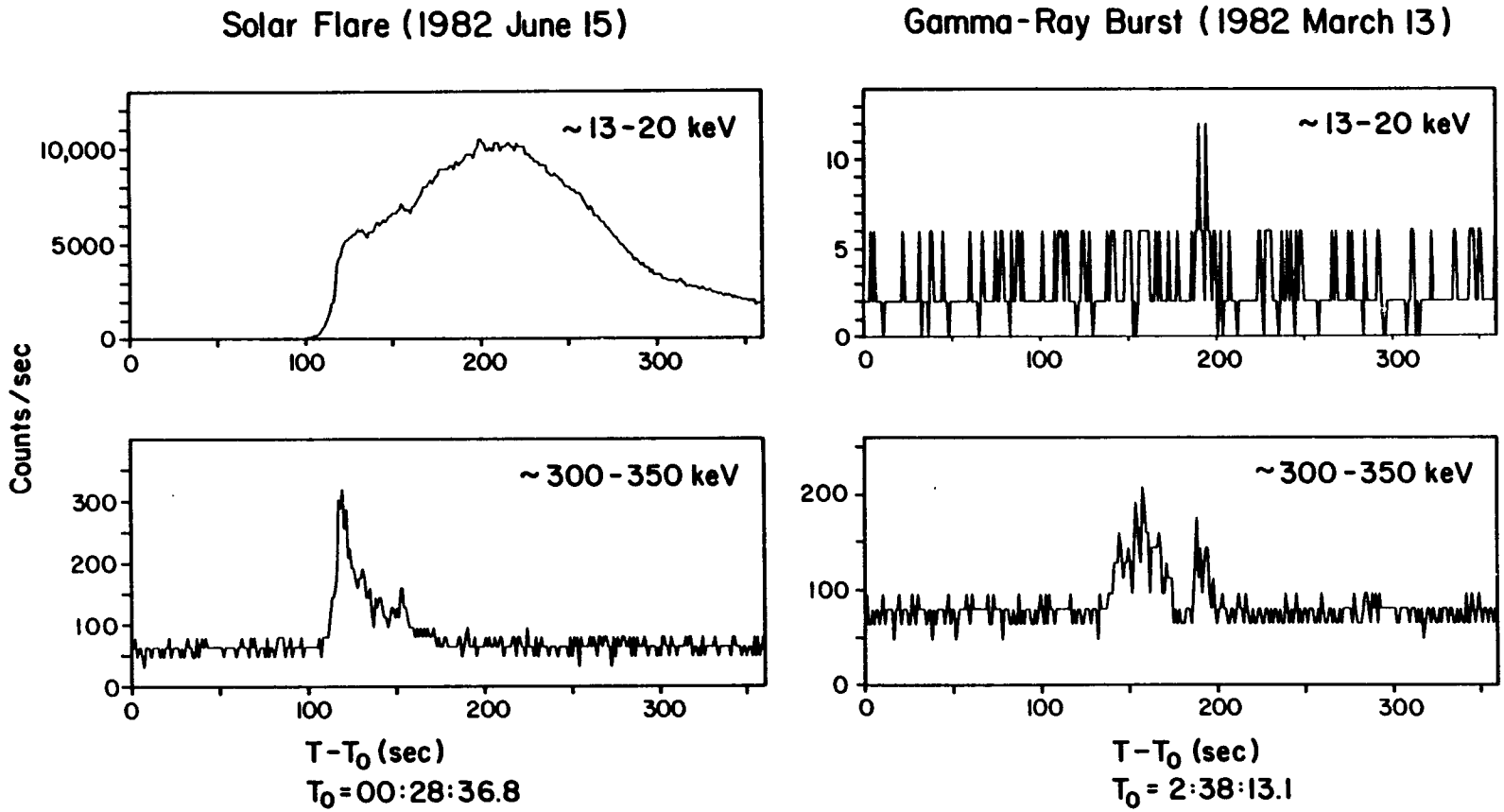

Fig. I-6: The GRS response to a solar flare and a gamma-ray burst in two energy bands, soft (13-20 keV) and hard (~300 keV) X-rays. The strong, extended thermal emission in the low-energy X-rays is a characteristic feature of solar flares.

data sets are indeed distinct, and that only a very small fraction of the events identified as bursts might actually be flares.

Also note that the ratio of cosmic events detected by both HXRBS and GRS to the total number of such events observed by GRS during the time period covered by the published HXRBS event list (Dennis *et al.* 1983) is $\sim 0.20(14/65)$. This is consistent with the ratio predicted based on the relative solid angles viewed by the two instruments (~ 0.17). However, there are other factors which affect this so the good agreement may be only coincidental.

GRS Bursts and the Class of Classical Gamma-Ray Bursts

Because of the unique nature of the GRS and its differences from other burst detectors, a question arises about the relation between the events detected by the GRS and the bursts measured by more standard instruments. This question has two parts: 1) Are the GRS bursts a new phenomenon, or a subset of the category of classical gamma-ray bursts? 2) If GRS events *are* classical bursts, do they represent a biased or unbiased subset of such events?

A priori, GRS events would be expected to be classical gamma-ray bursts, i.e., the same events detected by standard burst instruments. While the spectrometer measures higher energy photons than other experiments, the ranges do overlap. Since GRS event searches are made at the lower end of the measured spectrum, any event observable by GRS has strong emission < 1 MeV and should therefore be detectable by standard instruments. The minimum timescale of the GRS event search (16.384 s) should not cause any problem. This reasoning is verified *a posteriori*: over 70% (50/71) of GRS gamma-ray bursts have in fact been observed by other instruments. During a period of good coverage by the interplanetary network (1981 November to 1983 January), at least 96% (28/29) of GRS events were detected by some other experiment; all 28 are listed as "confirmed cosmic" (K. Hurley 1985, private communication).

To evaluate the bias in this subset, the rate of classical gamma-ray bursts can be compared with the rate of GRS events. The only available independent measurements of the gamma-ray burst rate are based on the integrated fluence (S) above 30 keV (see the discussion of $\log N$-$\log S$ in the Introduction). Detection

by GRS depends on the fluence above 300 keV, so it is necessary to relate the GRS threshold $S(> 300$ keV) to a corresponding fluence above 30 keV. Since the GRS does not trigger on, or ordinarily measure, $S(> 30$ keV), the relation of the detection threshold to $S(> 30$ keV) depends on the spectral shape at low energies. (The same problem exists in all other instruments in varying degrees, since they do not trigger on the total fluence, but on the flux in one particular part of the spectrum.) However, the spectral shape is similar enough from burst to burst that $S(> 300$ keV)$/S(> 30$ keV) is roughly constant (range approximately a factor of 4–5, see Table II-1; see also Barat *et al.* 1982 for a discussion of this problem). One of the weakest GRS events (GB810225) was near enough to the center of the instrument field-of-view to measure with the auxiliary X-ray detectors, giving a spectrum down to about 13 keV. The estimated fluence $S(> 30$ keV) was $\sim 1 \times 10^{-5}$ ergs-cm^{-2}. In addition, there are twelve GRS events for which there are independently measured (albeit unpublished) fluences; all have $S(> 30$ keV) $\geq$ 1×10^{-5} ergs-cm^{-2}. Therefore this value is taken as the estimate of the GRS threshold. This implies (from log$N$-log$S$ results, e.g., Share *et al.* 1982) that approximately 50 bursts per year are intense enough to be detected by GRS.

Since the GRS does not continuously view all parts of the sky, only a fraction of these events will actually be detectable. The satellite altitude is $\sim$ 520 km which means that the earth blocks $\sim$ 3.9 sr, or 31% of the sky. The instrument is turned off during passage through the South Atlantic Anomaly (SAA), and for a portion of spacecraft night the instrument transmits only calibration data. The combination of these factors results in an approximately 50% duty cycle for an isotropic source population. The GRS sensitivity is greatly reduced outside the forward FOV by the side and back shields. This lowers the duty cycle further by a factor between 1 and 2. Thus the actual probability of any single burst above threshold being detectable is between 25% and 50%.

The GRS burst rate is $\sim$ 20 per year; correcting for the duty cycle implies a rate of "GRS-type" events of 40–80 per year. As shown above, GRS events are a subset of the set of classical gamma-ray bursts, and the *total* number of bursts above the instrument threshold is approximately 50 per year. Therefore, the subset of GRS-

type events is roughly as large as the entire set of gamma-ray bursts. There cannot then be any strong bias in the GRS data set. Since GRS bursts are a representative sample of all bursts, the GRS results apply generally to the whole population of gamma-ray bursts.

II. HIGH-ENERGY EMISSION IN GAMMA-RAY BURSTS

Prior to the launch of SMM, most gamma-ray burst experiments had little or no sensitivity above 1 MeV, and so, with a few notable exceptions (Gilman *et al.* 1980, Hueter 1984, Schwartz *et al.* 1985), high-energy emission was not observed. The spectral models developed to fit the observed spectra were generally quite soft, and the extrapolations of the fits predicted very little flux at high energies.

Based on these data, a theoretical consensus emerged that bursts were thermal phenomena from compact sources with very strong magnetic fields. This view provided additional reasons for believing that > 1 MeV emission was unimportant in bursts. In compact sources with high densities of energetic photons, photon-photon pair-production may strongly attenuate photons above ~ 1 MeV (Herterich 1974; Schmidt 1978; Cavallo and Rees 1978; Carrigan and Katz 1984). In strong magnetic fields flux above 1 MeV can be degraded by single-photon pair-production (see Section IV). And because losses make it difficult to produce or maintain either very high temperature plasmas (kT $>$ 511 keV) or the high-energy tails of low-energy thermal plasmas (Gould 1981, 1982a, b), few electrons would have sufficient energy to generate high-energy photons.

In this context observations above 1 MeV become particularly important. As discussed below (Section III), differences in spectral models are most pronounced at high energies, so they are easiest to test and differentiate there. Observations of the effects of the pair-production attenuation processes mentioned above would be intrinsically interesting because they require exotic environments, and have not yet been observed; they may also provide constraints on the bursts source (see Section IV).

The GRS has good sensitivity and spectral resolution at high energies, making it possible, for the first time, to study the high-energy component of a large number of gamma-ray bursts. The first experimental question is whether high-energy photons are emitted from gamma-ray burst sources. Related questions which are

addressed include whether > 1 MeV emission is present in all bursts, or only some subset, and whether there is evidence of a maximum emitted photon energy (or spectral cut-off) or a series of cut-offs. The energetic importance of high-energy emission is estimated by calculating the fraction of total observed burst energy in > 1 MeV photons. Use of the high-energy observations to test spectral models and place constraints on physical parameters at the burst site are covered in detail in Sections III and IV.

The conclusions of this section may be summarized as follows: 1) high-energy emission is a common feature of gamma-ray bursts, consistent with emission to at least 5 MeV in all bursts with no cut-offs; and 2) high-energy emission is (on the average) an energetically significant part of the total burst radiation, more than predicted by thermal models.

PRESENCE OF HIGH-ENERGY EMISSION IN BURSTS

The question of the presence of high-energy emission has two components: 1) Is the spectral shape above 1 MeV generally soft or hard? and 2) Do the spectra cut off at high energies? Burst spectra were characterized by models with exponential (or faster) declines in flux at high energies (e.g., optically-thin thermal bremsstrahlung) and were thought to be so soft that above 1 MeV emission would be undetectable and of negligible energetic importance. Secondly, even if the spectra were hard, there might be cut-offs of the emission in the MeV range. There are a number of physical processes which are expected to be important in burst sources which could cause spectral cut-offs. (A specific example is discussed in Section IV.)

A large number of GRS gamma-ray bursts have significant detected fluences at high energies. An examination of the observed burst spectra shows no obvious cut-off in any event. Finally, the number of events observed at high energies is consistent with all events emitting to high energies with a relatively hard spectrum and no cut-offs.

Data

High-energy emission is clearly a feature of the gamma-ray bursts observed by GRS. For example, Figures II-1 (GB800419) and II-2 (GB821104) are time histories

of two events which have a detectable photon flux up to at least several MeV. Note that these events span a wide timescale range: the first is very short ($\sim$ 2 s long), the second very long ($>$ 60 s). Both show emission from X-rays to at least several MeV gamma-rays ($>$ 2 decades in energy), indicating that $>$ 1 MeV emission is not limited to a specific class of burst. Nolan *et al.* (1984b) also show examples of burst emission to high energies using GRS data. Further, there is no obvious evidence of a limit on emitted photon energy, since no sharp cut-off is seen in *any* GRS event spectrum. However, a more quantitative test is needed to determine the presence and characteristics of high-energy emission in general, over the whole class of gamma-ray bursts.

As a test for the presence of high-energy emission in gamma-ray bursts the maximum detectable photon energy has been determined for each event. This is defined as the highest energy such that the total source counts above that energy are 3σ or more above the measured background. Note that this is not a definitive standard, since another criterion (differential instead of integral, for example) may yield a different result. In addition, subsets of the total burst accumulations in many cases have a higher maximum observed energy because of better signal/noise in shorter integrations. Finally, this information is based only on the GRS main-channel data and is subject to the sensitivity limitations of that instrument; another detector, for example the GRS high-energy matrix (which measures flux $>$ 10 MeV), may indicate a higher maximum energy. Thus the measured maximum energy presented here is a *lower limit* on the actual maximum emitted photon energy.

The number of events with significant emission at or above each energy (at 1 MeV intervals) is shown by the solid line in Figure II-5. It is clear that emission above 1 MeV is a common feature of gamma-ray bursts: over 60% (43/71) of all events have significant emission above 1 MeV, $\sim$ 41% (29/71) above 2 MeV, $\sim$ 25% (18/71) above 4 MeV, and 7% (5/71) above 7 MeV. While the number of events observed declines with energy, a fall-off of detectable events at higher energies is expected simply because of the declining instrument sensitivity to a falling photon spectrum. The question is whether the number of observed events requires any *additional* assumption of cut-offs or spectral softening. A quantitative

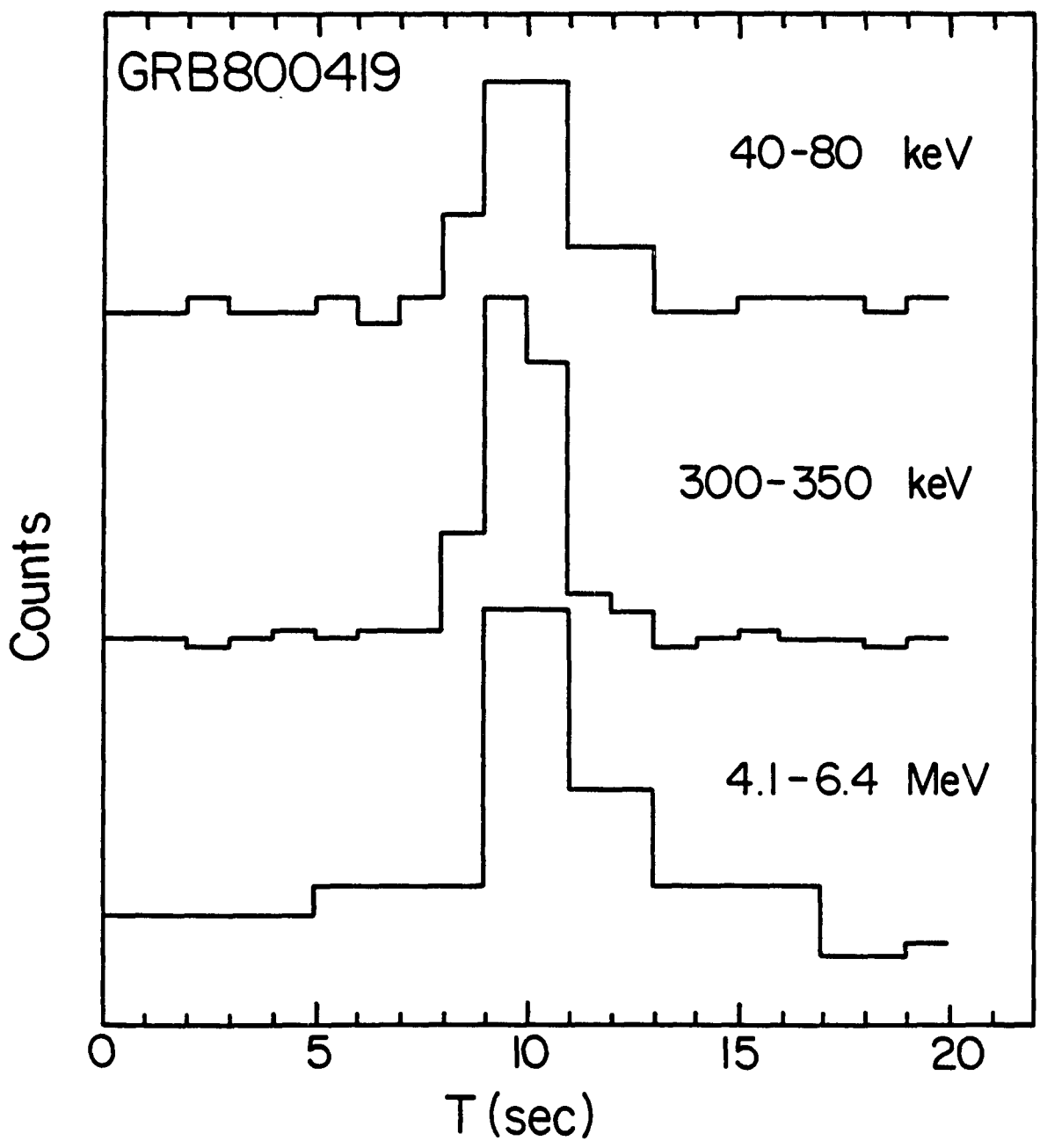

Fig. II-1: Time history of GB800419 in three energy bands, covering more than 2 decades in energy.

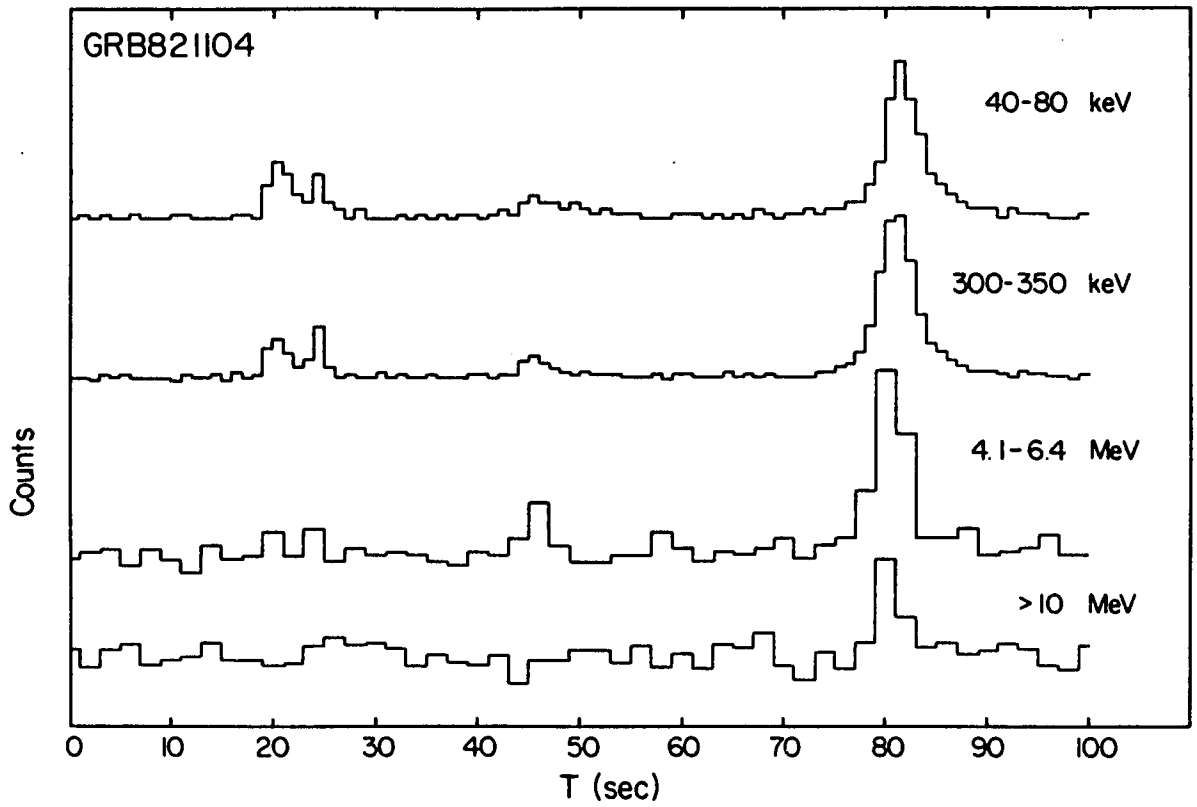

Fig. II-2: Time history of GB821104 in four bands, from 40 keV to > 10 MeV. Note the similarity of the event profile at different energies.

evaluation of this requires a comparison of the data with expectations based on the known instrument response.

Instrument Sensitivity and Detectability

It is probably worthwhile considering in some detail the factors which contribute to the energy-dependent detectability. Note that the detectability is not the relative instrumental sensitivity to the *same* photon flux in different energy bands, but the sensitivity to the flux from one event (with a certain spectral shape), at different energies. The declining detectability is not solely instrumental, but depends on the photon spectral shape. Three components affect the detectability of an event at different energies: 1) the instrument response to incident photons (Appendix A); 2) the background intensity, which sets the noise level, and falls at high energies; and 3) the incident photon spectrum, which generally declines with energy.

The significance of the source flux in a particular energy band is proportional to the counts produced in the instrument by that flux, in that energy range. The interaction of a photon in a scintillation detector can produce a count at the photon energy or below (see Appendix A); conversely, the counts in any energy band are a combination of counts produced by photons in that energy range and photons of higher energies. For this reason the sensitivity depends not only on the instrument characteristics (e.g., the effective area) and the flux, but also on the spectral shape. Secondly, the detectability is inversely proportional to the statistical noise, which is roughly the square root of the measured background in the relevant energy band. Figure II-3 shows the relative energy dependence of these two components (signal and noise), assuming an average source spectrum ($E^{-2.4}$) and average background. It is important to compare the slopes; the actual point at which the spectrum drops into the noise depends on the relative intensities of the source and background spectra. For a source spectrum softer than $\sim E^{-1.5}$, sensitivity falls with energy above 1 MeV. This is only an approximation since the noise spectrum has features and actually increases (decreasing sensitivity) in some energy bands.

Dividing the instrument response by the square root of the background gives the relative significance of the source flux with respect to the background, and shows how the statistical significance declines with energy (Figure II-4).

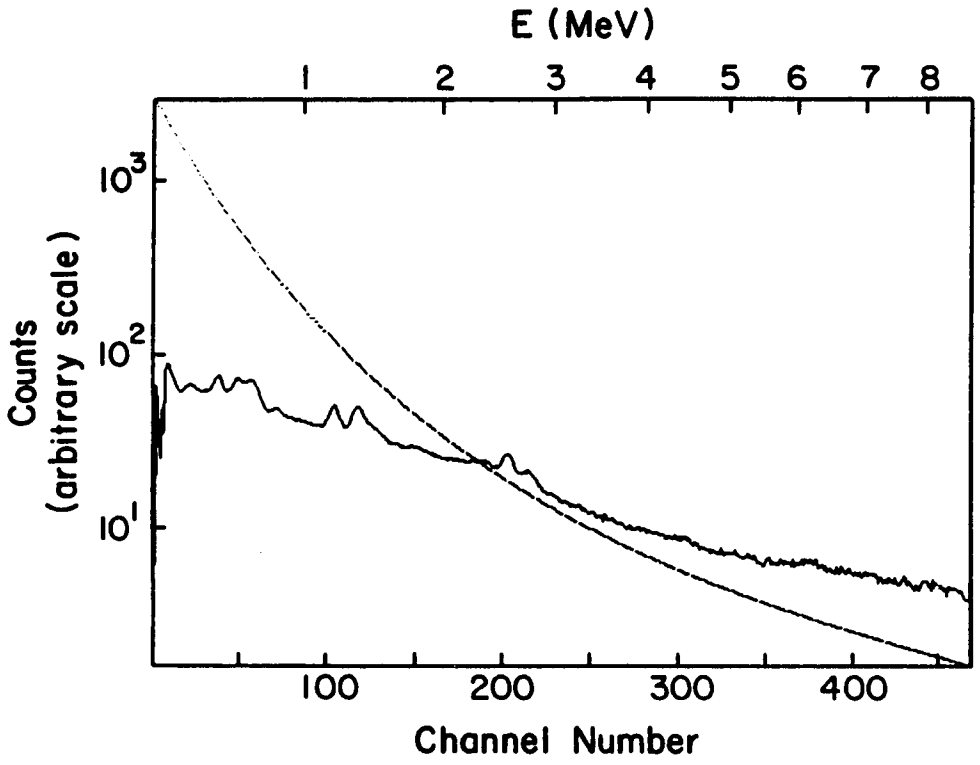

Fig. II-3: A comparison of the predicted instrument response to an $E^{-2.4}$ photon spectrum and the average noise level, defined as the square-root of the average background. The intensity of the power-law spectrum relative to the noise level is arbitrary. Instrument channels 1–470 are shown.

Analysis

To determine how the observed decline (with energy) of detectable events compares with what would be expected from the falling instrument sensitivity, the highest detectable energy *expected* and *observed* can be compared for each event. There is a measured background for each event, and the instrument response is known. In addition, however, some spectral model must be assumed, since instrument sensitivity depends on the spectral shape. A power-law model has been chosen since it is the hardest commonly-used spectral shape, and thus provides a conservative test. The test is made by fitting *each* spectrum below 1 MeV; the resulting power-law is then extrapolated to higher energies and the expected counts from that spectrum are compared to the observed background for that event. The *predicted* E_{max} is then determined by the same test as the *observed* E_{max}; that is,

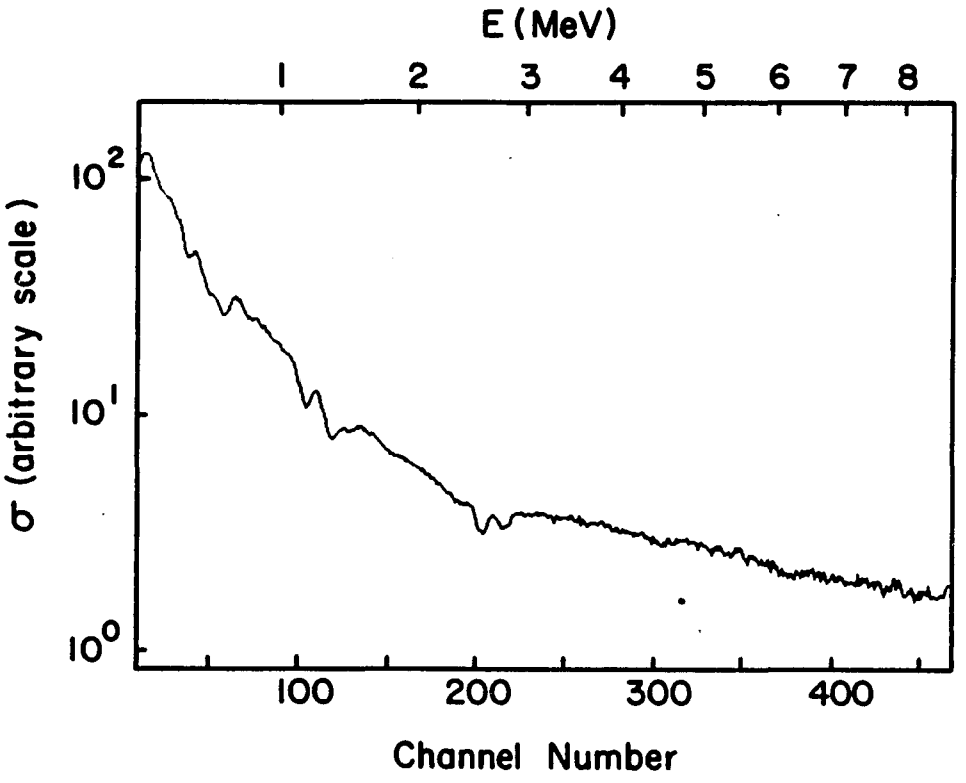

Fig. II-4: The energy dependence of the relative significance of the flux of an $E^{-2.4}$ photon spectrum. The significance (σ) is defined as the predicted instrument counts from the power law, divided by the square-root of the background. Instrument channels 10–470 are shown.

it is the highest energy for which the sum of the predicted counts above that energy are greater than 3σ above the background. The predicted maximum energies for all bursts were then compared to the actual observations. The results are displayed along with the data in Figure II-5. Figure II-6 shows the same comparison, with the data set restricted to those events which are thought to be in the forward field-of-view (FOV) of the instrument. This is done because for events outside the FOV the standard response function (used to fit and extrapolate the spectrum) is not a correct model of the instrument. Events are considered to be in the FOV if the source is well within the forward aperture based on timing by the GRS and other spacecraft (P. L. Nolan 1984, private communication), or if the GRS event is coincident with a HXRBS event (Dennis *et al.* 1983). HXRBS has a much smaller FOV than GRS ($\sim 40°$ *vs.* 100° FWHM) so that events detectable by HXRBS are

probably in the GRS forward aperture. No claim is made that these are *all* of the events in the GRS FOV, since the data available from other experiments are not complete. The FOV events are indicated on the burst list (Appendix B).

If the data were precisely described by the power-law model (without statistical variations or cut-offs), the predicted and observed E_{max} would agree in each case. With statistical fluctuations the total number of events observed and predicted should agree within error, unless the spectra soften (compared to the power-law model) or cut off (see below).

In fact, in both the complete and the partial data set the agreement between the prediction and the model is good. The largest discrepancy appears to be above 6 MeV in the total data set (Figure II-5). The statistical significance of this deficit can be calculated: seven events are observed and 17 predicted. The probability that 7 or fewer events would be observed as a fluctuation on a parent distribution with a mean of 17 is $\sim 3.5 \times 10^{-3}$, corresponding to a significance of $\sim 3.1\sigma$.

This difference is not necessarily an indication that some events do not have high-energy emission. There are other effects which can produce a deficit: 1) In making this test all burst spectra were assumed to be power laws. This is clearly not true in all cases (see Section III); some burst spectra have a distinct curvature *without* having an observable cut-off. Figure III-8 shows one example of such an event. 2) Spectra of events outside of the forward aperture will be more strongly attenuated at low energies than at high energies, making the spectra artificially harder below 1 MeV; thus the projected model spectrum will be harder than the data. When the data set for this test is limited to events which are thought to be within the field-of-view the deficit above 6 MeV is essentially eliminated. Figure II-6 shows this comparison. Since these effects are sufficient to explain the drop-off of detectable events above 6 MeV, there is no need to propose additional cut-offs. Thus the data are consistent with all events emitting to the highest energies (i.e., up to $\sim$ 9 MeV).

A comparison of the predicted and observed E_{max} can also be made on an event-by-event basis. It is possible that an examination of individual cases would show that the power-law model was not a good predictor of the maximum observable

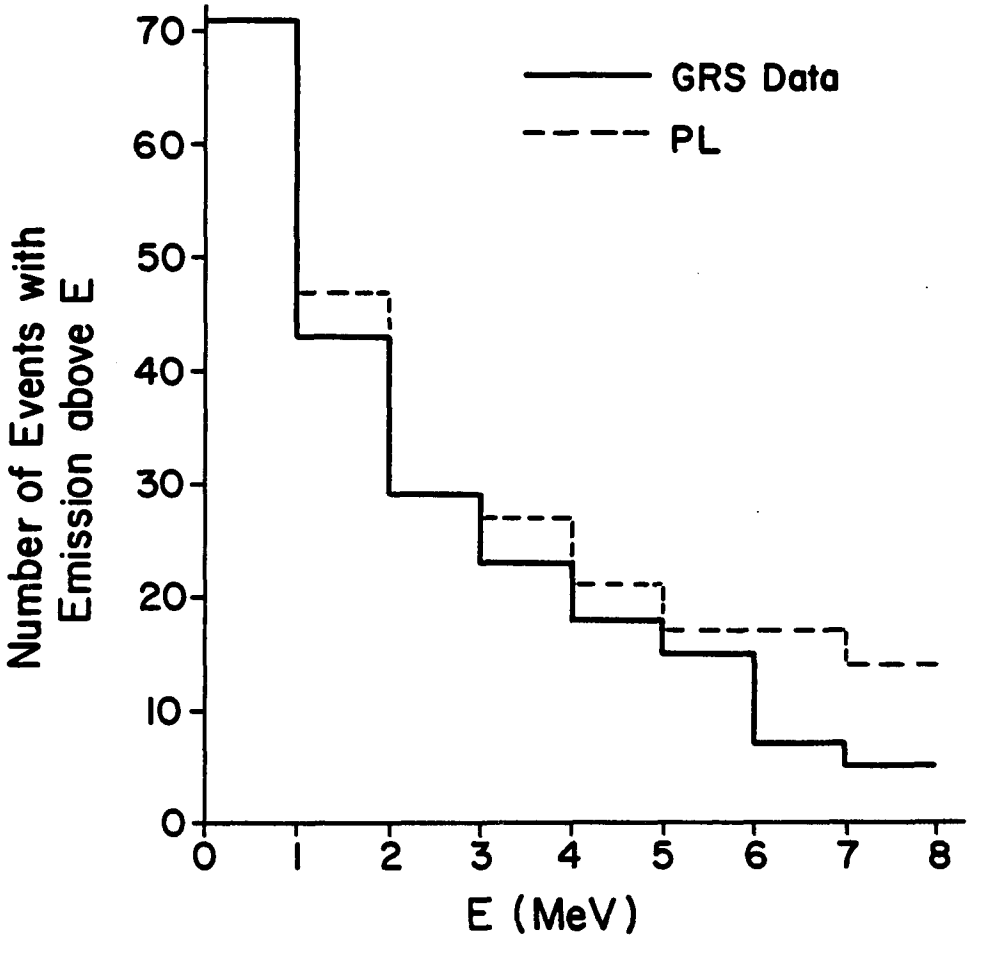

Fig. II-5: The number of events with significant flux above photon energy E *vs.* E, for all gamma-ray bursts. Also shown is the *predicted* number of observable events, assuming a power-law extrapolation of the low-energy (< 1 MeV) spectrum.

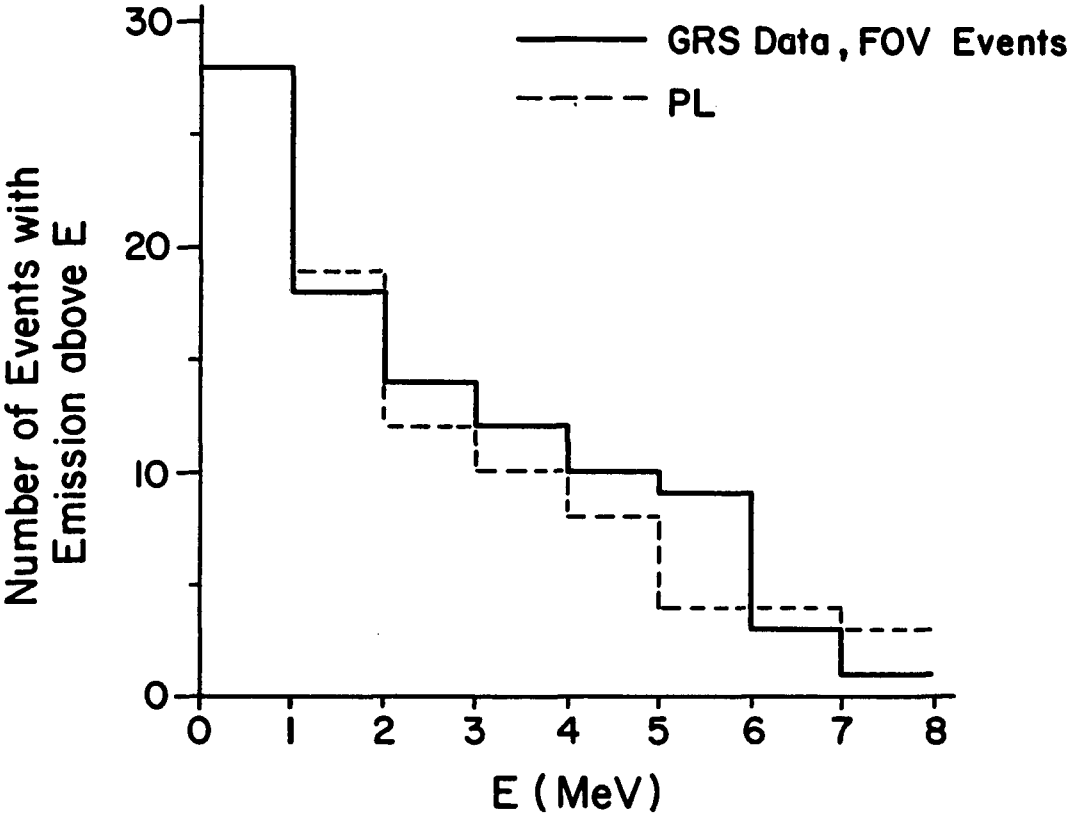

Fig. II-6: The same data as Figure II-5, but for only those events thought to be in the GRS forward field-of-view.

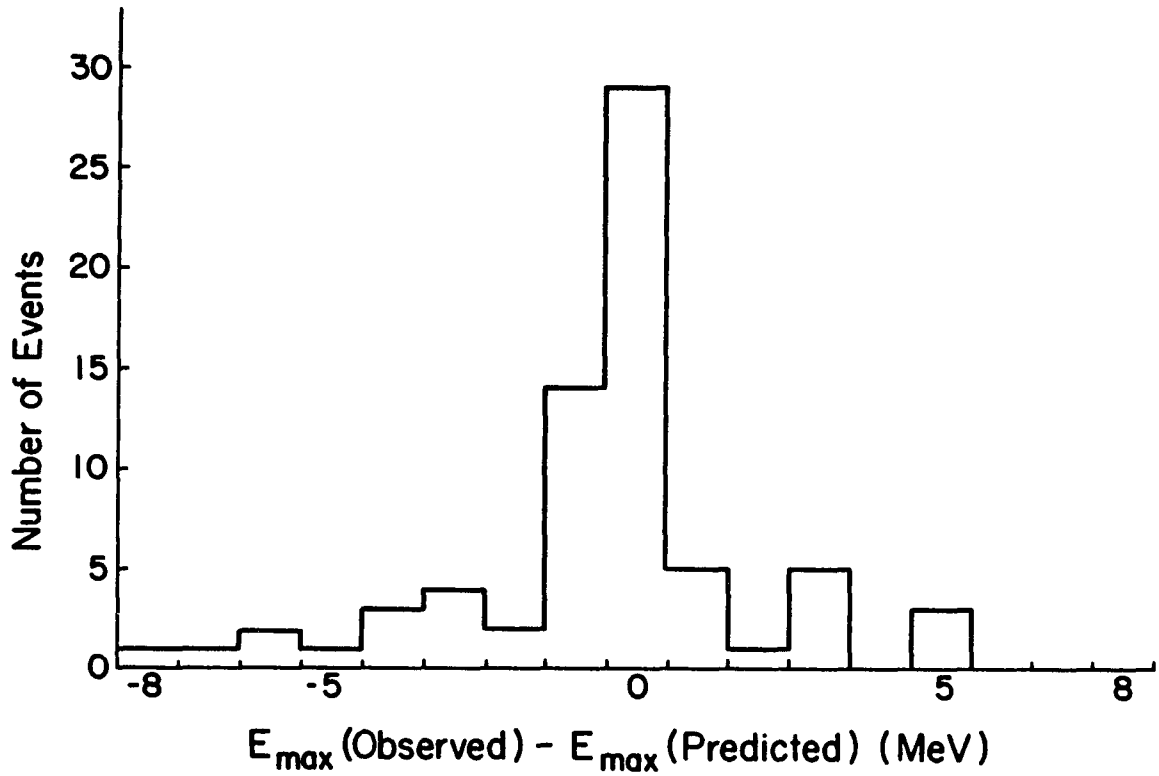

Fig. II-7: The difference ΔE between the observed and predicted E_{max} for each event, plotted as a histogram of the number of events at each value of ΔE *vs.* ΔE.

energies in specific bursts. Figure II-7 shows a histogram of the difference between observed and predicted energies for each event. The average difference is -0.52 ± 0.29, which is consistent with 0. Note that the prediction depends only on counts below 1 MeV; the agreement is actually remarkably good.

This technique can be used as a test of burst spectral models. Such a test is made for three spectral models in Section III.

Discussion and Conclusions

Spectral cut-offs. The physical reasons for expecting spectral cut-offs have been mentioned above; generally a cut-off may occur at a change of regime (e.g., from below to above kT in thermal spectra) or at the threshold of some attenuation process. Experimentally, however, spectral cut-offs may be difficult to detect. All spectra have an experimental high-energy cut-off equal to the maximum observed photon energy. This may well be the result of experimental limitations; indeed, the

maximum observed photon energy may be the upper end of the detector range. A directly observable cut-off would require a sharp softening or ending of the photon spectrum at a point where the flux would otherwise still be far above background. An examination of the GRS burst spectra shows *no* event with an obvious, sharp cut-off. Absent such a clear feature, the definition of a cut-off will be model dependent, based on the observed spectrum falling below an extrapolation using a specific model. Equivalently, the highest energy observed will fall below that predicted by the model. *If* the spectral model is physically correct, and *if* the data fall significantly below the extrapolated model spectrum, then there is a true (physically meaningful) cut-off. On the other hand, if the model is harder than the actual emission spectrum, then the data may fall below the extrapolation and indicate a cut-off where none is actually present.

The test made above can be interpreted as a test for cut-offs in the set of GRS bursts. If there was a general cut-off, a series of cut-offs, or even a general softening of the spectrum above 1 MeV, the data would fall below the predictions. In fact, however, the data and predictions are consistent, at least out to about 6 MeV. Again, the fall-off in the number of events observed at high energies is consistent with that expected based on the falling instrument sensitivity *alone*.

While there is a significant disagreement between the data and the model above 6 MeV, there are other factors which can cause this deficit. No additional assumption of spectral cut-offs is required.

Conclusions. The GRS has detected high-energy emission in a large fraction of the observed gamma-ray bursts. In no case is a sharp cut-off observed in a measured spectrum. A comparison of the maximum observed energies of events with those expected from a power-law extrapolation indicates that, overall, the spectra do not appreciably soften or cut off below 6 MeV. This does not, however, rule out the possibility that some individual spectra may cut off. For the complete data set there is, above 6 MeV, roughly a 3σ deficit below the number of events predicted by the power-law extrapolation. This would be evidence for cut-offs only if all event spectra were single power laws from sources in the field-of-view. Since these assumptions are not consistent with the data, such a conclusion cannot be drawn.

For events thought to be in the FOV, the data and model are in good agreement to the highest energies.

The data and the arguments above indicate E_{max} is an experimental artifact, not related to the physics of the burst. While the data are consistent with all bursts emitting to the highest energies ($\sim$ 9 MeV), this does *not* prove that all events emit to high energies. However, there is no strong evidence to the contrary either statistically or in individual events. Further, these results do *not* imply that all gamma-ray bursts have power-law spectra. The implications of the high-energy observations for spectral shape are discussed in Section III.

ENERGETIC IMPORTANCE OF > 1 MEV EMISSION

It has been shown that > 1 MeV emission is a common feature of gamma-ray bursts. To what extent is this emission a physically important part of the burst phenemenon—what fraction of the burst energy is in high-energy photons? This is related to important physical questions, including the nature of the acceleration/heating process and the optical depth, as well as to the question of spectral shape discussed in Section III. The analysis presented below indicates that the high-energy flux is an energetically important part of the complete burst. In particular, on the average over half of the total observed energy is in photons above 300 keV, $\sim$ 30% in photons above 1 MeV.

Fraction of Total Burst Energy in > 1 MeV Photons

To determine the energetic importance of the high-energy emission, the ratio $S(>1\ \text{MeV})/S(>30\ \text{keV})$ has been calculated, based on estimates of $S(>30\ \text{keV})$ from the GRS X-ray detectors. $S(>30\ \text{keV})$ is a commonly used measure of total burst fluence. Although the lower limit of 30 keV is an experimental one, not necessarily related to a physical limit, this is still the only commonly used measure of the total burst energy.

To find the total energy S from the GRS main-channel data the best-fit power law was found over the entire energy range (0.3–9 MeV). Then the energy in each channel (S_n) was determined by

$$S_n = (F_n/C_n)D_nE_n,$$

where F_n is the photon fluence in channel n (photons-cm^{-2}- channel^{-1}) implied by the fit, C_n is the predicted instrument response to that spectrum (counts-channel^{-1}), D_n is the actual observed counts in channel n, and E_n is the average energy of channel n. The S_n are then summed to get the total S for the spectrum. Note that in these calculations a maximum energy of 9 MeV was assumed. Extrapolating the spectra to higher energies would increase both the total fluence and the fraction of the emission at high energies.

Again, as in the case of sensitivity, the determination of energy content depends to some extent on the assumed spectral shape. In a harder spectrum a larger fraction of the counts observed at any energy will have been produced by photons *above* that energy, implying a higher total energy for the spectrum. In practice, for this instrument, the effect is relatively small. For example, for 45 GRS events with $S(> 300 \text{ keV}) > 8 \times 10^{-6}$ ergs-cm^{-2}, the values of $S(> 300 \text{ keV})$ derived assuming a thermal synchrotron model average $\sim$ 7% higher than those found assuming a power-law spectrum. Thermal bremsstrahlung gives values an average of $\sim$ 13% larger than the power-law model. This effect is negligible in the events analyzed below.

The GRS X-ray detector data (covering ~13 keV to 190 keV, and integrated over the same time as the main-channel spectrum) were used to estimate $S(>$ 30 keV). Because the X-ray detectors have a narrower FOV than the main detector, consideration was limited to events near the center of the main detector FOV. This was done by including only those events which were also detected by HXRBS. Recall that HXRBS has a smaller FOV than the GRS; however, the GRS X-ray detectors have a FOV that is smaller than HXRBS and asymmetric. In addition, the off-axis response of the X-ray detectors has not been measured. Therefore, there are possible systematic errors in the unfolding of the low-energy data. From 30 to 300 keV the estimate of the burst spectrum is based on the X-ray data and an extrapolation of the main-channel data. A comparison of GRS estimates of S(30–300 keV) with estimates from fits to HXRBS data (Norris 1983) for several events shows the GRS values to be systematically higher, but probably within the range of acceptable S implied by the errors on the fitted parameters given by Norris. If the

GRS measurements of $S(30-300$ keV) *are* systematically high, the actual fraction of the total burst energy in high-energy photons is correspondingly *higher* than that quoted below.

In addition to requiring HXRBS coincidence, only those events large enough to be well-measured by the GRS (roughly $S(>300$ keV$) > 8 \times 10^{-6}$ ergs-cm^{-2}) have been included. Eleven events are left for which $S(>30$ keV) can be compared with the energy content at higher energies.

The results of these calculations are presented in Table II-1. On the average, for these events, over 50% of the total observed energy is in photons with $E > 300$ keV, almost 30% above 1 MeV, and almost 20% above 2 MeV.

TABLE II-1

DATE	TIME	S(> 30 KEV) (MEV)	S(> 300 KEV) / S(> 30 KEV)	S(> 1 MEV) / S(> 30 KEV)	S(> 2 MEV) / S(> 30 KEV)
80/03/07	05:08	32	0.50	0.17	0.09
80/04/19	01:20	40	0.62	0.32	0.20
80/08/15	18:21	27	0.72	0.37	0.26
80/11/19	17:06	18	0.57	0.26	0.17
81/03/01	12:35	13	0.78	0.54	0.38
81/10/16	23:53	220	0.34	0.07	0.03
82/01/25	17:56	12	0.87	0.70	0.52
82/03/01	02:36	160	0.16	0.01	–0.01
82/05/30	09:49	20	0.51	0.23	0.10
82/11/04	03:30	180	0.61	0.34	0.22
83/02/10	12:20	39	0.33	0.08	0.03
		AVERAGE:	0.55±0.06	0.28±0.06	0.18±0.05

As a further test, the same fractions have been calculated for seven other GRS events using the unpublished measurements of $S(>30$ keV) which are available from different experiments. These results are combined with the values of $S(>$ 1 MeV) from the GRS data. It is found that, for these bursts, the average of

$S(> 1\ \mathrm{MeV})/S(> 30\ \mathrm{keV})$ is 0.23, consistent with the number derived from GRS data alone.

Conclusions

High-energy emission can be, and generally is, an energetically important part of bursts. It is not just a minor "tail" added on to the main phenomenon taking place at low energies.

If high-energy emission is a separate component (e.g., broadened, blue-shifted 0.511 MeV line, or a continuum of nuclear lines), that component requires a large part of the total observed burst energy (30–50%, depending on where the boundary between the two components is). The total amount of energy in that component obviously depends on the relative efficiencies of the low- and high-energy production and loss mechanisms, including the probability of escape for photons. Note that most opacities (e.g., Compton scattering, assuming plasma temperature is low) will enhance the low-energy emission with respect to the high-energy emission. Thus the observed ratios are probably lower limits on the production ratios. These observations may seriously constrain some two-component models.

In addition, as Katz (1982) and Epstein (1985a) have pointed out, models which produce radiation at high optical depths (thermonuclear, accretion) would be expected to have quite soft spectra, like X-ray bursts: an approximately blackbody spectrum with most of the observed energy in the soft X-rays ($\sim$ 1 keV). This seemed to be in serious disagreement with the data before; the GRS observations make the conflict much worse.

III. HIGH-ENERGY EMISSION AND SPECTRAL MODELS

A complete burst theory would describe the source of the burst energy, the mechanism by which this energy is coupled to charged particles (heating or acceleration), and the process by which the resulting energetic particles radiate, producing the observed photon spectrum. There is at present no such theory; however, the different parts can to some extent be addressed separately. For example, several different theories for the energy source have been advanced, including thermonuclear explosions and sudden mass accretion. Working backward from the spectra (which provide coupled information on the energetic particle distribution and the radiation mechanism), several spectral models have been proposed to explain the observations.

There are two physical questions involved in such a model: 1) What is the dominant radiation mechanism? This is largely determined by the values at the radiation site of a small number of parameters, notably the magnetic field strength, the electron density, and the temperature. 2) What is the energetic particle spectrum? This is the result of the interaction of the initial source of energy with the ambient medium, including all acceleration and loss mechanisms. Almost all calculations have assumed a thermal distribution, partially for physical reasons but mostly for convenience. The model must first be shown to fit the data adequately; then, under the assumption that the model is correct, deductions can be made about the conditions at the burst site.

This section begins with a description of the standard burst spectral models which have been used to fit and interpret the observations. Included are discussions of some of the relevant physics (i.e., the implications of, and the problems with, each model), and the experimental evidence, pre-GRS. Three of these models are then tested against the GRS data. Particular attention is paid to tests at high energies, since it is only above 1 MeV that the differences between the models become pronounced.

REVIEW OF SPECTRAL MODELS OF GAMMA-RAY BURSTS

A number of simple spectral models have been used to fit burst spectra. They are connected to the physics of the sources, and have physical implications, but they are probably too simple to be realistic. On the other hand, the data are generally not good enough to support an increase in complexity. For example, burst spectra have been measured which vary on timescales as short as any burst instrument spectral accumulation time (Golenetskii *et al.* 1983). But the introduction of time-evolution (e.g., multi-temperature instead of single-temperature fits) allows for an almost infinite increase in free parameters and a corresponding decrease in information. A specific theory (for example, a functional relation between temperature and intensity), with better constraints, would be needed to make a realistic test.

Historically, the first spectral models used to fit data were phenomenological, i.e., they were used to describe rather than explain the data. They were not explicitly based on physics or a physical model. The first functional form fit to burst spectra was a simple exponential; this was later modified, in some cases, by the addition of a power-law tail. A "universal" spectrum was proposed based on IMP-7 data (Cline and Desai 1975; Cline 1975). It consisted of a 150 keV exponential below 400 keV and a tangent $E^{-2.5}$ power law above that energy. Alternatively, it could be represented as a combination of a $\sim E^{-1}$ power law below 100 keV and a $\sim E^{-2.5}$ above a few hundred keV. This model was able to fit all the spectra available at that time. It is still a relatively good description of the data, on average, but it has no explicit physical content.

The first widely-applied spectral model based on a specific radiation mechanism and particle distribution was optically-thin thermal bremsstrahlung (OTTB), having the form

$$dN/dE = A < g > E^{-1} \exp(-E/kT) \text{ (photons} - \text{cm}^{-2} - \text{MeV}^{-1})$$

The temperature-averaged Gaunt factor $< g >$ is a quantum mechanical correction of order unity in the energy and temperature range of interest (Tucker 1975). Some applications of this model have included this factor (e.g., Gilman *et al.* 1980); others have not (e.g., Mazets and Golenetskii 1981; Mazets *et al.* 1983).

OTTB was used to fit the spectrum of the 1972 April 27 burst measured by detectors on the Apollo 16 spacecraft (Gilman *et al.* 1980). In this case single-temperature OTTB, with $kT \approx 500$ keV, fit the spectrum well from 2 keV up to 2 MeV. There was, however, a significant excess fluence above the model at higher energies. OTTB became the standard description of burst spectra, chiefly because it was found to fit (without the Gaunt factor) most of the 150 burst spectra detected by the KONUS instruments on Venera 11 and 12 (Mazets and Golenetskii 1981). It also had an attractively simple physical interpretation as the radiation from free-free interactions in a very hot, single-temperature plasma.

This simple functional form was able to correctly describe a large number of gamma-ray burst spectra from ~ 30 keV to ~ 1 MeV, though lines and absorption were invoked to explain some deviations, notably significant deficits at low energies. However, there were physical difficulties with the thermal bremsstrahlung interpretation of burst spectra, first noted by Helfand and Long (1979) in connection with the 1979 March 5 event and later discussed by Fenimore *et al.* (1982b), Katz (1982), Lamb (1982), and Liang (1982), among others. The luminosity of a source emitting by thermal bremsstrahlung is given by (assuming a plasma with cosmic abundances):

$$L_{TB} = 1.85 \times 10^{-22} {n_e}^2 T^{1/2} V \text{ ergs} - \text{s}^{-1}$$

(cf. Tucker 1975, eq. 5-64′), where n_e is the electron density (in cm^{-3}), T the temperature in units of $m_e c^2$, and V the volume of the emitting material (in cm^3). For isotropic emission the observed fluence S (ergs-cm^{-2}) is related to the source luminosity by $L = 4\pi D^2 S$, where D is the distance to the source. As Fenimore *et al.* (1982b) point out, if the sources are spherical and optically-thin to electron scattering ($\tau_{es} = n_e \sigma_c r < 1$), they must be quite close (within about a hundred parsecs), even assuming a rather large source (3×10^9 cm). If the emitting material is confined near the surface of a neutron star the radius would be on the order of 10^6 cm. In that case the sources would have to be only a few (< 5) parsecs away, which is inconsistent with the idea that the sources are neutron stars. Alternatively, for different source geometries the sources may be far away, but this requires a very thin emission region (aspect ratio greater than $1 : 10^4$). Finally, it was difficult to

fit the occasionally observed hard spectra with OTTB, requiring either physically unrealistic temperatures or the assumption of a second, harder component.

An alternative radiation mechanism which seemed to solve many of the problems of the bremsstrahlung model was thermal synchrotron (TS) emission, first proposed for the 1979 March 5 burst by Ramaty, Lingenfelter, and Bussard (1981), and further discussed by many others, including Lamb (1982), Katz (1982), and Liang (1982). Since cyclotron lines were thought to indicate the presence of very strong magnetic fields ($> 10^{12}$ G) in burst sources (see Section IV), and synchrotron radiation is much more efficient than bremsstrahlung in strong fields, it was a natural possibility for the radiation mechanism of all bursts. Indeed, the efficiency of synchrotron radiation is high enough to mitigate some of the problems of total burst energy.

The luminosity of a thermal source of temperature kT radiating by synchrotron emission in a magnetic field B is given by:

$$L_{TS} = 2.7 \times 10^9 n_e (B/10^{12}\ \mathrm{G})^2 F(T) T^2 V\ \mathrm{ergs - s^{-1}}$$

(Liang 1982, eq. 2), with T again in units of $m_e c^2$; $F(T) \approx T^{-1}$ for $T \ll 1$ and $F(T) = T^2/K_2(1/T)$ for $T \geq 1$. The luminosities of OTTB and TS as functions of n_e and the strength of the magnetic field B, assuming $T = 300$ keV, are compared in Figure III-1. The line indicates the conditions under which the luminosities are equal: above the line, bremsstrahlung dominates; below it, synchrotron. In particular, at the high field strengths thought to be present at burst sites, TS is much more efficient than OTTB.

In order to determine whether this model could accurately (at least as accurately as OTTB) describe the observed burst spectra, Liang (1983) and Liang, Jernigan, and Rodrigues (1983) tested it against 150 published KONUS photon spectra (Mazets *et al.* 1981a, b, c).The form used in fitting the KONUS data was the approximate result (adapted from Petrosian 1981, eq. 26),

$$dN/dE = A \exp(-(4.5E/E_{crit})^{1/3})$$

where $E_{crit} = E_B T^2 \sin\theta$, with E_B the Larmor energy, T the temperature in units of $m_e c^2$, and θ the angle of observation with respect to the magnetic field direction.

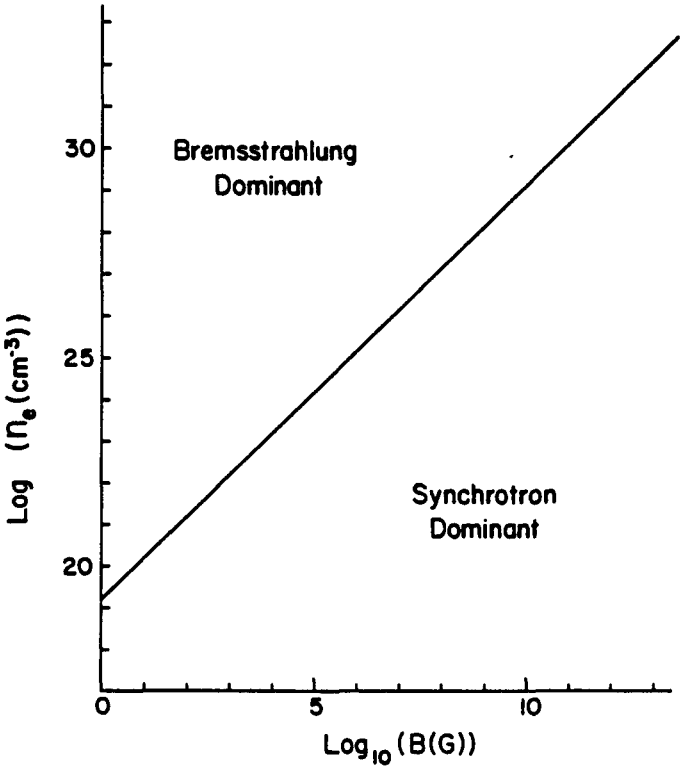

Fig. III-1: Radiation regimes, assuming a thermal plasma with kT = 300 keV, based on the approximate luminosities given in the text. After a plot by Epstein (1985a).

This approximation was derived by Petrosian assuming $T \leq 1$ and $E \gg E_B/T$. Unfortunately (but unavoidably), these fits were made to unfolded photon spectra; this is incorrect, since the derived photon spectrum depends upon the assumed spectral model. The best fit was determined by eye (not χ^2); again, this could not be avoided since χ^2 could not be calculated properly based on the published data. Since no statistical test of goodness-of-fit was made, no quantitative measure of the acceptability of the model was available; however, the authors contend that "over 80% of the fits should be considered satisfactory" (Liang, Jernigan, and Rodrigues 1983). This made it roughly as good a candidate as OTTB for the universal burst spectral shape on descriptive grounds, and it seemed to be preferable on physical grounds.

This model had the further advantage that the derived parameters produced a

fairly consistent physical picture of the burst source (Liang 1983; Liang, Jernigan, and Rodrigues 1983). Other advantages of TS over OTTB included the fact that it produced a somewhat harder spectrum, and required lower temperatures to fit the data.

As Imamura, Epstein, and Petrosian (1985) point out, the approximate TS spectral shape given above is good only for cases where E_{ph} (the energy of the radiated photon) is significantly less than the average electron energy, since the derivation of that formula did not include energy conservation. This means that spectra are significantly softer at high energies. Hard spectra (at least in some cases) can still be fit by TS. Imamura, Epstein, and Petrosian provide one example of a fit using the revised calculations, the spectrum of GRB820125 from GRS data. A satisfactory fit can be made in this case, but it requires a very high temperature (> 2 MeV). This vitiates one of the advantages of TS model, i.e., that it needed much lower temperatures to fit hard spectra. In addition, it should be noted that GRB820125 is an atypical GRS spectrum since it shows clear curvature (see analysis below).

In addition, like OTTB, there are physical difficulties with the TS model. These are discussed by Lamb (1982), Liang (1984), and Fenimore, Klebesadel, and Laros (1984), among others. The cooling times in such high fields are very fast ($\sim 10^{-16}$ s), requiring continuous, rapid acceleration throughout the burst and thermalization on a timescale much shorter than can be accomplished by collisions. In addition, the TS model does not solve the problem of thin emission layers. Liang (1983) derives emission layer thicknesses of 2×10^{-5} and 5×10^{-5} cm for two bursts, based on parameters deduced assuming thermal synchrotron emission. In addition, as Fenimore, Klebesadel, and Laros (1984) point out, TS requires invoking a separate mechanism to explain emission below the first harmonic.

A third model of gamma-ray burst spectra has been proposed based on the inverse Compton process (Fenimore *et al.* 1982a). In this case the observed spectrum is produced when soft X-ray photons from a low temperature blackbody source traverse an overlying hot ($kT_{hot} > 100$ keV) e^+e^- plasma. The low-energy photons gain energy (on the average) from collisions with the higher-energy electrons and

positrons, hardening the spectrum to that of a gamma-ray burst. In one specific case Fenimore *et al.* (1982a) applied this model to spectra from a gamma-ray burst (GB781104) using data from ISEE-3. The calculated inverse Compton (IC) spectra provided good fits to the three measured spectra obtained during the burst, describing the data much better than the thermal bremsstrahlung model. Parameters derived from the fit indicated a blackbody source of temperature 2.4 keV, and an overlying hot plasma with $kT_{hot} \approx 160$ keV. A blackbody source of this temperature can result from a number of processes, including those that produce X-ray bursts. Indeed, most of the popular gamma-ray burst models are more likely to result in such a spectrum than in one like the typical gamma-ray burst (Katz 1982). Fenimore *et al.* do not speculate on the means of producing or maintaining the hot plasma, but point out that this is a problem common to all burst models.

IC is better at low field strengths, and for shorter source distances ($\sim$ 300 pc). If high fields are present, as may be indicated by the low-energy spectral features (see Section IV), inverse Compton cannot produce a monotonic spectrum and is much less efficient than synchrotron emission (Fenimore, Klebesadel, and Laros 1984). The total luminosity is relatively low, requiring sources to be fairly close (hundreds of parsecs). Because IC is softer at high energies than TS (with a roughly exponential fall-off above a few times kT_{hot}), it may be necessary to invoke a separate component to explain the high-energy emission. In addition, IC may be inconsistent with the observed L_x/L_{gamma} (Liang 1984).

The advantages of this scenario, as noted by Fenimore *et al.* (1982a) and Fenimore, Klebesadel, and Laros (1984), are that it provides a natural explanation for the low-energy X-rays and also for the two-component spectra observed in some bursts.

A final spectral form, which has been used mostly to fit GRS spectra, is the power law (PL). Although this model is descriptive and not tied directly to a specific emission mechanism or burst model, the power law is a common spectral form in astrophysical sources. It can be produced by a number of processes, including synchrotron self-Compton, where the emitted synchrotron spectrum is modified by the scattering of photons on the energetic electrons. Such spectra are seen in this

energy range from (for example) active galactic nuclei (Rothschild *et al.* 1983), the Crab nebula (Mandrou *et al.* 1977), and Centaurus A (Baity *et al.* 1981), as well as in the diffuse galactic background (Trombka *et al.* 1977). If burst spectra are indeed power laws, a break (or flattening) would be required at low energies to be consistent with the data, which generally show a flattening of the spectrum below $\sim$ 200 keV.

FITTED SPECTRAL PARAMETERS, 0.3–9 MeV

The results of fitting spectral models to GRS data are presented, with two purposes: 1) to characterize the observed spectra, and compare the results to previous experiments; and, 2) to test the spectral models against the data. Comparisons emphasizing high energies are the subject of the following section. The models tested are OTTB, TS, and PL. IC fits have not been done, since they are difficult to calculate correctly.

Like all experiments, the GRS can only measure time-averaged properties. However, the problem here is worse than usual since the GRS spectral integration time (16.384 s) is significantly longer than that of any dedicated burst instrument. While some events extend into more than one 16 s interval, in order to treat the events consistently the results for the *complete* burst are presented in each case.

Average Fitted Parameters

The results of these fits over the entire energy range (0.3–9 MeV) of the GRS main detector are presented in Figures III-2, III-3, and III-4 as histograms of the fitted parameters for OTTB, TS, and PL respectively. For comparison, Figures III-2 and III-3 also show the same information for 148 KONUS spectra, from fits by Norris (1983). PL fits to the KONUS spectra are not available. No Gaunt factor has been included for GRS OTTB fits; this is consistent with the way the KONUS OTTB fits were made by Norris. The averages of the fitted parameters over all events for GRS and KONUS are presented in Table III-1. Data from GRB781119 were excluded from the OTTB average since no best-fit temperature was given for this event by Norris. (Norris 1983 lists $T \geq 9000$ keV for this event; if we assume $T = 9000$ keV and include this in the calculation, the average temperature rises to

330 ± 70 keV.) The errors listed are the errors on the *mean*: the standard deviation of the distribution is greater by a factor of the square root of the number of events.

TABLE III-1

AVERAGE VALUES OF SPECTRAL PARAMETERS FIT TO GRS AND KONUS DATA

	ALL EVENTS (71)	FOV EVENTS (28)	KONUS (148)
PL INDEX	2.43 ± 0.12	2.51 ± 0.11	N/A
TS E_{CRIT} (keV)	19 ± 3	14 ± 4	5.6 ± 0.8
OTTB kT (keV)	1020 ± 160	800 ± 180	270 ± 40

While the KONUS results are included for comparison it should be noted that they were not derived in the same way as the GRS parameters. The KONUS averages include multiple spectra for some events, and, because of the way that the KONUS instruments accumulate spectra, data for longer events may be incomplete. The inclusion of multiple spectra from single events will tend to make the KONUS average softer. Since the most intense parts of bursts are also generally the hardest, the hard component will dominate in a spectral sum such as used in this analysis. The KONUS experiment, on the other hand, may record several weaker soft spectra in addition to the hard spectrum at the rising edge and peak of the burst. This is apparently a small effect in the KONUS data set, since the average of *peak* burst temperatures is only negligibly higher than the overall average. Also, the parameters used here were derived from fits to unfolded photon spectra, as discussed above in the section on the thermal synchrotron model.

Even taking into account these qualifications, the KONUS fits are clearly softer, on the average, than those from GRS. There are at least two possible explanations for the difference: 1) because of selection effects, the GRS detects a higher proportion of events with hard spectra; and 2) since the GRS fits are done over a different energy range, higher temperatures are fit to the same type of events. Both

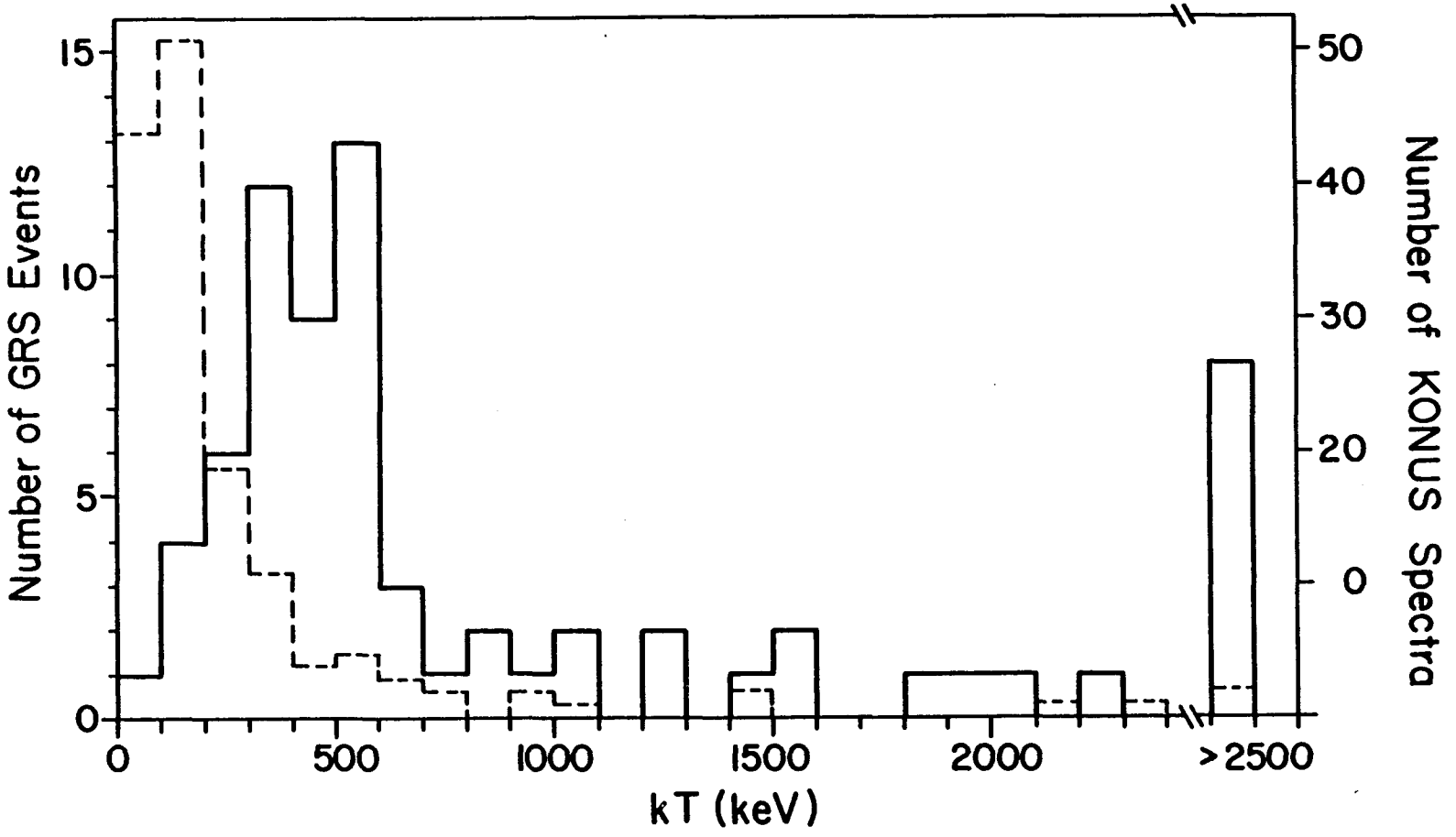

Fig. III-2: Histogram of the best-fit temperatures for the 71 GRS burst spectra from 0.3–9 MeV, assuming optically-thin thermal bremsstrahlung and the nominal instrument response. For comparison, the results for OTTB fits to 148 KONUS spectra (Norris 1983) are also shown. The solid line indicates the GRS data, and the dotted line the KONUS results.

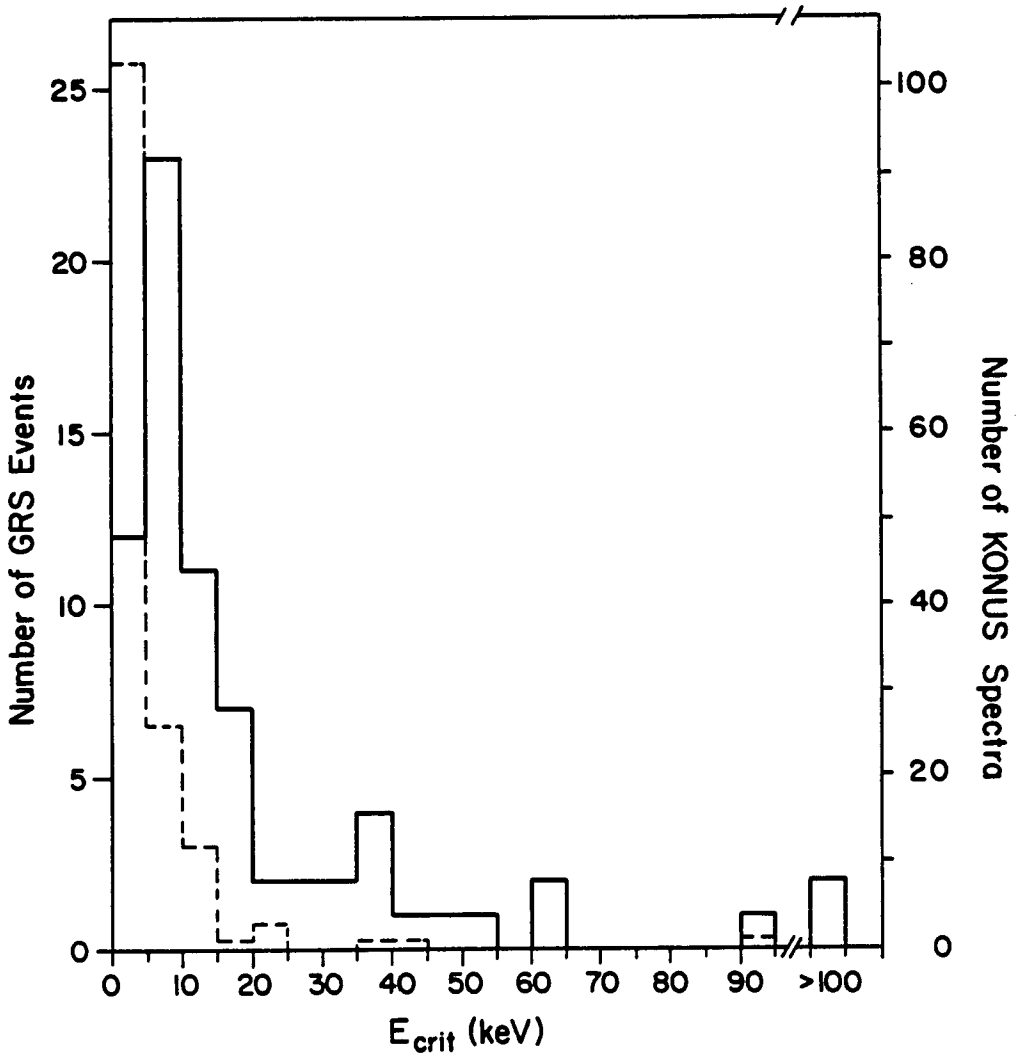

Fig. III-3: Histogram of the fitted values of E_{CRIT} for 71 GRS bursts from 0.3–9 MeV, assuming thermal synchrotron emission and the nominal instrument response. The results for TS fits to 148 KONUS spectra (Norris 1983) are shown for comparison. The solid line indicates the GRS data, and the dotted line the KONUS results.

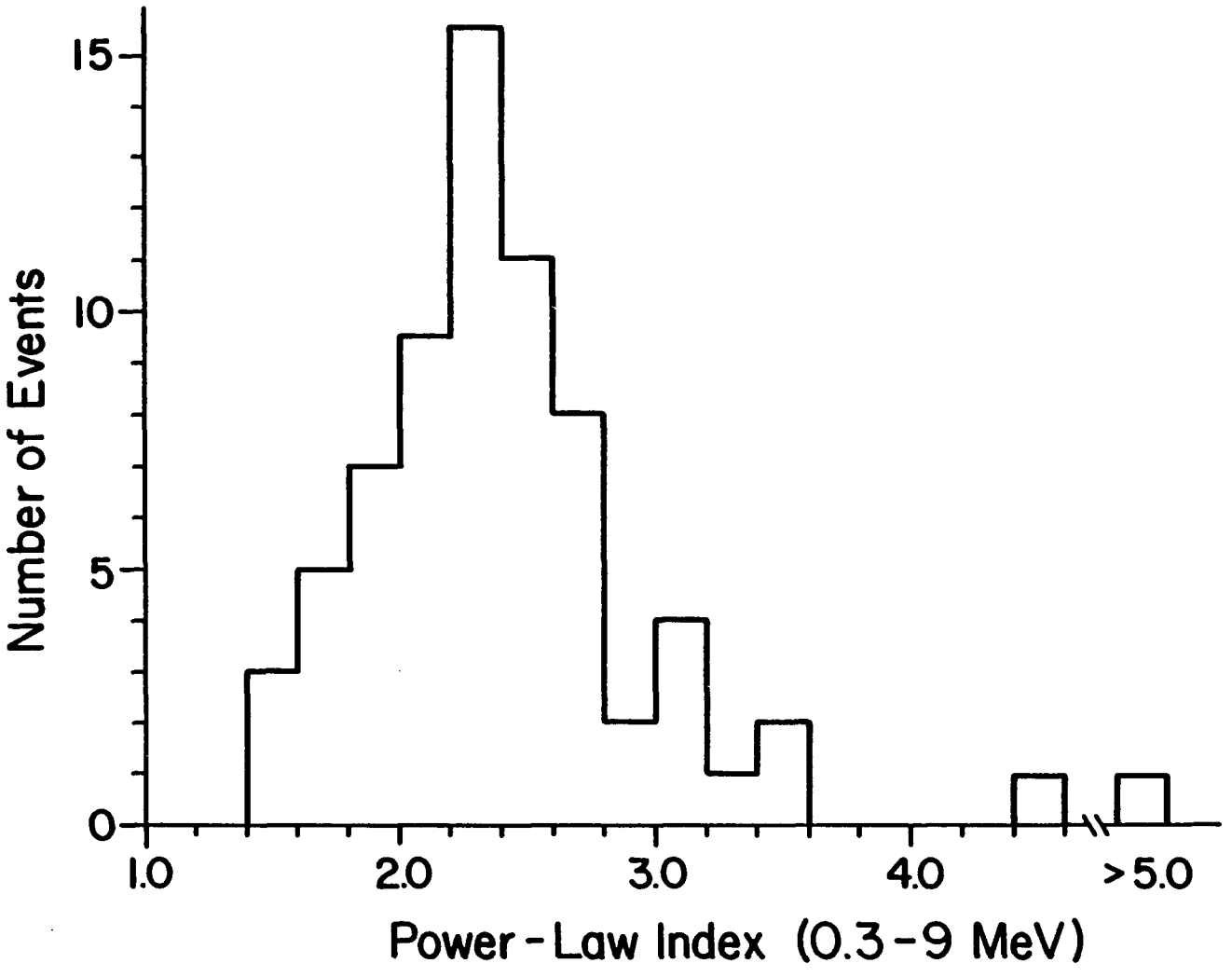

Fig. III-4: Histogram of the best-fit power-law spectral indices for 71 GRS bursts from 0.3 to 9 MeV, assuming the nominal instrument response.

of these effects are undoubtedly present and contribute to the observed differences. There are certainly very soft events that are detected by KONUS but missed by GRS because of its higher photon energy threshold. On the other hand, as Higdon and Lingenfelter (1985) point out, the KONUS experiments will miss many bursts with harder spectra. In fact, Higdon and Lingenfelter calculate that the actual intrinsic burst temperature distribution, corrected for KONUS selection biases, peaks at about 1.1 MeV. This is consistent with the GRS results. The results of Section I would seem to place a limit on the degree to which such selection effects could bias the GRS data set, unless there are serious problems with the logN-logS measurements.

The second explanation is supported by the fact that gamma-ray burst spectra are generally harder than either of the thermal models (see below); therefore, the higher the energy range, the higher the temperature which will be fit to the data. For example, in the GRS data the average temperature fitted to the 28 FOV events is 800 ± 180 for 0.3–9 MeV, but only 540 ± 160 for 0.3–1 MeV.

Comparisons for Individual Events

For a limited number of events the fitted parameters from GRS and KONUS *can* be compared. For one burst (GB811231), details of such a comparison have been published (Nolan *et al.* 1984a). In this instance, for the first spectral interval discussed by Nolan *et al.*, the data of KONUS and GRS are in good agreement. Mazets *et al.* (1983) find a temperature from a thermal bremsstrahlung fit of 400 keV. The GRS data are consistent with this, having a best-fit temperature of 420 keV. In the later intervals where Mazets *et al.* find a strong annihilation line, the GRS and KONUS data significantly disagree, with the GRS data being softer. This discrepancy remains unexplained. The burst of 1982 March 28 was also observed by GRS and KONUS; the KONUS spectra have been published in Mazets *et al.* (1983). The sum of the four KONUS spectra would produce an observed temperature for the entire burst of 360 keV in the GRS detector. The best-fit temperature for the GRS spectrum is 340 keV, again in good agreement. Finally, for the first peak of GB820320 the combined fits of Mazets *et al.* (1983) are equivalent to a single spectrum with kT = 580 keV. The GRS data for the same peak have a best-fit

temperature which is significantly higher, kT = 960 keV. This event is probably *not* in the GRS FOV.

From this limited comparison, with mixed results, no conclusions can be drawn about the source of the disagreement between the KONUS and GRS data sets. Direct comparisons of the complete data sets (not possible at present) are the only way to finally resolve this question.

There is another relevant example of experiments differing in measured kT and E_{max} for the same burst which does not involve GRS. The very short 1979 June 13 event was detected by several instruments, including the KONUS experiments on Venera 11 and 12. Barat *et al.* (1984a) present data for this burst from the Signe experiments on Venera 11 and 12 and from the detector on PVO. While KONUS measured a soft event, with an OTTB kT of $\sim$ 70 keV and a maximum photon energy of 225 keV, the other instruments found the spectrum could be fit by a simple exponential with kT $\approx$ 400 keV, extending up to at least 2 MeV. The total fluence determined from the KONUS fits was an order of magnitude or more smaller than S found by the other experiments. While this was clearly an unusual event, there does not seem to be any reason to think that the experimental problems are unique.

Acceptability of Models

Is there evidence from overall χ^2 that one of these models is strongly preferred in this energy range? The distribution of reduced χ^2 for the 71 events, for each of the three models fit from 300 keV to 9 MeV, is plotted in Fig. III-5. It is apparent from this figure that, based on this test, none of the models is clearly better than the others over the whole data set. This impression is verified by considering the averages of reduced χ^2 over the whole data set (71 events), and the FOV subset (28 events). As seen in Table III-2, this test gives no significant preference to any spectral model.

Overall χ^2 *does* indicate a clear preference among models in some individual cases. Table III-3 lists those events for which the power-law fit was significantly better than either of the thermal models, and the events for which one of the thermal models was preferred over the power law. For 9 events the power-law

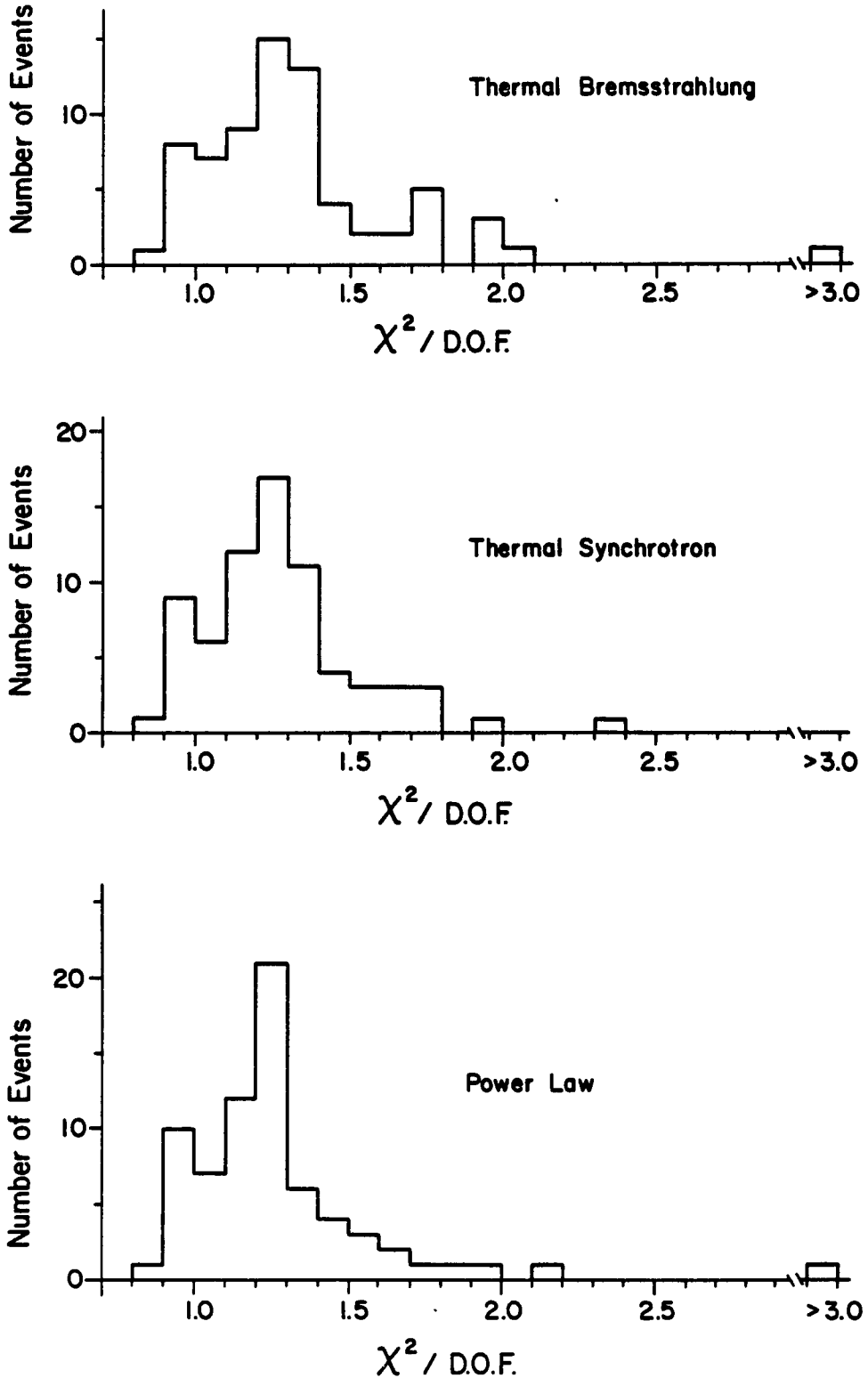

Fig. III-5: Distribution of reduced chi-square for the three tested models fit from 0.3 to 9 MeV.

TABLE III-2

AVERAGE REDUCED CHI-SQUARED VALUES

	ALL EVENTS	FOV EVENTS
PL:	1.275 ± 0.035	1.335 ± 0.081
TS:	1.279 ± 0.031	1.352 ± 0.058
OTTB:	1.334 ± 0.040	1.461 ± 0.086

Average D.O.F. = 181

model was substantially better than either of the thermal models; for 6 events one of the thermal models was preferred. The most reliable data are from the 28 FOV events. Eight of these are best fit by power laws, two by a thermal model.

The criterion used to determine a "significant" difference in goodness-of-fit was a difference in reduced χ^2 of 0.1 or more. Because of varying numbers of degrees of freedom and χ^2 values, an increment of 0.1 does not represent a constant change in probability. It is used as a rough guide to indicate a substantial difference in goodness-of-fit. For example, assuming the average χ^2 and d.o.f., 0.1 roughly corresponds to the difference between the 95% confidence level ($\chi^2 = 1.180$) and 99% confidence level ($\chi^2 = 1.261$).

If a confidence level of 95% or better is defined to be an acceptable fit, 30 events can be fit by power laws, 25 by thermal synchrotron, and 20 by thermal bremsstrahlung. For the 28 FOV events, 12 can be fit by PL, 9 by TS, and 6 by OTTB. There is a significant overlap; for example, in both cases all but one of the events fit by thermal synchrotron can also be fit by a power law.

Figures III-6 through III-8 demonstrate the range of spectral shapes observed by GRS. GB801220 (Fig. III-6) shows a strong curvature; this event had the greatest difference in χ^2 between the power-law and the thermal models, which were strongly preferred (see Table III-3). GB821104 (Fig. III-7) was much better fit by a power-law than by a thermal spectrum. Finally, over the whole energy range GB810301 (Fig. III-8) is (roughly) equally well-fit by each of the model spectra.

TABLE III-3

DATE	TIME	IN FOV?	DOF	REDUCED CHI-SQ. 0.3–9 MEV PL	TS	OTTB	PREFERRED MODEL
80/04/19	01:20	X	155	1.13	1.56	1.97	PL
80/08/15	18:21	X	168	1.22	1.46	1.60	PL
81/12/31	01:37	X	243	1.22	1.44	1.74	PL
82/03/03	16:21	X	176	1.21	1.39	1.52	PL
82/03/13	02:40	X	229	1.50	1.65	1.74	PL
82/03/28	14:37	X	112	1.19	1.30	1.35	PL
82/05/30	09:49	X	130	1.00	1.14	1.29	PL
82/11/04	03:30	X	265	1.38	2.40	3.21	PL
83/01/21	21:12		212	1.39	1.74	1.97	PL
80/12/20	18:30	X	187	3.20	1.13	1.06	TB OR TS
81/04/08	00:49		146	2.16	1.65	1.62	TB OR TS
81/08/14	10:09		185	1.42	1.32	1.31	TB OR TS
81/10/16	23:53	X	183	1.51	1.39	2.04	TS
82/02/14	01:23		113	1.12	1.04	1.02	TB OR TS
82/03/20	13:10		220	1.88	1.56	1.70	TS

X $\Rightarrow$ IN FOV

TESTS OF MODELS AT HIGH ENERGIES

The results of the previous section show that, except in a small fraction ($\sim$ 20%) of the cases, overall χ^2 is not able to distinguish between even very different spectral models. As Liang, Jernigan, and Rodrigues (1983) point out, in the limited energy range of most burst observations the standard models (OTTB, TS, IC) have very similar shapes; thus if one fits the data, it is likely that the others will also. Apparently this is also true, in many cases, of the power-law model. Only the behavior at high energies differentiates between the models. Overall χ^2 is not the most sensitive

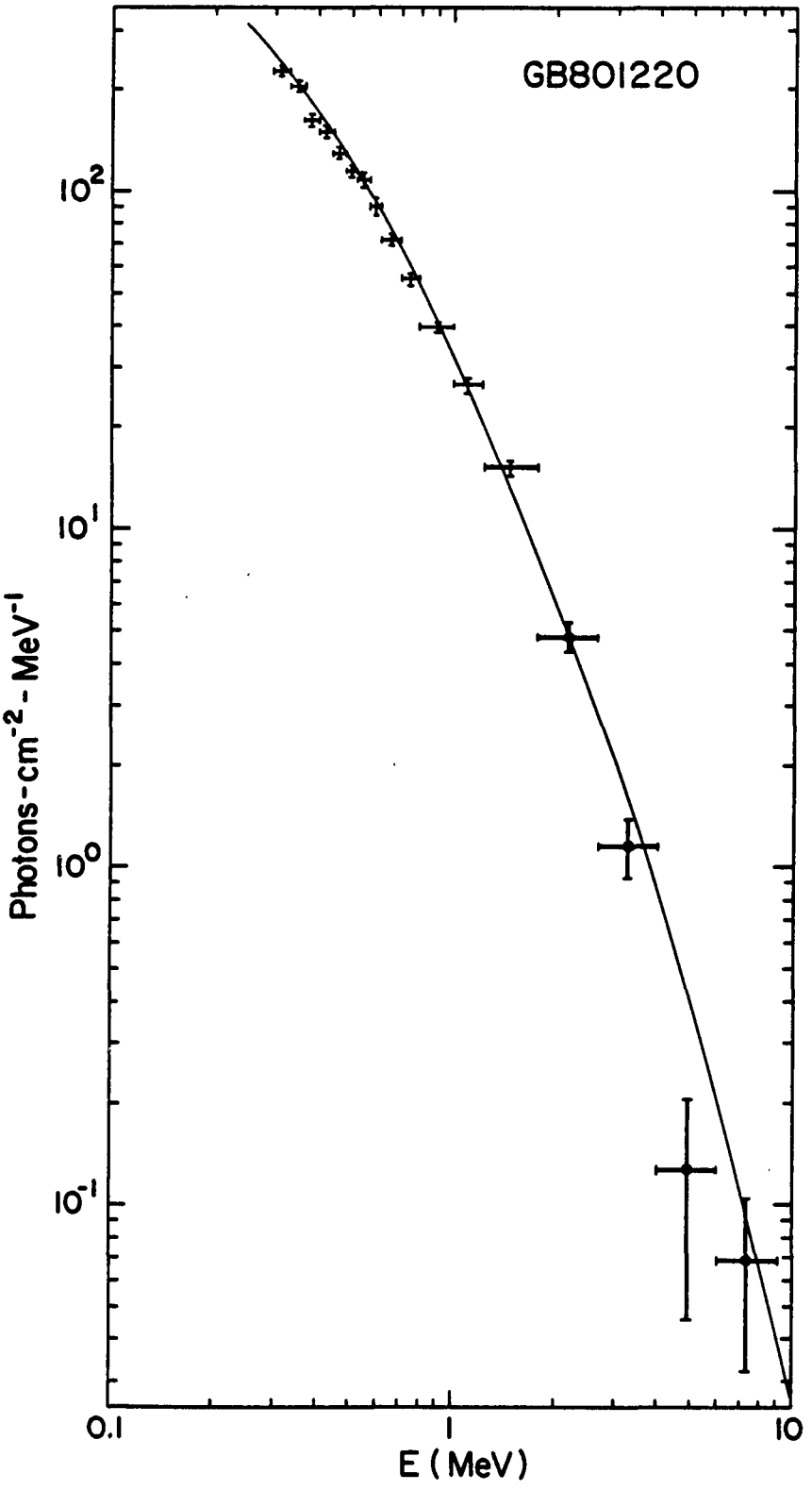

Fig. III-6: GRS photon spectrum for the burst of 1981 December 20, assuming the nominal instrument response and the best-fit TS spectrum, which is also shown (E_{CRIT} = 19 keV).

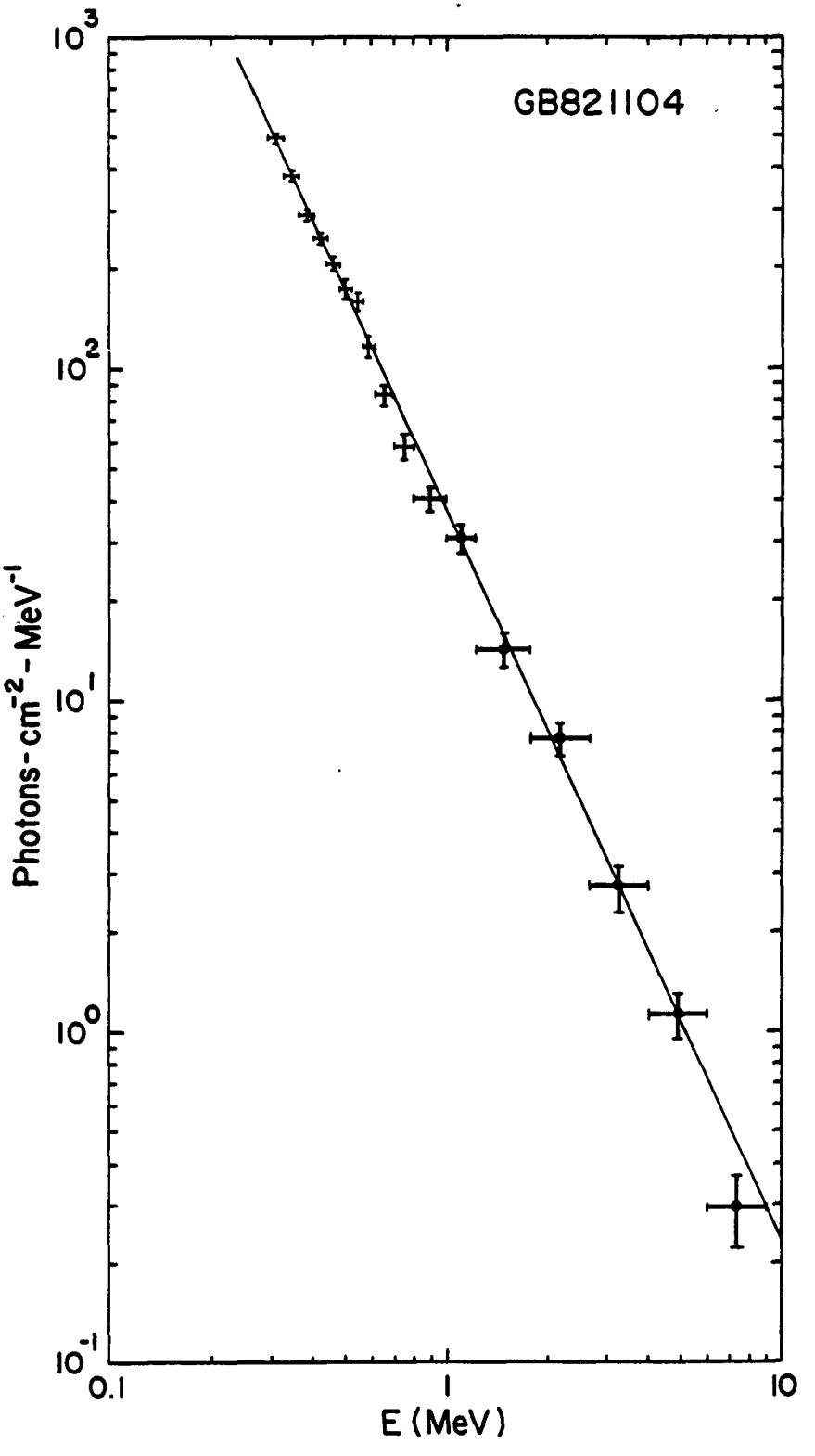

Fig. III-7: GRS photon spectrum for the burst of 1982 November 4, assuming the nominal instrument response and the best-fit power law ($E^{-2.2}$), which is also shown.

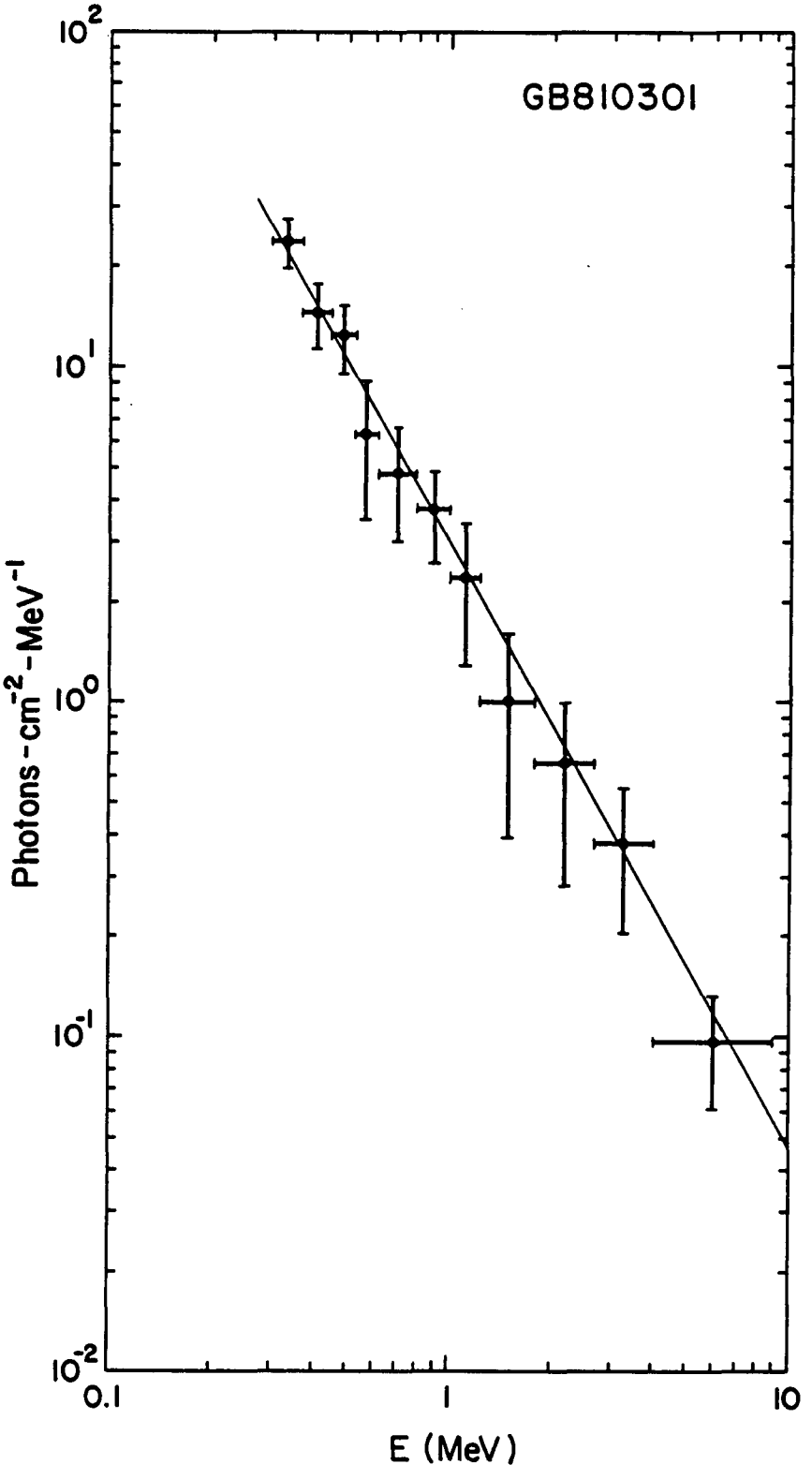

Fig. III-8: GRS photon spectrum for the burst of 1981 March 1, assuming nominal instrument response and the best-fit power law ($E^{-1.8}$), which is also shown.

test for models that disagree only in a limited energy region, especially if the counts in that region are of relatively low significance.

Fits done over the entire range are driven by, and the χ^2 is dominated by, the low-energy, high-statistics (highest intensity) channels. Counts above 1 MeV may be significant, yet still have little effect on the fit and contribute little to total χ^2. Since the models disagree strongly only at high energies, such a test will not be a sensitive way to distinguish between the different spectral forms.

The best way to differentiate between the models is to test them where they differ; in this case, above 1 MeV. Three tests of the models at high energies were performed: 1) evaluation of the χ^2 above 1 MeV for each model; 2) test for significant fluence above or below the extrapolated fit for each event; and, 3) comparison of the highest detectable energy, predicted and observed. The last two, in particular, show that the two thermal models are too soft to account for the observed emission above 1 MeV.

In the first test, each of the three models was fit to the data *below* 1 MeV for each total burst accumulation. The extrapolation of that fitted spectrum was then compared to the data *above* 1 MeV by means of χ^2. The result for the 28 FOV events are shown in Table III-4. In roughly half of the cases (13/28), the PL model gives a substantially better fit to the data at high energies. In 5 of the 28 spectra one of the thermal models is significantly better, in one case (GRB801220) dramatically so. In the remaining 10 spectra there is no substantial difference between the χ^2 values of the three models.

Do the data depart from the models in a systematic way? Using the same fits determined above, the predicted and observed counts above 1 MeV can be compared. A model can then be rejected if the extrapolation of the fit falls significantly ($> 3\sigma$) above or below the data. Table III-5 shows the results of this test, both for the complete data set and (in parentheses) for the FOV events.

For an event to be harder than a model by this standard it must at least have significant flux above the background above 1 MeV. There are 18 FOV events which have significant flux $>$ 1 MeV. In 50% of these (9/18), TS is substantially softer than the data; 67% of the OTTB fits are too soft.

TABLE III-4

DATE	TIME	DOF > 1 MEV	REDUCED CHI-SQ. > 1 MEV PL	TS	OTTB	PREFERRED MODEL
80/03/07	05:07	131	1.306	1.406	1.469	PL
80/04/19	01:19	77	1.251	2.308	3.077	PL
80/04/21	03:08	88	1.090	1.094	1.095	
80/08/15	18:21	89	1.234	1.680	1.917	PL
80/09/20	14:10	102	1.246	1.268	1.011	TB
80/11/19	17:06	54	1.078	1.263	1.469	PL
80/12/20	18:30	108	10.30	1.177	1.732	TS
81/02/25	04:47	140	1.035	1.035	1.035	
81/03/01	12:35	83	1.248	1.613	1.780	PL
81/10/16	23:53	104	1.461	1.296	2.016	TS
81/12/31	01:37	164	1.317	1.736	2.173	PL
82/01/18	12:20	116	1.215	1.216	1.216	
82/01/21	09:00	169	1.483	1.453	1.438	
82/01/25	17:56	53	2.959	1.457	1.415	TS OR TB
82/02/01	08:19	44	1.502	1.468	1.607	
82/02/24	20:29	75	1.313	1.313	1.313	
82/03/01	02:36	174	1.755	1.809	1.849	
82/03/03	16:21	97	1.511	1.964	2.106	PL
82/03/13	02:40	150	1.450	1.667	1.817	PL
82/03/24	12:21	190	2.060	2.083	2.107	
82/03/28	14:37	47	1.619	1.868	1.953	PL
82/05/02	21:15	97	1.011	0.940	0.943	
82/05/30	09:49	58	0.981	1.307	1.645	PL
82/08/20	13:59	63	1.435	1.543	1.614	PL
82/08/28	13:50	60	0.933	0.785	0.783	TS OR TB
82/11/04	03:30	186	1.404	3.411	4.360	PL
83/02/10	12:20	84	1.117	1.231	1.405	PL
83/08/24	02:20	162	1.325	1.339	1.344	

TABLE III-5

NUMBER OF (FOV) EVENTS WITH SPECTRA SIGNIFICANTLY HARDER OR SOFTER THAN MODELS ABOVE 1 MEV

	DATA HARDER THAN MODEL	DATA SOFTER THAN MODEL
PL:	1 (1)	13 (5)
TS:	11 (9)	4 (1)
OTTB:	21 (12)	3 (1)

Finally, a more sensitive (though perhaps less straightforward) test can be made: comparison of the maximum observable energy seen in the data with that predicted by the three models. This method has been described in Section II. This test is especially suitable here since it maximizes sensitivity at high energies, to deviations at high energies.

The results are presented in Figures III-9 and III-10. Figures III-9a and III-9b show the comparison of observed to predicted E_{max} for the three models. Here the model spectra have been fit only to 1 MeV and extrapolated to higher energies; if the model is correct, it should be able to predict the high-energy behavior from the low-energy data. It is clear that the two thermal models fall far short of explaining the observed high-energy emission. Above 2 MeV, for example, OTTB predicts 6 observable events, and TS 7 observable events; 29 events are actually detected. In the next figure (III-10), the predicted E_{max} is based on spectral fits over the whole range of data, 0.3–9 MeV. Even in this case, using all the high-energy data, the thermal models are clearly too soft. The results for the power-law fits have already been discussed in Section II.

The same effect can be seen by calculating, for each event, the difference between the *observed* maximum energy and that predicted by the three models fit below 1 MeV. Such a comparison was presented for the power-law model in Section II. The differences are -0.52 ± 0.29 (1.8σ) for PL, $1.20 \pm 0.26(4.7\sigma)$ for TS, and $1.48 \pm 0.28(5.2\sigma)$ for OTTB, averaged over all 71 events. That is, the two thermal

models, on the average, predict a maximum energy which is more than an MeV below the observed maximum. The power-law average is not significantly different from zero.

Note that these results differ slightly from Matz *et al.* (1985) due to a modification of the fitting technique and, in some cases, different burst accumulations (Matz *et al.* did not use total burst accumulations for every event, but the accumulation giving the highest observed energy). These changes do not affect the conclusions of Matz *et al.*

DISCUSSION AND CONCLUSIONS

Effects of Spectral Evolution

The GRS spectral integration time is long compared to burst timescales, and in particular is longer than the observed timescale for spectral variability at low energies. Spectral variability on somewhat longer timescales ($\geq$ 1 s) is also clearly present at high energies in the GRS data (Norris *et al.* 1986). If the spectral shape does change over the course of the burst, the spectrum should harden at higher energies where the harder (higher temperature) component dominates. The importance of this effect depends on the range of spectral variability and the relation between spectral hardness and intensity. It is at least a possibility that this effect could change the interpretation of the above results. That is, the spectral fits made at low energies would be dominated by the softer components and then the extrapolation of these fits to high energies would fall below the data where the harder component dominates. Figure III-10 shows that the high-energy deficit of OTTB and TS is essentially unchanged when all the data to 9 MeV are included in the fit. Still, these fits are dominated by the lower-energy emission and are not a sensitive test for the effects of spectral evolution.

What temperatures would be required, assuming OTTB or TS, to explain the observed high-energy emission? Based on fits above 1 MeV (to events with significant emission above 1 MeV), the average temperature required to explain the high-energy data is > 2.8 MeV, assuming the emission is produced by OTTB. Therefore there must be a large amount of energy in an unphysically hot plasma if the high-energy component is to be explained by spectral evolution of a thermal

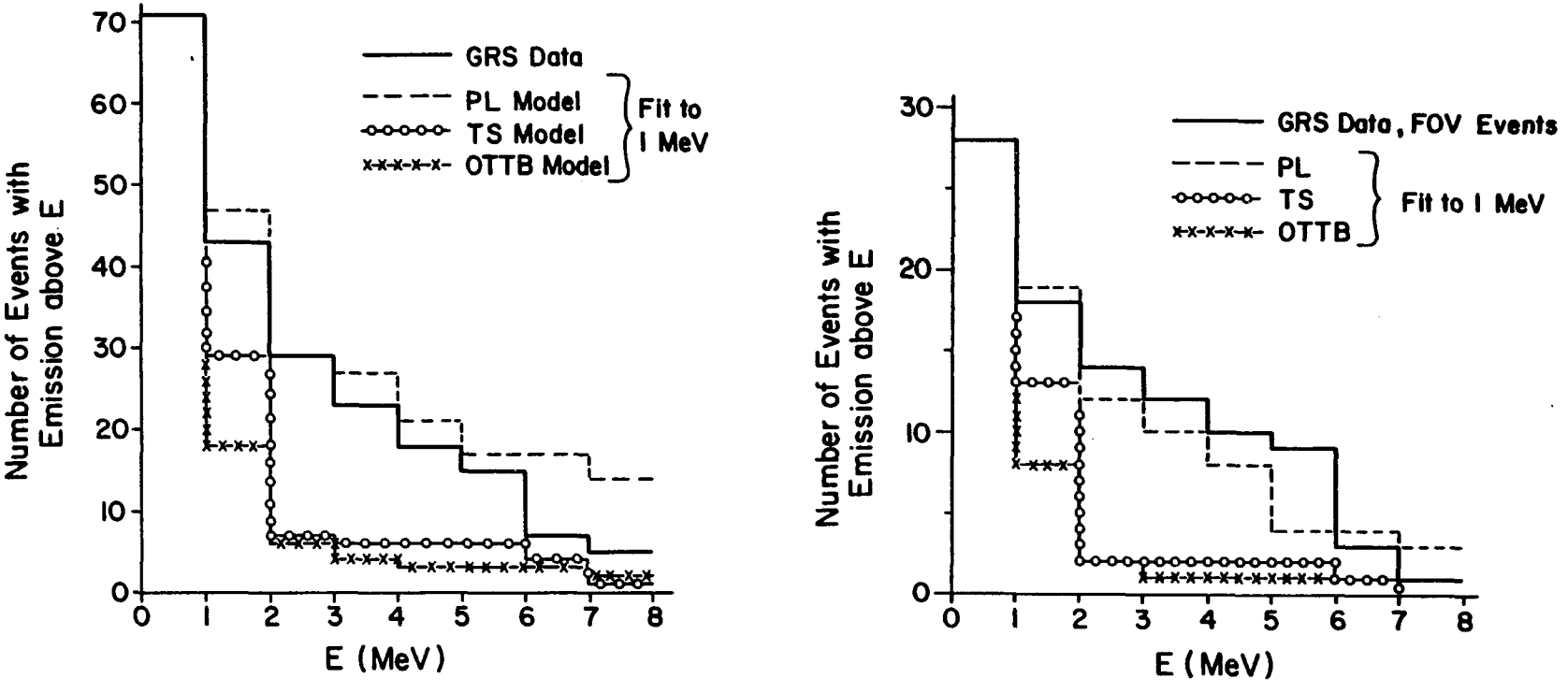

Fig. III-9: Observed and predicted number of events *vs.* E_{max}, assuming extrapolations of the spectra fit below 1 MeV. 9a: for all 71 events. 9b: for 28 events thought to be in the forward field-of-view.

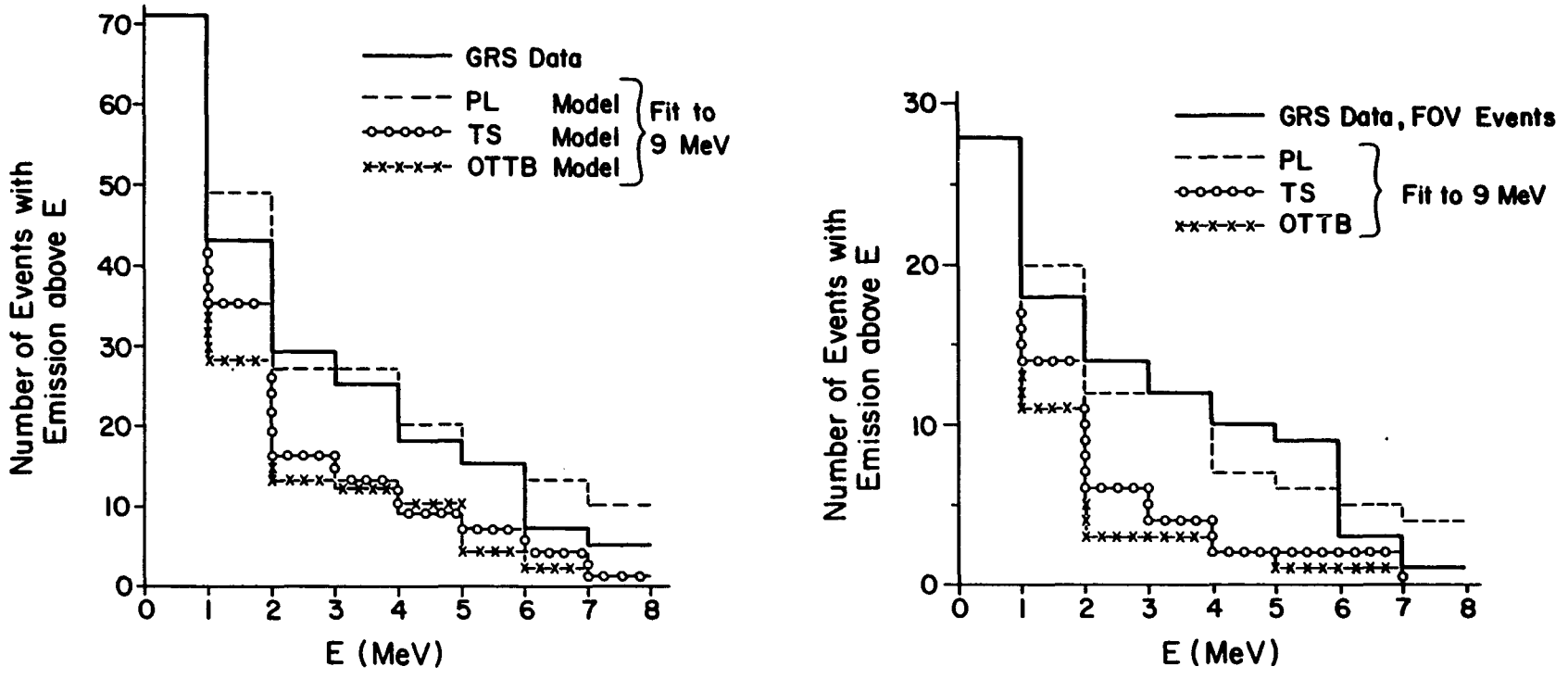

Fig. III-10: Observed and predicted number of events *vs.* E_{max}. The predicted values are from spectra fit over the entire energy range (0.3–9 MeV), without extrapolation. 10a: for all 71 events. 10b: for 28 events thought to be in the forward field-of-view.

plasma.

A comparison of this temperature to the average temperatures fit over the whole spectral range (see Table III-1) would seem to indicate a spectral hardening, but it is actually an artifact of the model used to fit the data. As mentioned above, if a model is systematically softer than the data, the higher the energy range fit, the harder the fitted model spectrum. An examination of the spectra does not reveal any obvious bends to flatter spectra at higher energies, and a comparison of power-law spectral indices fit below and above 1 MeV (Figure III-11) shows no systematic hardening. Indeed there is a slight (insignificant) softening overall.

Even in the cases for which a power-law spectrum is the preferred model, it cannot be stated conclusively that the *fundamental* spectral shape is not OTTB or TS. It is possible, for example, to produce a power-law spectrum from a superposition of different temperature thermal synchrotron spectra (G. H. Share 1985, private communication). However, if the observed spectra are the result of such a superposition, the spectral evolution must be such that it usually produces an integrated spectrum of roughly power-law shape. In addition, as mentioned above, very high temperatures would be required. It is worth investigating whether this is physically realistic and consistent with the known spectral evolution of bursts.

Conclusions

Of the three models tested against the GRS data, none is adequate to explain all of the observed burst spectra. In particular, a number of spectra show distinct curvature and are well-described by a single-temperature thermal model. The two clearest instances of this are the intense events GB811220 and GB820125.

While none of the models fits all of the spectra, PL provides the best overall fit to the data: in all the χ^2 tests it is preferred in more cases than the thermal models, especially for FOV events. It also gives the best explanation of the high-energy emission. Overall, the thermal models fail to explain the strong high-energy emission detected by GRS, even when fitted over the entire range of the data. However, in a significant number of events the PL fit is harder than the data.

The fact that a number of events (10–20%) have spectra with clear evidence of curvature at least raises the possibility that distinct classes of events (with,

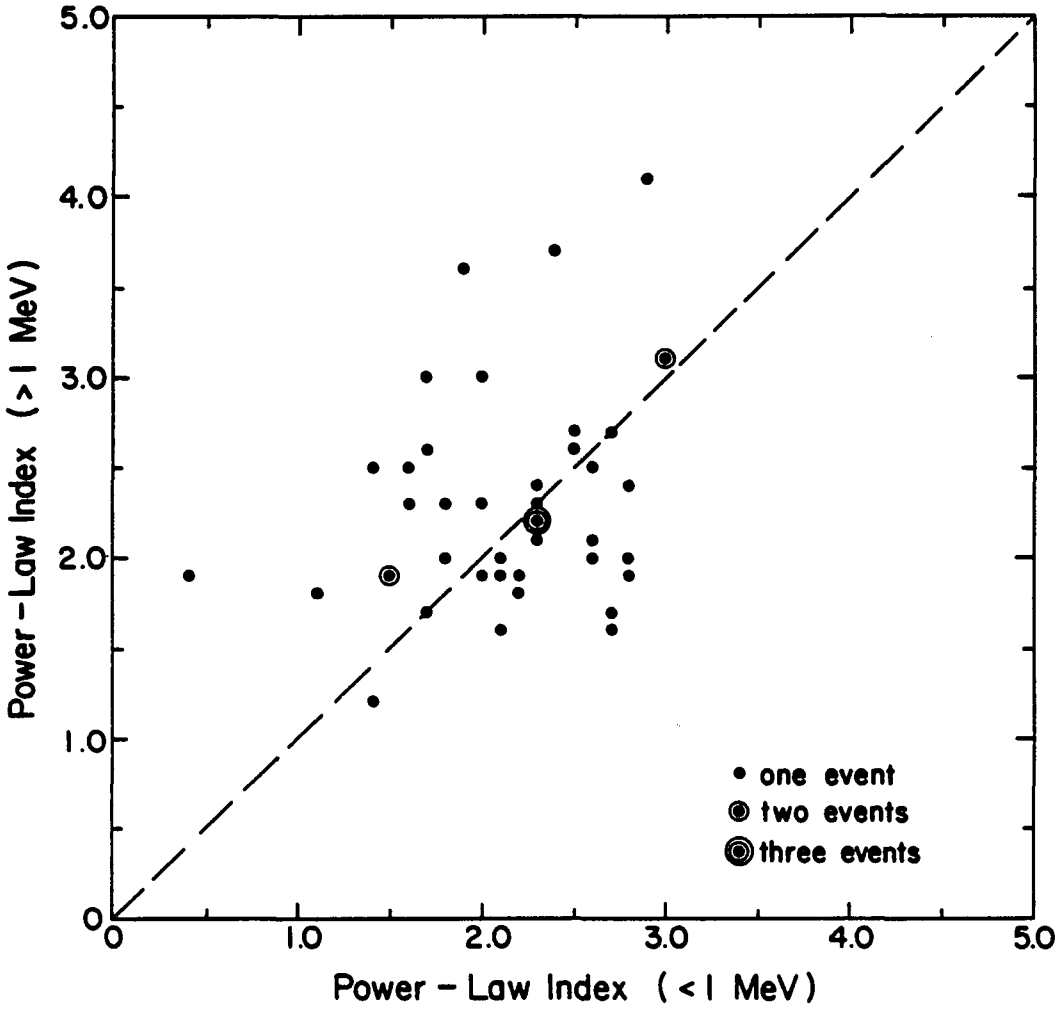

Fig. III-11: The spectral indices fit to GRS gamma-ray burst spectra below and above 1 MeV for the 43 events with significant emission > 1 MeV.

presumably, corresponding physical differences in the sources) may exist which can be differentiated by spectral shape. On the other hand, it is possible that these events may differ only in their spectral evolution during the burst, producing an apparently different spectral shape from basically the same physics. There is no obvious difference in the time histories which would support the theory of separate classes.

Let me emphasize that the conclusion of this section is *not* that all burst spectra are power laws. On the contrary, none of the models tested is consistent with all the observed spectra. Even for those events where it provides the best description of the data PL is not necessarily the real fundamental spectral shape, since it is possible that evolution could mimic it from thermal spectra. The strongest conclusions are negative: no model adequately describes all the data, and the two single-temperature thermal models are generally not consistent with the high-energy data.

IV. MAGNETIC FIELD, PAIR-PRODUCTION, AND BEAMING

In Section II it was shown that high-energy emission is a common feature in gamma-ray bursts; indeed, the data are consistent with *all* events emitting to high energies. However, the detection of events depends only on the low-energy flux, since searches for events have only been made on data below 1 MeV. If all events observed at low energies are also seen at high energies, then the low- and high-energy flux must be emitted in the same solid angle: high-energy emission cannot be more tightly beamed than low-energy emission, or only a fraction of the events seen at low energies would also be observed above 1 MeV. In practice, not all events are actually observed to have significant flux at high energies, but the data can still be used to place a *limit* on the relative beaming of the high-energy emission with respect to the low-energy emission.

One process that could cause such beaming is single-photon pair-production in a very strong ($> 10^{12}$ G) magnetic field. Based on this process the GRS data can be used to derive an upper limit on the typical magnetic field strength at burst sites. Experimental and theoretical arguments have been made which indicate that the typical fields of burst sources are $> 10^{12}$ G; however, these arguments have weaknesses that make them unconvincing. Because knowledge of the field strength is critical to an understanding of gamma-ray bursts, a reliable estimate is important.

In this section the arguments and data which led to the original estimates of the magnetic field strength are reviewed. Then single-photon pair-production is described, with an emphasis on the observable consequences of this process. Finally, the results on single-photon pair-production are used in conjunction with the GRS data to derive an upper limit of 1×10^{12} G on the typical magnetic field at the burst radiation site.

PREVIOUS ESTIMATES OF THE MAGNETIC FIELD STRENGTH

There are essentially three arguments that very strong ($B > 10^{12}$ G) fields are present at the site of gamma-ray bursts: 1) such fields provide perhaps the only way to confine high temperature thermal plasmas (which were thought to be the source of burst radiation) on the timescales of bursts; 2) low-energy features (30–70 keV) observed in some burst spectra, when interpreted as cyclotron or synchrotron features, implied fields of $(2\text{–}6)\times 10^{12}$ G.; 3) bursts are thought to originate on neutron stars, where high fields are expected. The first two points deserve more detailed discussion; the question of the nature of the source object has been treated in the Introduction.

Confinement of High Temperature Plasmas

The confinement argument was originally presented by Colgate and Petschek (1981), whose treatment is followed here. A hot plasma will tend to expand, cool, and rapidly dissipate. If the plasma is optically thick and radiation dominated (Lamb 1984a), the dominant force will be the radiation pressure. For isotropic black-body emission the radiation pressure is $\sigma T^4/3c$, where σ is the Stefan-Boltzman constant and T the black body temperature. The gas can be constrained by gravity alone as long as

$$GMm_p/r^2 \leq \sigma_T P_{rad}$$

(cf. Tucker 1975, pg. 161). For a "typical" neutron star with $M = M_\odot$ and $r = 10^6$ cm, this relation implies a maximum temperature of ~ 1.2 keV. Typical temperatures obtained from thermal fits to burst spectra are *hundreds* of keV. A temperature of 300 keV implies a radiation force $\sim 4 \times 10^9$ times the gravitational. With no other constraint, expansion and cooling occur on a timescale of $\sim 10^{-12}$ s, much much shorter than typical burst durations (0.1–100 s).

If the plasma is not continuously replenished or reheated throughout the burst some additional means of confining the plasma is needed. The best available mechanism is the magnetic field pressure, which acts against expansion perpendicular to the field lines. The condition for confinement in this case is:

$$\frac{\sigma T^4}{3c} \leq \frac{B^2}{8\pi}$$

or

$$T \leq 170(B/10^{12}\mathrm{G})^{1/2}(\mathrm{keV}).$$

For ordinary burst temperatures, then, a field $\geq 10^{12}$ G is required. As Colgate and Petschek (1981) point out, some additional force is needed to prevent expansion parallel to the field lines. In an accretion model this is easily provided by the ram pressure of the infalling matter. However, thick overlying material may allow photons to escape only at large angles to the field, which may cause other problems (see below). Another possibility is that the field is complex (non-dipole) and expansion is limited because field lines are closed in a short distance.

There are several problems with this argument. First, the observed spectra of gamma-ray bursts, unlike X-ray bursts, are not blackbody. Addressing this problem, Fenimore, Klebesadel, and Laros (1984) make a more general argument which is independent of the shape of the emitted spectrum, simply by substituting L/A (where L is the total luminosity and A is the total emitting area) for the blackbody expression for luminosity per unit area (σT^4), giving

$$\frac{(L/A)}{3c} \leq \frac{B^2}{8\pi}$$

or, for $S = 10^{-5}$ ergs-cm^{-2}-s^{-1},

$$B > 5.6 \times 10^9 (D/1\ \mathrm{kpc})(A/1\ \mathrm{km}^2)^{-1/2}\ \mathrm{G}$$

(Fenimore, Klebesadel, and Laros 1984, eq. 2 and 3). Using this to derive a magnetic field constraint from an observed burst requires estimates of both source size and distance. Values of L/A derived from the TS model applied to spectra showing evidence of self-absorption (Liang, Jernigan, and Rodrigues 1983) would require fields on the order of 10^{10} G.

The assumption that the plasma is optically thick may also be violated. Lamb (1984a) argues, based on the lack of Wien peaks and the presence of sharp "annihilation" lines, that the burst emission region is optically thin. Analyses of burst spectra using various models (Fenimore *et al.* 1982; Liang 1983) imply that at least some sources are very optically-thin. In this case the photons "decouple" from the

gas and the radiation pressure does not dominate the expansion. Then only the gas pressure of the plasma must be confined, requiring

$$p_{gas} = nkT < B^2/(8\pi)$$

or

$$(B/10^{12}\mathrm{G})^2 > (4 \times 10^{-32}) n_e(\mathrm{cm}^{-3}) T(\mathrm{keV})$$

for confinement perpendicular to the field. This point has been previously mentioned by Liang (1982). Based on the maximum density estimates of Lamb (1984a, eq. 17; see also his eq. 61 and 62), this constraint requires fields no higher than $\sim 10^9$ G for a typical source at 10 kpc. For nearer sources the field needed is even less.

The need to confine the hot plasma followed from the fact that, unconstrained, the plasma would expand and cool in a time much shorter than the typical burst duration and produce radiation much softer than observed. However, even in a confined plasma the problem of replenishment remains, since other cooling mechanisms act as fast or faster than expansion. For example, Lamb (1984a) gives the synchrotron cooling timescale

$$t_{syn} = \frac{3\pi m_e c}{\sigma_T B^2} \doteq 3.9 \times 10^{-16} (B/10^{12}\mathrm{G})^{-2} \ \mathrm{s}$$

which is about four orders of magnitude *faster* than the expansion timescale for $B = 10^{12}$ G. So the gas cools (perpendicular to the field) by other means before it can expand. Far from solving the replenishment problem, the large fields invoked for confinement have made it worse. For fields $> 10^{10}$ G, t_{syn} is faster than the expansion time, and so confinement is not a problem.

In summary, the confinement argument is quite model dependent, and specific assumptions made to derive the high field limit ($> 10^{12}$G) seem to be incorrect. For these reasons, the argument does not provide convincing evidence for the presence of superstrong fields at burst sites.

Low-Energy Spectral Features

Low-energy spectral features have been observed in about 10–15% of the bursts detected by the KONUS experiment. The energies of these "lines" range from about

20 keV to 70 keV, with equivalent widths of 3 to 30 keV (Mazets *et al.* 1981d). In addition there are a number of "wide absorption bands" which extend to the lower end of the measured spectral range. Two other experiments have observed similar spectral features: Hueter (1984) published results from the High Energy X-Ray and Low Energy Gamma-Ray Experiment on HEAO-1 showing a narrow absorption feature at 55 ± 5 keV with an equivalent width of 13 ± 3 keV in the spectrum of GB780325. Dennis *et al.* (1982) reported the measurement by the HXRBS experiment on SMM of a broad absorption band below $\sim$ 150 keV in the burst of 1980 April 19. However, they noted that this spectrum does not require a feature but can be explained by a different continuum shape.

If these features are interpreted as cyclotron absorption lines, the ambient field can be easily derived from the relationship of the field strength to the cyclotron frequency

$$\omega_c = \frac{eB}{m_e c}$$

or

$$E_c = \hbar\omega_c \doteq 11.6(B/10^{12}\mathrm{G})\ \mathrm{keV}.$$

A line at 55 keV implies $B = 4.8 \times 10^{12}$ G; the range of fields implied by all the observations is $(2\text{–}6)\times 10^{12}$ G, without correcting for possible redshift. However, there are both experimental and theoretical difficulties with this interpretation.

Thermal motion in the absorbing medium will broaden, or even wash out the lines if the plasma is hot. The narrowness of the lines implies that the temperature of the absorbing material along the line-of-sight is $\leq$ 50 keV (Lamb 1984b), much cooler than the temperatures inferred from spectral fits of thermal models. There are two ways to avoid this conflict. First, there may be a cool layer of gas above the emission region. This suffers from being an ad hoc hypothesis invoked solely to explain the line features. In addition, it requires that the magnetic field be very strong even at fairly large distances from the source object. Second, in high fields synchrotron radiation efficiently cools motion perpendicular, but not parallel, to the field. At large viewing angles, then, the thermal motion along the line-of-sight, and thus the thermal line broadening, may be slight even though the temperature of the plasma is high. This effect is described by Lamb (1984b).

In addition, if the features are indeed cyclotron lines, higher harmonics are expected to be visible. Bussard and Lamb (1982) showed that, given fairly general assumptions (e.g., that cyclotron scattering, not absorption, is dominant), the second harmonic will be even darker (with respect to the surrounding continuum) than the first. Decay of higher Landau states will tend to fill in the first harmonic, since single level transitions are strongly preferred (Daugherty and Ventura 1978). The synchrotron spectra of Lamb (1984b) show this effect. But no higher harmonics have been observed. Bussard and Lamb (1982) point out, however, that a variation in the field (of a factor of two or more) in the emission region could explain this. Thus the lack of higher harmonics may not be a serious problem.

In light of these theoretical problems, alternative explanations for the source of the features have been proposed. One possibility is that the features are the result of an evolving low-energy cut-off (Norris 1983, Lamb 1982). This hypothesis is based on the fact that spectral evolution is observed to take place on timescales much shorter than KONUS accumulation time of 4s; in particular, in one burst observed by Signe (GB791119: Barat *et al.* 1981; Knight, Matteson, and Peterson 1981; Barat 1983) a spectral turnover was present at $\sim$ 500 keV in the early spectra but not those taken later. As Norris (1983, Fig. 5.36) shows, such an evolving spectrum can mimic an absorption feature. If the spectral turnover is due to the synchrotron cut-off, the line may supply information about the magnetic field. However, it may have another cause unrelated to the field.

A second theory is that the lines may be produced by the superposition of two separate spectral components: a hard, high-energy spectrum with a low-energy cut-off in the range of the "cyclotron" lines, and a soft low-energy thermal spectrum (Lasota and Belli 1983). The specific model of Lasota and Belli is an optically-thin thermal synchrotron spectrum with a turnover due to self-absorption, combined with a blackbody spectrum (though they also consider two synchrotron components, somewhat as above). This hypothesis is supported by the observations of GB790329 which show a soft spectrum persisting between the main burst peaks. Lasota and Belli analyze the spectra of four bursts as measured by the KONUS experiments. They show that the main burst spectra (with low-energy features) can be fit by

a two component spectrum as described above. The blackbody model generally fits better than that with two synchrotron components. The temperatures inferred from the blackbody fits are in the range of 7 to 12 keV. In this model the magnetic field strength cannot be directly deduced from the fitted parameters.

In addition, experimental questions have been raised about whether there are any lines at all. The broad features which extend to the lower limits of measured energy spectra are in fact only deficits below the extended fitted continuum, assuming optically-thin thermal bremsstrahlung. As several authors have shown (Dennis *et al.* 1982; Fenimore, Klebesadel, and Laros 1983), these features disappear with different assumptions about the continuum shape. Other problems arise because of the difficulty in unfolding gamma-ray burst spectra. As discussed in Appendix A, even a monoenergetic photon source produces a complicated response in a scintillation detector. As a result the observed counts at any energy are produced not only by photons of that same energy, but also by higher-energy photons which have deposited only part of their energy in the detector. Therefore it is not possible, in general, to derive the incident *photon* spectrum unambiguously from the observed *counts* spectrum. Some spectral model must be assumed. The model is used to produce a predicted counts spectrum, which is compared to the data. This predicted counts spectrum is used to deduce a (model-dependent) sensitivity at each energy which can be used to derive a photon spectrum. At any energy E,

$$F_{obs} = C_{obs}(F_{pred}/C_{pred}),$$

where F is the photon flux and C is the counts. The predicted flux and counts are produced by the spectral model and the instrument response function. The flatter the model spectrum, the larger the relative contribution at any energy from photons of higher energy, and thus the smaller the predicted sensitivity $S = (C_{pred}/F_{pred})$. Because of the dependence of the sensitivity on the assumed spectral shape, points in the unfolded photon spectrum "move" to more closely match the model. This "obliging" behavior of data points was discussed by Fenimore, Klebesadel, and Laros (1983). The result is that if a line is assumed, a linelike feature can be produced in the unfolded spectrum though none is actually present. The importance of this effect depends on the instrument response function and, in particular, on the degree

of Compton supression. If the analysis is properly done this effect will not change the statistical significance of features.

A second problem, pointed out by Fenimore *et al.* (1982b), results from the fact that the K-edge of I (at about 32 keV) is in the same energy range as the features. At the K-edge the attenuation coefficient, and thus the detection efficiency, changes discontinuously by about an order of magnitude, and any small gain shift which is not corrected for can produce spurious absorption features in the unfolded spectrum. Real-looking features can be produced by this process, at least in a limited energy range. It is probably *not* possible to produce all the observed narrow features in this manner.

Finally, even if the features are real and are produced by cyclotron absorption they are only present in ~10–15% of all bursts. Since lower fields would produce lines below the range of the KONUS detectors, the observed features might well represent only the high end of the field strength distribution. That is, there is no reason to suppose, *a priori*, that the measured fields are typical.

To summarize, despite the possible experimental problems, it is likely that real low-energy features have been observed in some bursts. However, the theoretical problems with the interpretation of the features as cyclotron lines, combined with the existence of plausible alternative hypotheses, make the lines at best an ambiguous measure of the source magnetic field. The small fraction of events with such features further implies that any measured field may not be typical.

Conclusions

Neither the theoretical arguments nor the experimental evidence provide a compelling case for the presence of very strong magnetic fields in gamma-ray burst sources. Since much of interest depends on the source field strength, it would be useful to have an independent measure of the magnetic field.

SINGLE-PHOTON PAIR-PRODUCTION IN SUPERSTRONG FIELDS

At the high field strengths inferred for burst sources new physics becomes important. Of particular interest, it is possible for a single high-energy photon to produce an electron-positron pair. This process provides an independent way to measure the strength of the ambient field based on the observed spectra.

High-energy photons (> 1.022 MeV) moving through a region of very strong magnetic field ($> 10^{12}$ G) may "annihilate," becoming an electron-positron pair. The particles carry away the excess energy of the photon (above the rest mass of the particles) as kinetic energy. Momentum is conserved by the interaction with the magnetic field. The secondary particles then radiate photons as they move in the magnetic field; if these photons are of high enough energy, they may again produce pairs. This process continues until the photon energies are below the pair-production threshold or the photons escape from the high-field region. The effect of this is that strong magnetic fields can act as efficient attenuators of high-energy photons.

Single-photon pair-production requires superstrong fields and high photon energies, and has thus never been observed in the laboratory. However, it is a straightforward result of quantum electrodynamics. The physics of single-photon pair-production in superstrong magnetic fields has been discussed by (among others) Erber (1966), Tsai and Erber (1974), and Daugherty and Harding (1983); it was first applied in an astrophysical situation in connection with pulsars (Sturrock 1971). Cascades in pulsars ("electromagnetic showers") have been extensively studied and modelled (e.g., Daugherty and Harding 1982).

Theory

Most of the following is based on Daugherty and Harding (1983), to which the reader is referred for a more complete treatment; the discussion here is limited to a relation of the results of that paper.

For our purposes the primary result can be conveniently expressed as a pair-production attenuation coefficient for the high-energy photons, as a function of photon energy and magnetic field strength. The exact expression (eq. 6a and 6b in Daughery and Harding (1983)) is rather involved, but an accurate approximation

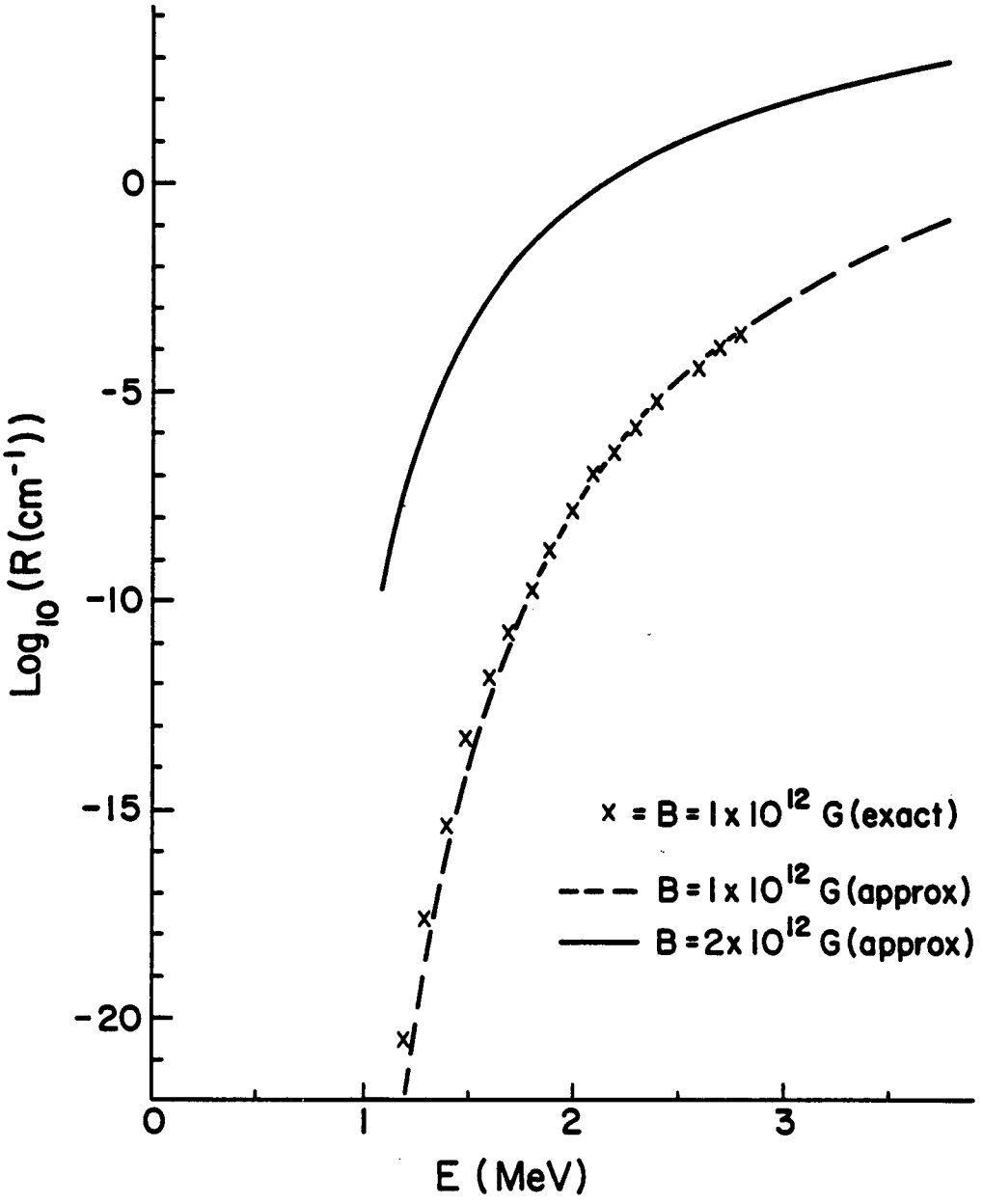

Fig. IV-1: The approximate single-photon pair-production attenuation coefficient for two values of the magnetic field. Also shown are some exact values for B = 1×10^{12} G, from Daugherty and Harding (1983), Fig. 5.

has been derived by the same authors:

$$R_0 = 0.23 C_0 B' \exp(-4f(E', B')/(3E'B')),$$

for $E' = E/(2mc^2)$ above threshold ($E' = 1$), $B' = B/(4.414 \times 10^{13}\mathrm{G})$. $C_0 = 2\pi\alpha/\lambda$, the fine-structure constant times 2π divided by the Compton wavelength. The function f, derived by the authors from a fit to the exact attenuation coefficient, is:

$$f(E', B') = 1 + 0.42 E'^{-2.7} B'^{-0.0038}.$$

This assumes that the photon is propagating perpendicular to the magnetic field. For an arbitrary angle θ between the direction of photon propagation and the magnetic field, the appropriate Lorentz transformation must be made:

$$R(E, \mathrm{B}) = \sin\theta R_0(E \sin\theta, \mathrm{B})$$

(Daugherty and Harding 1983, eq. 22). Figure IV-1 compares the exact and approximate attenuation coefficients for two values of the magnetic field over a range of photon energies. The continuous curves come from the evaluation of the above expression for R_0 and the individual points from the exact expression in Daugherty and Harding (1983). Clearly the agreement is excellent and no significant error will be introduced by using the approximation.

Two points about the attenuation coefficient are particularly important for the following application: the dependence on photon energy and the dependence on the photon propagation angle.

Energy dependence. As Figure IV-1 shows, the attenuation coefficient rises very rapidly, e.g., more than 10 orders of magnitude between 1.2 and 2 MeV for $B = 1 \times 10^{12}$ G. A large increase in attenuation over small energy range may produce a sharp cut-off in the observed spectrum. However, a *sharp* cut-off is not required for the argument below, which depends only on the absence of emission above some energy, and the fact that there are no cut-offs below threshold, 1.022 MeV.

When a photon is transformed into an electron-positron pair, 1.022 MeV of the original energy is in the rest mass of the particles and the remainder is in kinetic energy. The kinetic energy is rapidly lost by synchrotron radiation, producing

(generally) many photons of low energy. The synchrotron radiation length is very short compared to the attenuation length, and the electrons reradiate promptly. The peak of the radiated spectrum, and thus most of the photons, are at relatively low energy. Thus a single high-energy photon is rapidly converted into a large number of low-energy photons. Any photons produced above threshold are again subject to the process of attenuation and synchrotron radiation. If the original photon spectrum declines with energy, there are few higher energy photons to "fill in" the attenuated spectrum through their own attenuation. In any case, even very high-energy photons are degraded, within a few attenuation lengths, to below the threshold for this process. Therefore a large number of attenuation lengths combined with the rapidly rising attenuation coefficient should give a strong cut-off.

Calculations have shown that the resulting spectrum does indeed have a sharp cut-off at a critical energy which depends on the field strength B and the sine of the angle θ between the photon direction and the direction of the magnetic field (Õgelman, Ayasli, and Hacinliyan 1977). These authors made a calculation in which individual photons, and their secondaries, were followed as they traversed the field. The result is that the emergent photon spectrum cuts off rather sharply above threshold, while it softens below threshold. Although these authors used an old approximation which is not accurate near threshold (see Daugherty and Harding (1983)), the results are qualitatively correct.

Angular dependence. The second notable feature of the attenuation coefficient is the strong dependence on angle derived from the Lorentz transform. This produces an angle-dependent threshold, and thus an angle-dependent cut-off.

This effect is illustrated by Figure IV-2 which shows the cut-off energy as a function of angle for two field strengths. Here it has been assumed that the cut-off occurs at the photon energy for which the attenuation length equals 10 cm. This choice is discussed in more detail below; however, the threshold depends only weakly on this value.

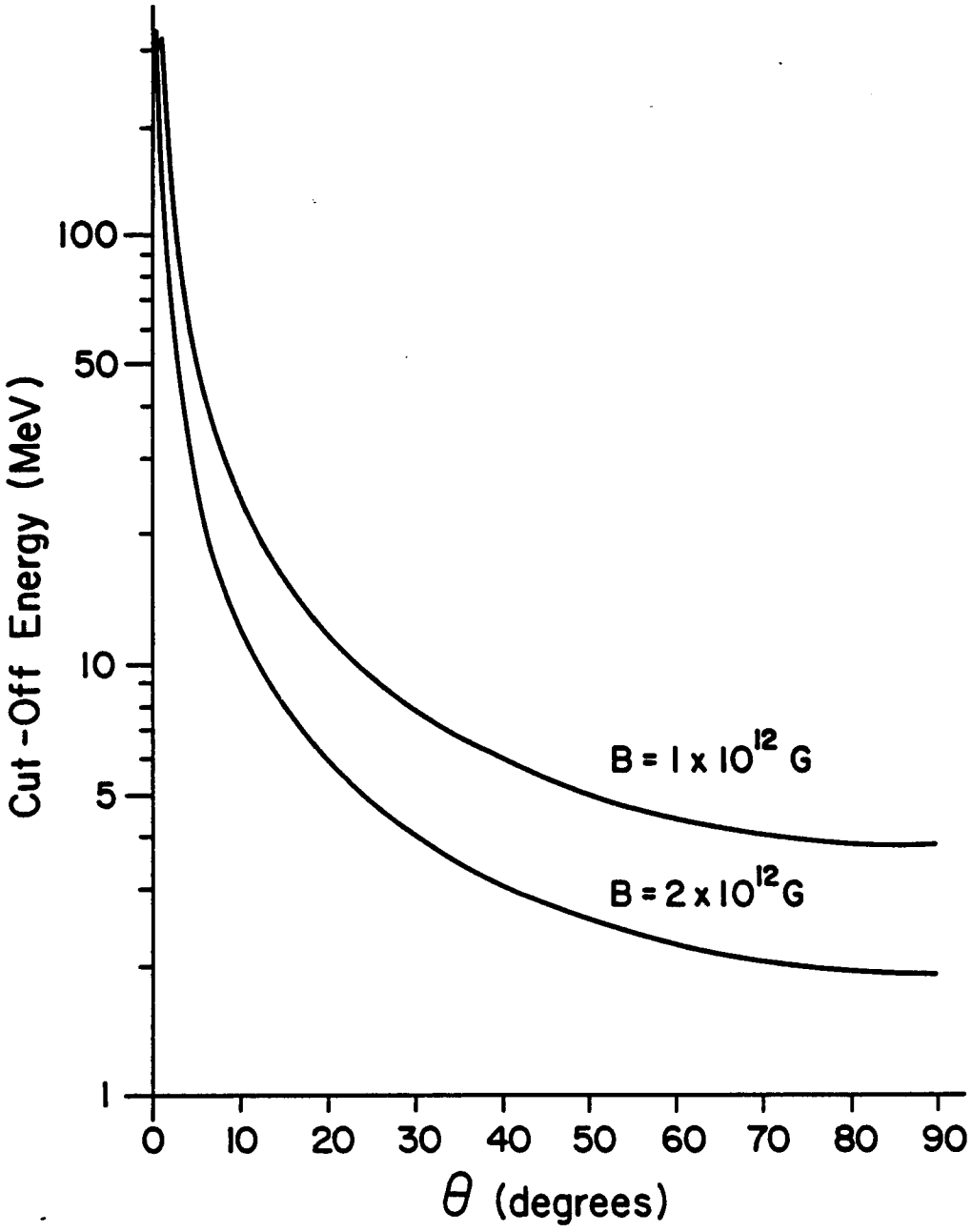

Fig. IV-2: The cut-off energy as a function of angle for two magnetic field strengths, using the approximate form of the attenuation coefficient given in the text and assuming that the cut-off occurs when the attenuation length equals 10 cm.

GRS DATA AND ANALYSIS

The results of the previous section can be used to derive an independent limit on the magnetic field strength at the sites of gamma-ray bursts. Single-photon pair-production can produce a cut-off in the observed gamma-ray spectrum; the energy at which this cut-off occurs depends upon the strength of the magnetic field and the angle θ defined above. Therefore the highest observable energy in each event implies a coupled limit on B and θ for that event. Under certain conditions (in certain models) the value of θ can be assumed. In that case, for each event an upper limit on the B field can be deduced. This is discussed below. A more general limit (requiring fewer assumptions), applying to the whole class of gamma-ray bursts, can be derived using statistical arguments.

Statistical Analysis

Using our whole data set and relying on the relation between the spectral cut-off energy and the angle of observation with respect to the field we can derive an upper limit on the "typical" magnetic field strength. The emission below 1.022 MeV is not attenuated by the field and may be isotropic. If the low-energy emission *is* isotropic and the source is near the stellar surface, these photons will be observable over a solid angle of approximately 2π sr. In a strong field the higher energy photons may be attenuated by single-photon pair-production. For a fixed field strength and configuration there is a maximum angle for which any photon above 1.022 MeV can escape, and this angle *decreases* with increasing photon energy (see Figure IV-2). Thus, at higher photon energies the burst is observable over a smaller solid angle.

Because our burst list is based on the detection of photons below the threshold for this process, our data set presumably represents a random sample of observation angles (assuming the low-energy emission is isotropic). At any given field strength, then, the fraction of all bursts which are observable above any photon energy should be less than or equal to the solid angle of escape for that energy, divided by 2π sr, the solid angle of escape for low-energy photons. Then the *actual* fraction of events observed at high energies gives an upper limit on the typical field strength at the radiation site.

GRS Data. A measurement of the source magnetic field strength can be made

by comparing the fraction of all events *observed* at high energies with the fraction *predicted* assuming a particular field strength. Fig. IV-3 shows such a comparison for two magnetic field strengths. To calculate the predicted fractions the solid angle of emission was found for photon energies in 1 MeV increments. The ratio of this solid angle to 2π sr is the fraction of events which would be detectable at that energy, given: 1) a random sample of observation angles, 2) isotropic low-energy emission, 3) no other attenuation processes (which would lower the observed fraction), and 4) a perfect detector. However, the detector is not perfect; as previously discussed, it has a declining sensitivity to falling spectra even if no cut-offs are present. To account for the instrument response, the fraction of events predicted is multiplied by the fraction of events which would be detectable, assuming a power law with no softening or cut-off. The result is the fraction of events which would be detectable by GRS as a function of energy, for the specific field assumed.

The solid line indicates the percentage of events actually observed at or above photon energy E. The dashed and dotted lines indicate the fraction of events we would expect to observe for fields of 1×10^{12} G and 2×10^{12} G, respectively. If the actual spectrum is softer than a power law, we would expect even fewer events. Above 5 MeV, the binomial probabilities for seeing the observed number of events or more, assuming that the *predicted* fractions are correct, are $\sim 9.3 \times 10^{-4}$ (corresponding to 3.1σ significance) for 1×10^{12} G and $\sim 1.7 \times 10^{-11}$ (6.6σ) for 2×10^{12} G. Even if we exclude the effects of declining instrument sensitivity, the prediction for a 2×10^{12} G field differs by 3.1σ from the observations.

For these calculations we have estimated the spectral cut-off to be at the photon energy for which the attenuation length equals 10 cm, using the approximate form of the attenuation coefficient given by Daugherty and Harding (1983). This length is much less than the expected physical scale size of the magnetic field, so this assumption produces a conservative limit on the field. The results are not sensitive to the chosen attenuation length. Under the less-general assumption of a dipole field, we can set a slightly lower limit on the typical field strength: 8×10^{11} G at 3.7σ significance.

These observations do *not* exclude the possibility that some burst sources have

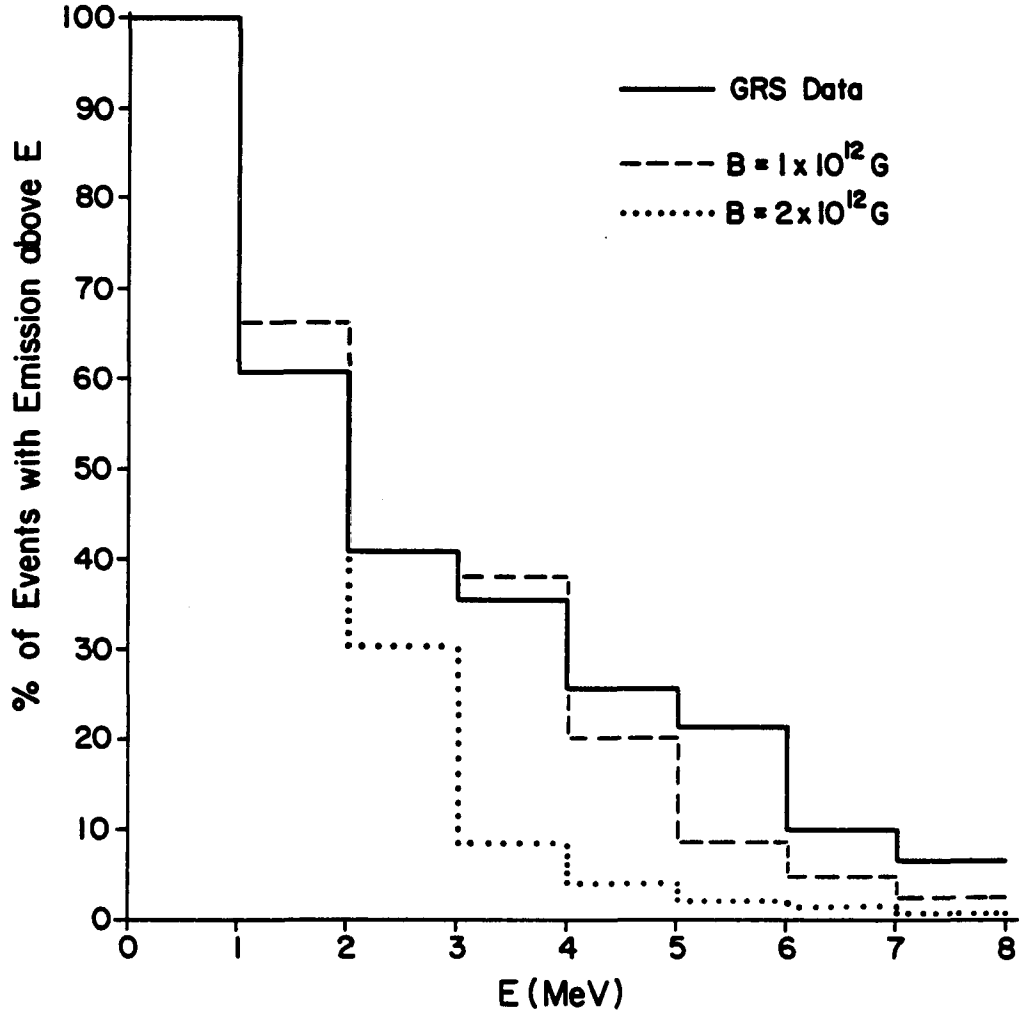

Fig. IV-3: The number of events with maximum observed energy greater than or equal to E *vs.* E, along with the number of events *expected* to be observable assuming isotropic low-energy emission and the two magnetic field strengths listed.

fields of greater than 2×10^{12} G, but most must be weaker and, indeed, the typical field strength must be less than 1×10^{12} G. This indicates that the magnetic fields inferred from the KONUS data cannot be representative of the entire source population. This is not surprising since fields of lesser strength would produce features outside the effective energy range of the KONUS instruments.

In certain models most of the emission is expected to come out at large angles to the field. Examples of this are emission by synchrotron radiation, or accretion models where there is a large amount of overlying matter. If we assume $\theta = 90°$, we can get a stronger constraint on the field, and indeed a limit for each event. Under this assumption, observed emission above 4 MeV (18/71 events) implies a field of less than 1×10^{12} G; emission above 8 MeV (3/71 events) would require $B < 5 \times 10^{11}$ G under these assumptions.

Discussion

It is possible to conceive of models which avoid this constraint on the field. The difficulty is in constructing a realistic model which avoids this limit and is not inconsistent with the data supporting strong fields. For example, both low- and high-energy emission could be beamed due to bulk motion along the field lines. It is not clear, though, that the observed narrow features could be produced in such an environment. Alternatively, the high-energy emission might be a separate component, originating in a low-field region away from the strong fields in which the < 1 MeV photons are produced. While this may be implausible, we cannot rule it out based on our data alone. However, we have found no strong evidence that the observed spectra are composed of separate high- and low-energy components. In neither of these cases would the plasma be confined, so the original argument for high fields would be invalid.

The conclusions of this section do not depend on the GRS data set being strictly unbiased. All that is required is that we not be biased in favor of events without observable cut-offs. Since our search for events covered E ~300–400 keV and the pair-production process increases flux < 1 MeV and decreases flux > 1 MeV, we are actually *more* likely to detect events with cut-offs produced by this process. Thus removal of bias from our sample would strengthen, not weaken, our conclusions.

CONCLUSIONS

Based on the pair-production attenuation of high-energy photons and assuming isotropic low-energy emission, we have placed an independent limit on the typical field strength at burst sites that is below the level deduced from the KONUS data. It is important to note that the geometrical argument used to place a limit on the magnetic field applies equally well to any model which requires high-energy emission to be selectively beamed. The observations argue against *any* scheme of isotropic low-energy emission and highly beamed high-energy emission. Low- and high-energy emission must, in general, have roughly similar angular distributions. *Both* the high- and low-energy radiation may be beamed; then the limit on the field could be avoided, but many more sources would be required.

This limit on preferential beaming will constrain certain types of models and radiation mechanisms. For example, Woosley (1984) predicts possible strong beaming of high-energy emission; Hameury *et al.* (1985) do also. It is very constraining on models (e.g., those powered by accretion or radiating by synchrotron emission) with most radiation coming out perpendicular to field. The limit may constrain some models which require a very high field (e.g., models which require funneling of accretion flow to the poles, or confinement of accreted matter at the poles).

V. SUMMARY AND CONCLUSIONS

Early observations produced a picture of gamma-ray bursts as events with relatively soft spectra; despite the name given to these transients, most of the energy seemed to be in X-rays, with little or no high-energy emission. This picture was accepted for a number of reasons. While most burst instruments were effectively limited to energies below 1 MeV, the spectral models which were used to fit the data at low energies were generally quite soft, and thus predicted very little flux at gamma-ray energies. In addition, the conditions which were thought to exist at bursts radiation sites (high photon density, strong fields, thermal particle distributions) were expected to severely limit high-energy emission.

The GRS results have caused a change in this view. Gamma-ray bursts are truly a gamma-ray phenomenon. High-energy emission is a common feature of bursts; the data are consistent with emission to greater than 5 MeV in all events. There is no indication in the data than any event has a sharp spectral cut-off. Emission above 1 MeV is energetically a large part of the total observed burst energy. These results affect ideas about particle acceleration and heating, the radiation mechanism, the environment at the source, distances to the sources, etc. Bursts have often been treated as thermal phenomena, but the presence of high-energy emission, the requirement of very high temperatures to fit the data, and the large fraction of total energy in high-energy photons make thermal models seem unlikely.

Consistent with this, the thermal spectral models which fit the data at low energies do not in general explain the high-energy radiation as well as a harder model such as a power law. There are a number of exceptions to this, however, and in particular there are spectra with evident curvature which can only be well-fit by a thermal model. Whether the differences in spectra indicate the existence of different classes of bursts is not clear.

The origin of this emission is an important question: is it produced by the same process as the low-energy flux, or is it a hard "tail" from some other mechanism,

added to a basically soft spectrum? Although two-component models have been proposed (Mazets *et al.* 1983; Matz *et al.* 1984), there is no strong indication of separate components in our data. There are no obvious breaks or bends to harder spectra in the GRS energy range, and no systematic hardening of spectra at high energies. Burst emission shows similar time behavior and peak structure at all measured energies (although spectral evolution is observed). The fact that high-energy emission is observed in many events also argues against some types of two-component models. If there is a second component, it is roughly as important energetically as the low-energy component and can hardly be described as a "tail."

The GRS observations also allow a limit to be placed on the magnetic field at the emission site which is independent of the previously used methods of estimating the field strength. The GRS limit is below those earlier results. Given the theoretical and experimental difficulties with the earlier estimates, there is currently no strong reason to believe that there are very strong fields at burst sites. Further, the GRS observations place a limit on the degree to which high-energy photons can be *preferentially* beamed by any process.

It will be interesting to see future theoretical efforts which take these results into account. However, it seems unlikely that theory, or observations by bigger and better instruments, will make rapid progress on the fundamental issues: where are the sources, what are the sources, and how are bursts produced. The best hope is that one or more burst sources will be associated with identifiable objects. Unfortunately, the results of such attempts to date are not encouraging.

APPENDICES

APPENDIX A

THE GRS RESPONSE FUNCTION

The response function for the Gamma-Ray Spectrometer is based on work originally done by D. J. Forrest and B. M. Gardner, implemented, with modifications, in Fortran on a Honeywell Level 6 Computer by J. M. Ryan. In its current form it has been extensively revised by D. J. Forrest with assistance from and programming by this author.

It is an unfortunate experimental fact that a monoenergetic photon beam does not produce a monoenergetic response in a scintillation detector. Instead, because of the number of different ways a photon can interact, depositing some or all of its energy in the detector, a complicated spectrum results with counts from the low-energy threshold up to slightly above the input photon energy. Analysis of complicated observed spectra which may contain multiple lines and continua requires a good understanding of this instrument dependent response. In fact, even with a perfect knowledge of the instrument response it would not be possible to perform the inverse operation unambiguously to derive a unique photon spectrum from the observed counts spectrum.

In the energy region of interest (< 10 MeV) the three basic processes by which an incoming photon interacts in the detector are 1) photoelectric, 2) Compton scattering, and 3) pair-production. Good discussions of these processes in relation to gamma-ray detectors are contained in Evans (1955) and Chupp (1976).

Each of these processes contributes one or more features to the counts spectrum of a monoenergetic photon beam. Actual observed spectra are superpositons of many of these monoenergetic spectra at different energies and intensities. An empirical approach has been taken to the analysis of the components of the GRS response. The various features of the instrument response to nuclear line spectra

(photopeak, first escape peak, Compton tail, and Compton edge feature) were independently measured using pre-flight calibration data and, to a lesser extent, in-flight data. The characteristic parameters of these features (e.g., intensity, width) were measured for different incident photon energies. The data so obtained were then fit to piecewise analytic functions of the original photon energy. The measurements of absolute efficiency and the photofraction were based in part on data from Berger and Seltzer (1972). Figures A-1 through A-8 depict both the original data and the fitted functions used in the response program for the several components.

With these functions the idealized exact electron energy deposit spectrum can be produced for any input gamma-ray line. This spectrum is then smoothed by the instrument resolution, which was also measured from the calibration data. Finally, the channel-to-energy relation is used to transform the smoothed spectrum into the predicted instrument response in counts *vs.* channel number. Continuum spectra are produced as a sum of gamma-ray lines of appropriate energy and intensity. As an illustration of the resulting spectra, Figures A-9 through A-11 compare the predicted instrument response to the measured calibration spectra. See also Fig. I-4 for an in-flight comparison.

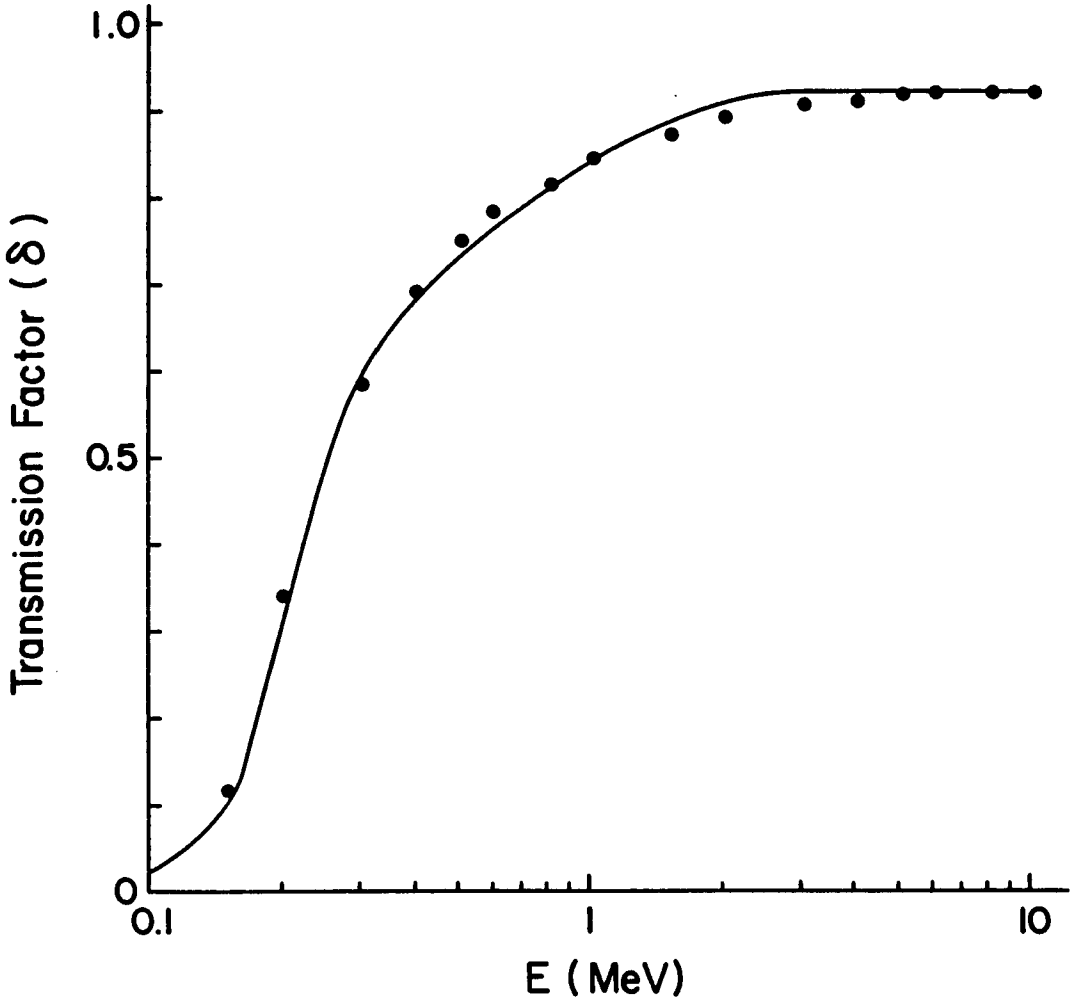

Fig. A-1: The fraction of the incident photon flux which passes through the material in front of the detector: $(0.307\text{g} - \text{cm}^{-2})$ Al + $(0.827\text{g} - \text{cm}^{-2})$ Pb + $(1.0\text{g} - \text{cm}^{-2})$ plastic + $(0.432\text{g} - \text{cm}^{-2})$ stainless steel. The actual values, calculated from the known attenuation coefficients, are shown as points. The analytic approximation used in the response function is shown as a line.

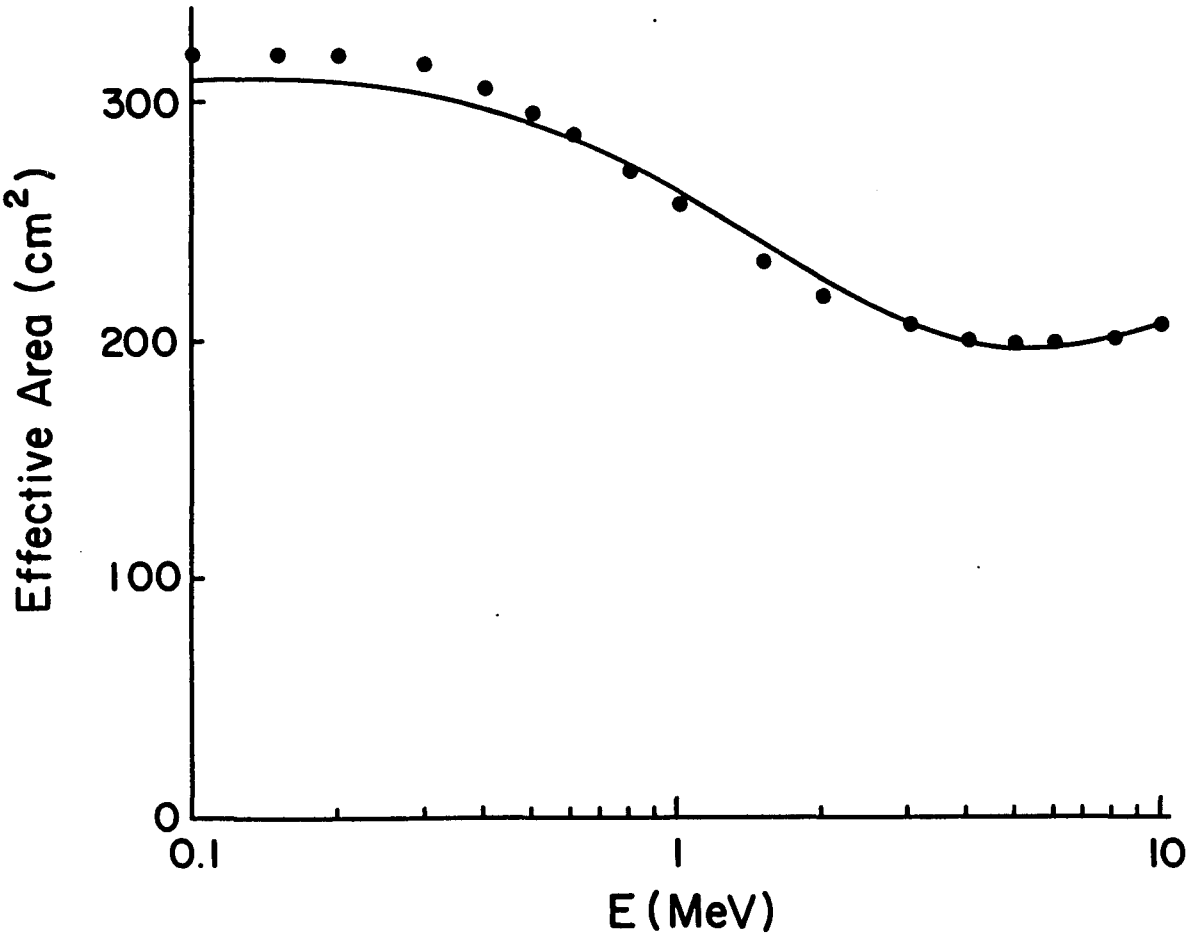

Fig. A-2: The effective area (A) of the main detector (in cm^2) as a function of incident photon energy. The effective area is the interaction efficiency (ϵ) times the geometrical area of the detector. The values of ϵ are taken from Berger and Seltzer (1972); these were used to produce the plotted points. The line is the analytic function used in the response function.

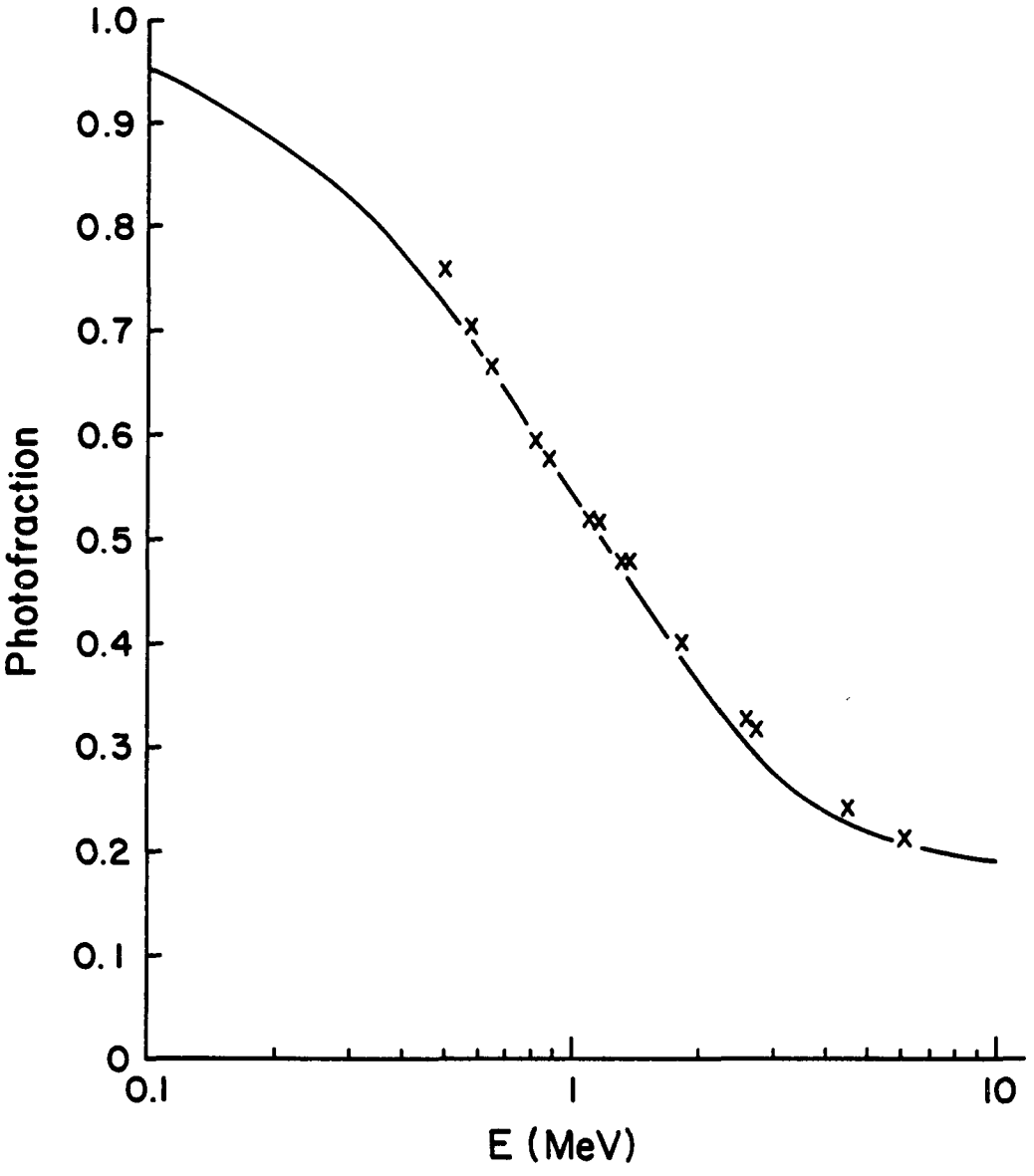

Fig. A-3: The photofraction P_0, which is the fraction of interacting photons which produce a count in the photopeak. The photofraction for a single 3 in. × 3 in. NaI crystal is given by Berger and Seltzer (1972). This is equivalent to the photofraction in the GRS "singles" mode, made up of those events producing signals in only one of the seven detectors. The "totals" mode includes these events and also those producing signals in more than one detector. The photofraction for the totals mode (which is shown) is the singles photofraction multiplied by the observed ratio of counts in the totals photopeak to counts in the singles photopeak. The points indicate values measured in the calibration data; the line is the response function approximation. All features in the response function are scaled to the photopeak area $= \delta \times A \times P_0$.

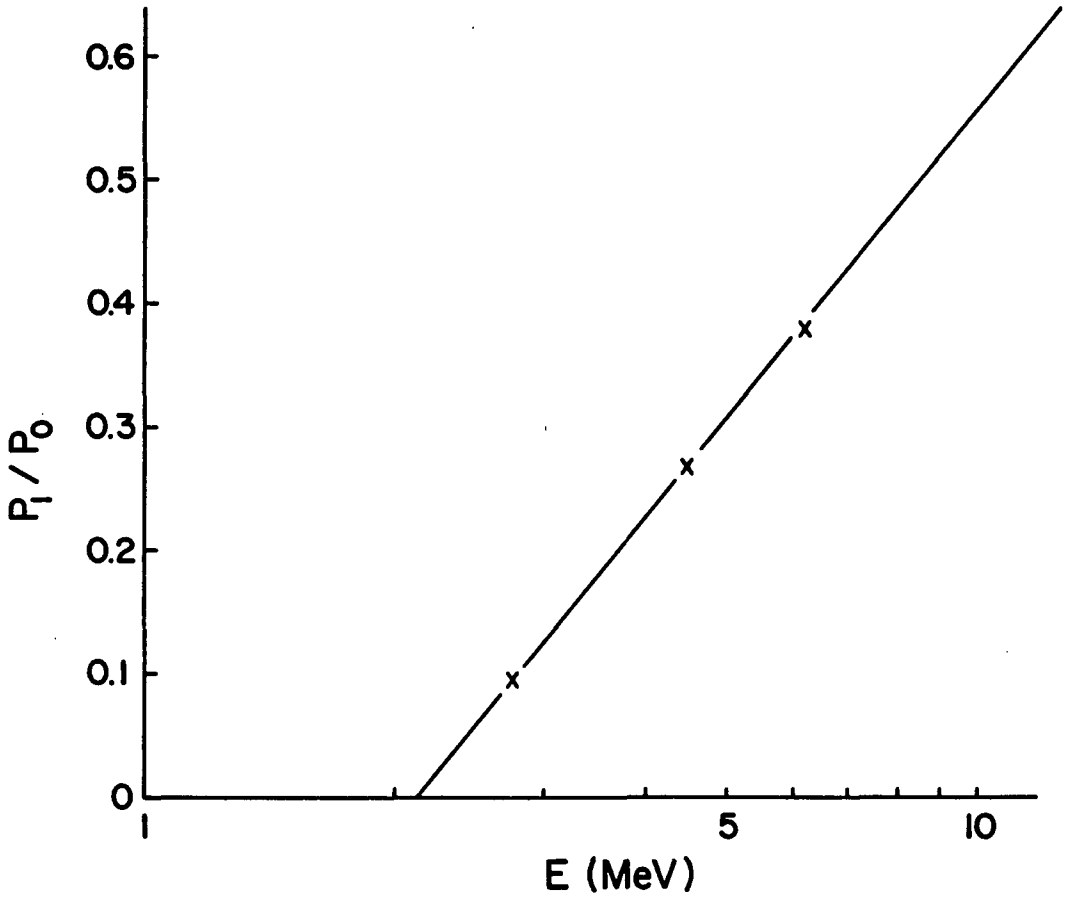

Fig. A-4: The ratio of the fraction of photons producing a count in the first escape peak (P_1) to the photofraction (P_0). The points indicate measurements from calibration data, and the line is the analytic approximation.

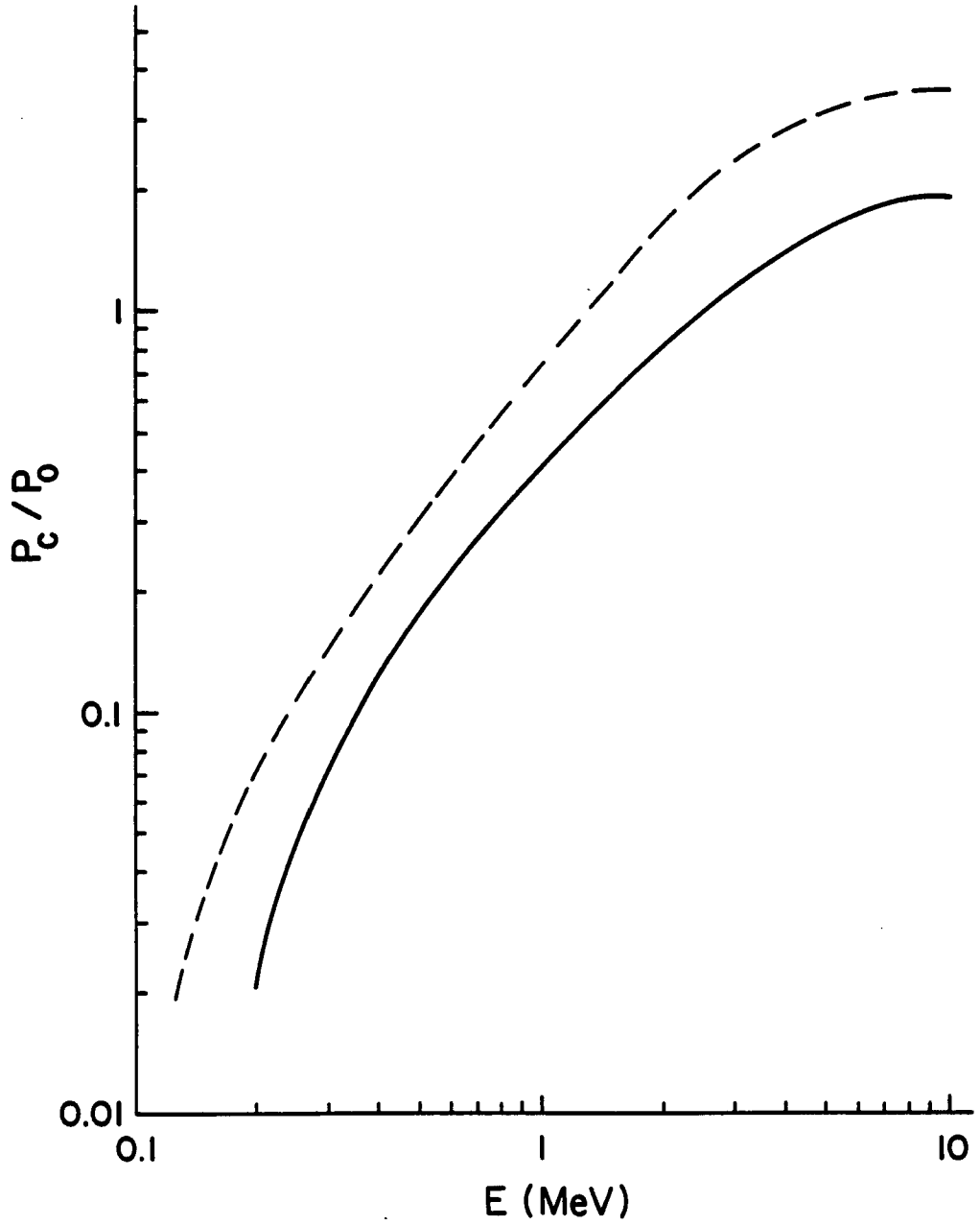

Fig. A-5: The ratio of the fraction of photons producing a count in the Compton tail (P_C), excluding the edge feature, to the photofraction (P_0). The solid line is the analytic approximation used in the response function ($P_C = (1 - P_0 - P_1)/2$). The dashed line is the upper limit, assuming no Compton suppression by the shields. The actual value of this parameter depends on the shield thresholds, which are not well known. In addition, the preflight calibration spectra are contaminated by photons which scattered in the room and were then detected; the result is that the Compton tails are artificially high in those spectra (Fig A-9 to A-11). See Dunphy and Forrest (1985) for a discussuion of this problem. Fortunately, the response is not very sensitive to the height or shape of the Compton tail.

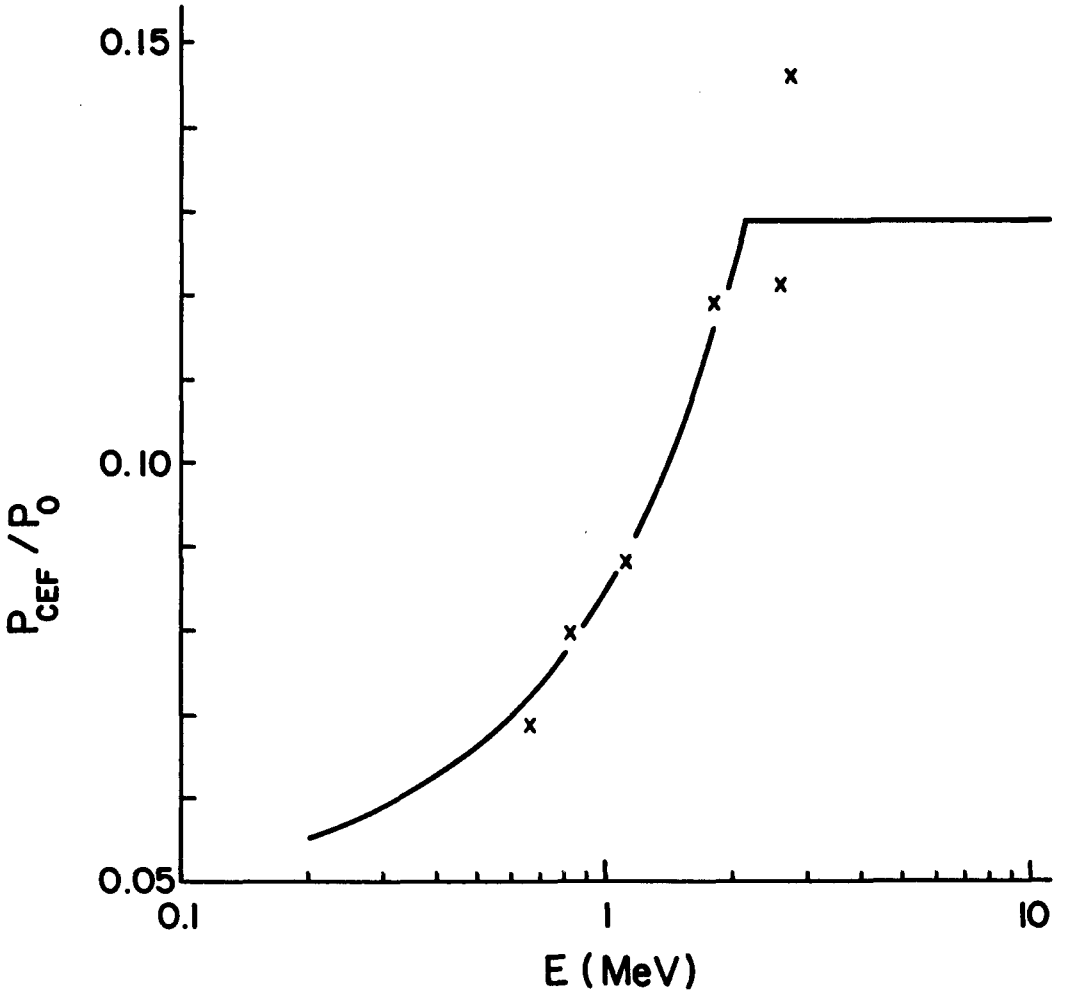

Fig. A-6: The ratio of the fraction of photons producing a count in the Compton edge feature (P_{CEF}) to the photofraction as a function of incident photon energy. The Compton edge feature is a broad peak with a peak energy two σ below the Compton edge. The points are measured from calibration data and the line is the fit used in the response function.

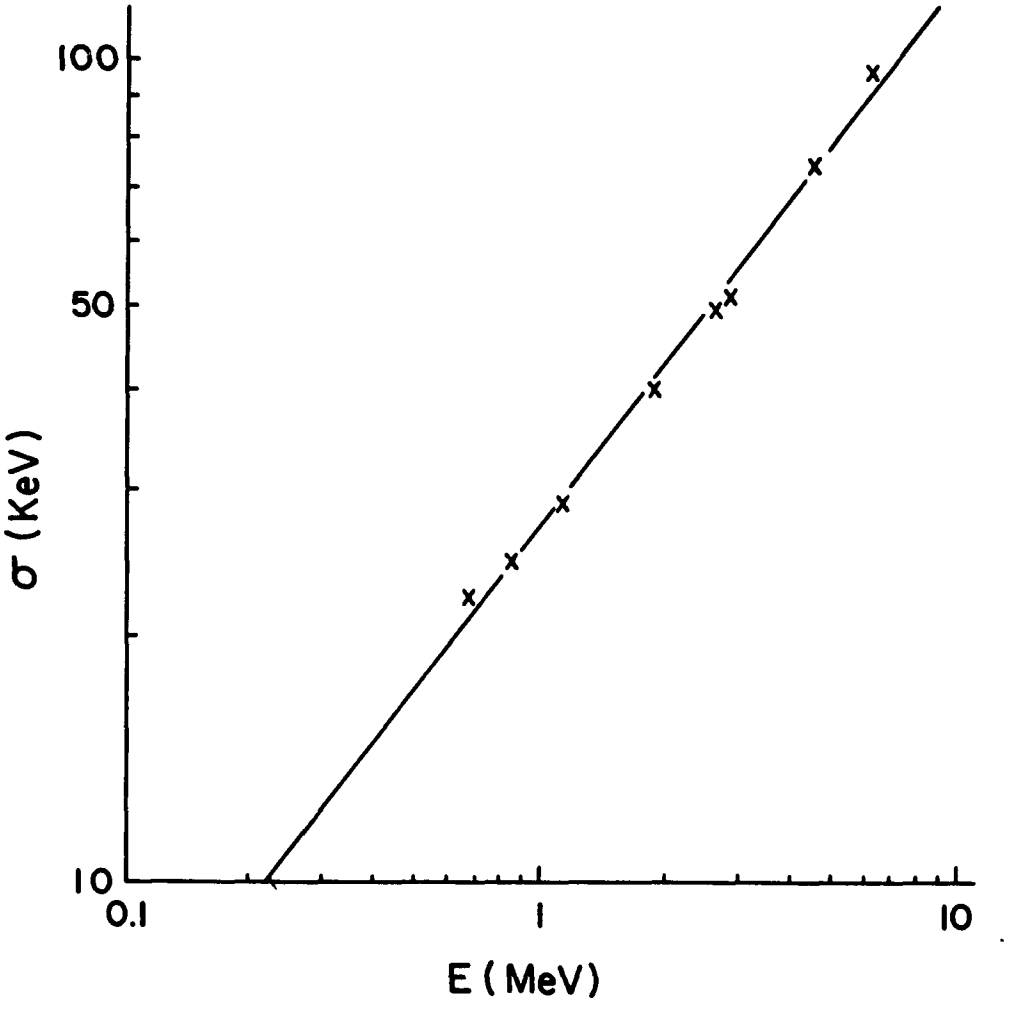

Fig. A-7: The resolution (σ) of the GRS in keV as a function of energy. The points are measured from calibration data and the line is the fit used in the response function.

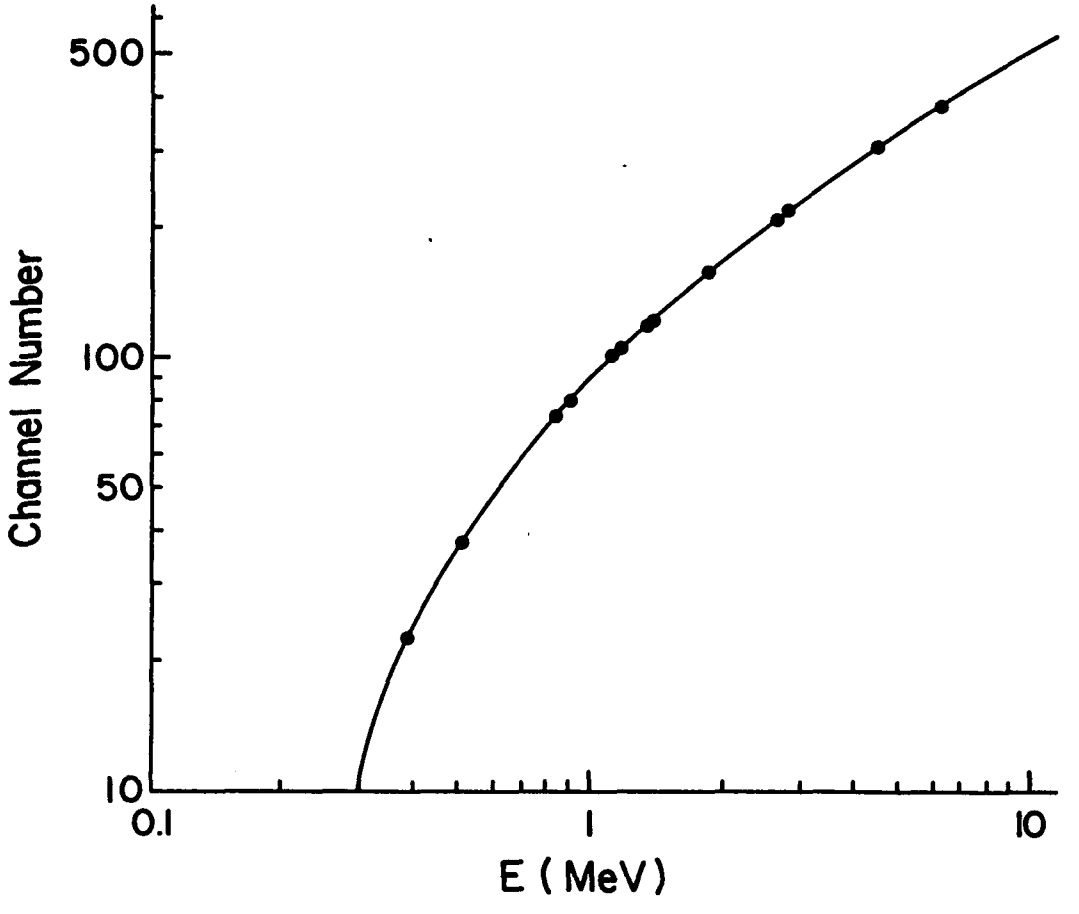

Fig. A-8: The relation between GRS channel number and energy. The points are measured from calibration data and the line is the fit used in the response function.

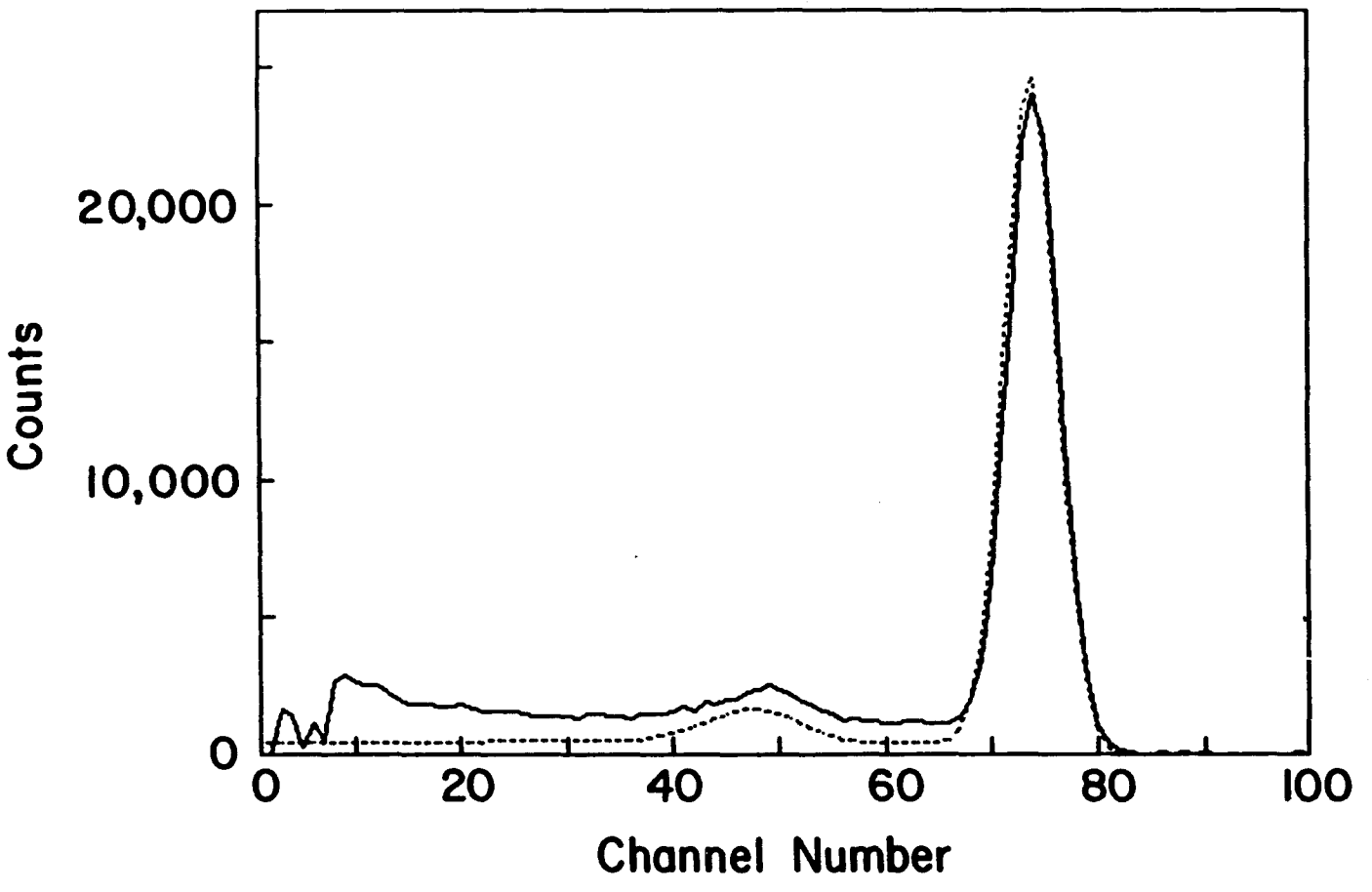

Fig. A-9: A comparison of the pre-flight calibration data (solid line) and the instrument response (dotted line) for the 0.835 MeV line from ^{54}Mn.

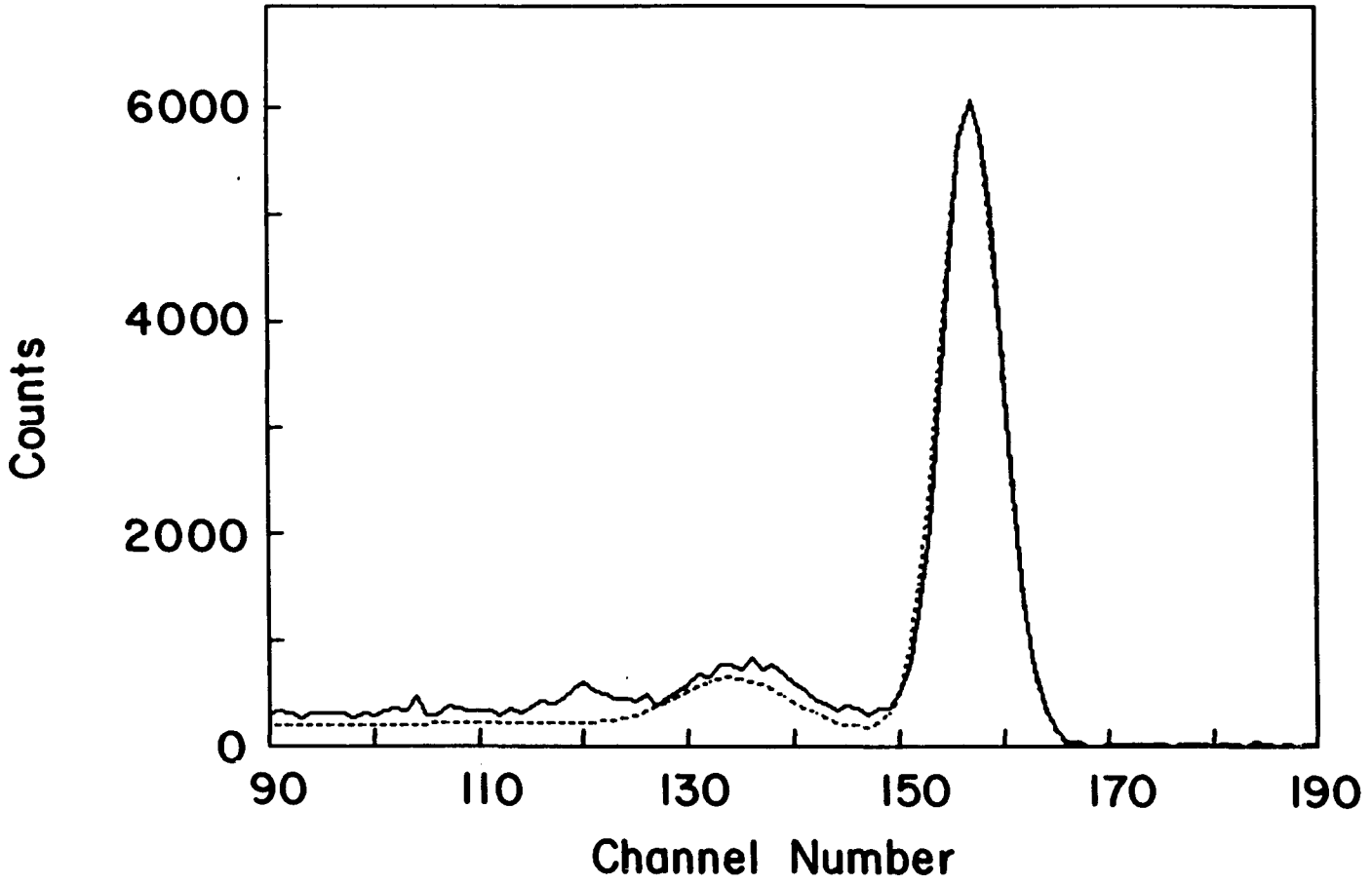

Fig. A-10: A comparison of the pre-flight calibration data (solid line) and the instrument response (dotted line) for the 1.836 MeV line from ^{88}Y.

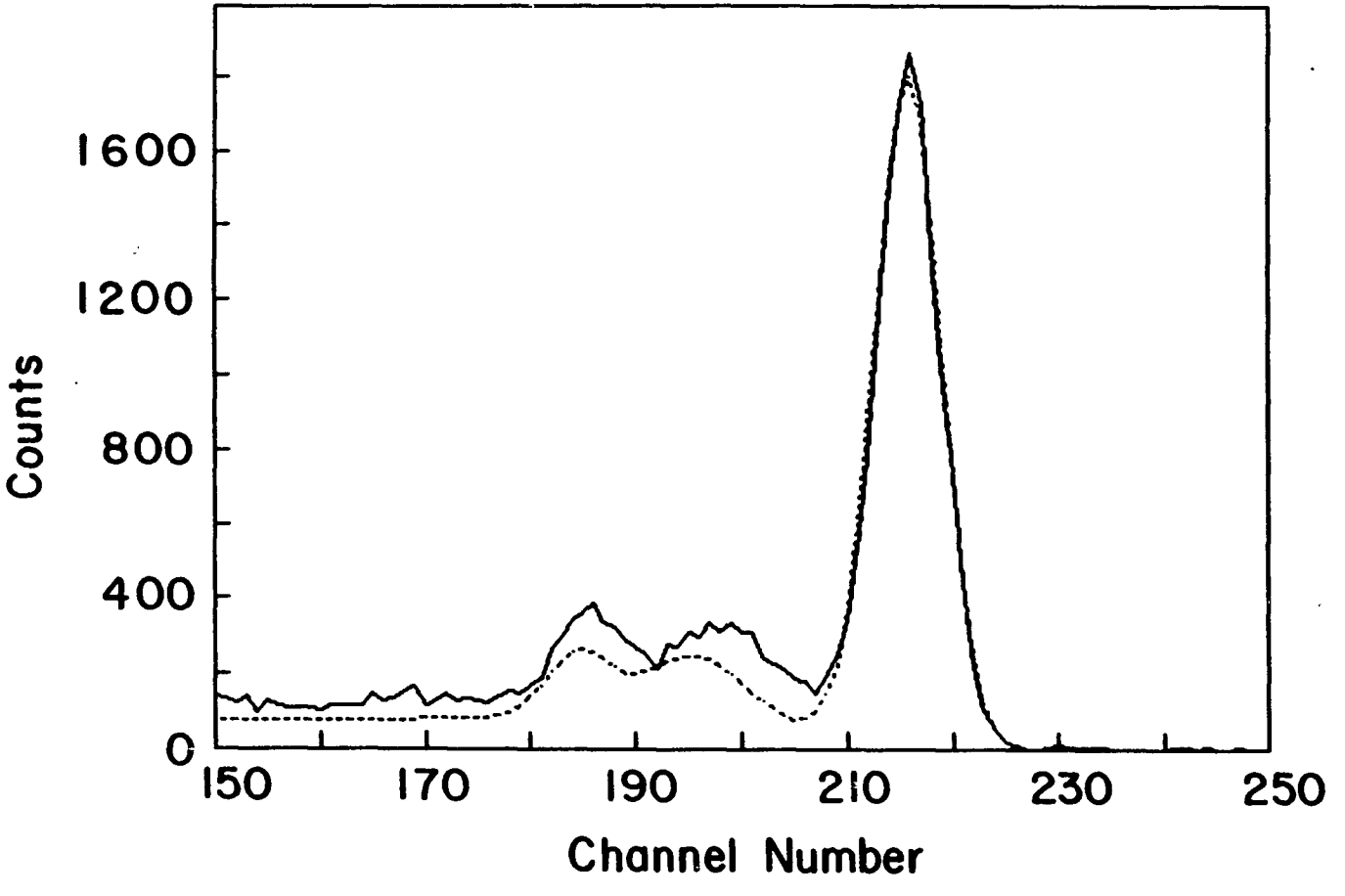

Fig. A-11: A comparison of the pre-flight calibration data (solid line) and the instrument response (dotted line) for the 2.754 MeV line from ^{24}Na.

APPENDIX B

THE SMM/GRS GAMMA-RAY BURST LIST

Following is a list of the 71 gamma-ray bursts analyzed in this work. Each event is identified by date and approximate GRS start time (UT, to the nearest minute). The other items included in the list are:

IN FOV? As described in the text, an event may be identified as in the GRS forward field-of-view by two methods. Timing comparisons with other instruments may provide a rough indication of the direction which is adequate to determine whether the event is in the instrument forward aperture. This work has been done by P. L. Nolan. Second, if a burst is coincident with an event detected by the smaller field-of-view HXRBS experiment it is also taken to be from a source within the aperture. These criteria are not exhaustive and the data are not complete; many events which are not listed as in the FOV may well be.

EMAX (MeV) The maximum energy for which there is detectable flux in the GRS main detectors, in 1 MeV steps (0 indicates EMAX< 1 MeV). The standard for detectability is that the integrated source counts above photon energy E be greater than or equal to 3σ above the measured background.

FITTED PARAMETERS The final three columns list the spectral parameters fit to each burst using three models described in the text. The approximate forms of the thermal synchrotron (TS) and optically-thin thermal bremsstrahlung (OTTB) spectra were used; for OTTB, the Gaunt factor was set equal to 1. The 95% confidence ranges were determined by the technique of Lampton, Margon, and Bowyer (1976).

The spectral fits reported here were made to the whole main detector energy range, 0.3-9 MeV (channels 10–476). All continuum fits were performed by comparing the observed counts spectrum to model spectra generated using the known

instrument response. The best-fit intensity is determined by χ^2 for successive values of the spectral parameters; the minimum of these gives the best-fit spectral parameter listed. To insure adequate statistics the data were binned to a minimum of 25 source counts per bin by summing channels until the minimum was reached. Due to limitations of computer time the tests are made against libraries of previously generated model spectra. The step sizes of the libraries were 0.1 for the PL index, 1 keV for TS E_{CRIT}, and 10 keV for OTTB kT. This limited resolution may result in a significant overestimation of the sizes of the 95% confidence ranges in certain cases. In cases where the values were very large ($E_{CRIT} > 70$ keV, or $kT > 2500$ keV) or small ($E_{CRIT} < 1$ keV) the step size was increased or decreased by a factor of 10.

SMM/GRS GAMMA-RAY BURST LIST

DATE	START TIME	IN FOV?	EMAX (MeV)	PL INDEX (95% RANGE)	TS E_{CRIT} (keV) (95% RANGE)	OTTB (keV) (95% RANGE)
80/03/07	05:07	T	1	2.7 (2.9–2.4)	5 (7–3)	330 (410–270)
80/03/24	23:58	F	2	2.1 (2.5–1.8)	11 (24–5)	480 (850–310)
80/04/19	01:20	T	5	2.3 (2.4–2.1)	11 (14–9)	590 (700–510)
80/04/21	03:08	T	0	3.5 (4.3–2.9)	2 (4–0.8)	170 (250–120)
80/05/12	23:32	F	0	1.7 (2.2–1.4)	38 (100–11)	1840 (6300–510)
80/05/24	15:54	F	0	2.6 (2.9–2.4)	5 (8–3)	360 (450–290)
80/06/02	13:20	F	4	1.6 (1.9–1.4)	61 (100–36)	3300 (5200–2090)
80/07/06	08:44	F	1	2.2 (2.5–1.9)	15 (24–8)	800 (1190–530)
80/07/09	07:24	F	0	2.6 (3.3–2.1)	5 (11–2)	350 (580–210)
80/08/12	18:55	F	3	2.1 (2.7–1.8)	7 (23–2)	360 (760–200)
80/08/15	18:21	T	5	2.5 (2.7–2.3)	6 (9–4)	380 (460–310)
80/09/19	19:21	F	1	2.1 (2.4–1.8)	16 (33–7)	690 (1650–380)
80/09/20	14:10	T	0	2.3 (3.3–1.8)	11 (35–2)	530 (2010–190)
80/10/16	06:04	F	3	2.1 (2.6–1.8)	16 (38–4)	550 (2130–280)
80/11/19	17:06	T	2	2.3 (2.6–2.1)	9 (13–6)	500 (640–390)
80/12/20	18:30	T	6	2.1 (2.2–1.9)	19 (21–17)	1010 (1080–950)
81/01/07	08:47	F	0	2.9 (4.4–2.0)	2 (8–0.6)	190 (400–100)
81/01/27	00:40	F	0	2.1 (3.0–1.7)	16 (45–3)	770 (2270–290)
81/01/29	04:15	F	5	1.4 (1.7–1.1)	120 (230–66)	5500 ($>$ 9900–3100)
81/02/25	04:47	T	0	4.4 (8.6–2.1)	0.7 (7– $<$ 0.1)	110 (360–40)
81/03/01	12:35	T	4	1.8 (2.1–1.6)	41 (63–25)	2470 (3600–1690)
81/03/04	08:50	F	0	2.6 (3.7–2.0)	8 (22–2)	500 (1180–210)
81/04/08	00:49	F	5	1.8 (1.9–1.6)	39 (47–32)	1930 (2280–1630)
81/04/24	09:59	F	3	2.0 (2.2–1.7)	26 (40–16)	1440 (2140–910)
81/06/05	05:13	F	0	2.2 (3.1–1.7)	21 (50–5)	1200 (2600–420)
81/07/21	19:08	F	7	1.7 (1.9–1.5)	54 (80–36)	3000 (4300–2060)
81/08/01	17:19	F	1	1.8 (2.2–1.5)	38 (67–19)	2010 (3400–1070)
81/08/05	06:33	F	0	3.0 (3.8–2.4)	3 (8–1)	280 (470–160)
81/08/14	10:09	F	1	3.0 (3.2–2.8)	3 (5–2)	270 (300–240)
81/09/06	11:57	F	0	2.5 (3.0–2.2)	6 (11–3)	400 (580–280)
81/09/09	04:23	F	0	2.7 (4.5–1.9)	4 (19–0.6)	280 (840–110)

SMM/GRS GAMMA-RAY BURST LIST

DATE	START TIME	IN FOV?	EMAX (MeV)	PL INDEX (95% RANGE)	TS E_{CRIT} (keV) (95% RANGE)	OTTB (keV) (95% RANGE)
81/10/06	05:13	F	1	2.2 (2.8–1.8)	10 (27–3)	540 (1230–260)
81/10/16	23:53	T	5	3.1 (3.2–2.9)	3 (4–2)	270 (290–260)
81/10/23	11:38	F	0	2.2 (2.8–1.8)	9 (22–4)	490 (950–280)
81/11/02	03:36	F	0	3.2 (4.0–2.6)	2 (5–1)	200 (310–130)
81/12/22	08:10	F	0	2.2 (3.0–1.8)	12 (31–3)	670 (1570–300)
81/12/31	01:37	T	3	2.6 (2.7–2.4)	6 (7–5)	390 (430–350)
82/01/18	12:20	T	0	2.5 (3.4–1.9)	6 (18–1)	410 (840–200)
82/01/21	09:00	T	0	2.6 (3.2–2.1)	5 (12–2)	350 (580–220)
82/01/25	17:56	T	5	1.5 (1.7–1.3)	90 (130–59)	4300 (6500–2900)
82/02/01	08:19	T	1	2.5 (2.9–2.2)	9 (14–5)	530 (770–370)
82/02/14	01:23	F	0	2.3 (2.6–2.0)	10 (16–6)	540 (770–400)
82/02/24	20:29	T	0	9.5 ($>$ 9.9–6.4)	0.1 (0.3– $<$ 0.1)	40 (70–20)
82/03/01	02:36	T	0	3.4 (3.6–3.2)	2 (3–1)	190 (220–170)
82/03/03	16:21	T	5	2.0 (2.2–1.8)	20 (31–12)	970 (1840–530)
82/03/13	02:40	T	6	2.6 (2.9–2.4)	4 (6–3)	300 (350–260)
82/03/20	13:10	F	7	1.9 (2.0–1.8)	30 (35–26)	1570 (1770–1380)
82/03/24	12:21	T	0	2.3 (2.6–2.0)	9 (15–5)	520 (760–370)
82/03/28	14:37	T	3	2.4 (2.8–2.0)	6 (12–3)	340 (520–230)
82/03/31	15:21	F	2	2.2 (2.5–2.0)	11 (16–7)	540 (740–410)
82/04/16	15:56	F	4	1.7 (2.0–1.5)	47 (80–28)	2800 (4100–1800)
82/05/02	13:17	F	1	2.3 (2.9–1.9)	10 (24–3)	520 (1160–260)
82/05/02	21:15	T	1	1.9 (2.4–1.6)	30 (58–13)	1580 (2900–800)
82/05/11	09:20	F	0	2.5 (2.9–2.2)	6 (12–3)	400 (600–270)
82/05/30	09:49	T	2	2.4 (2.6–2.2)	8 (12–5)	490 (640–380)
82/08/16	20:41:53	F	3	1.9 (2.1–1.7)	38 (54–24)	2230 (3000–1580)
82/08/20	13:59	T	5	2.5 (3.0–2.2)	5 (9–2)	310 (470–210)
82/08/25	11:34	F	1	1.9 (2.3–1.6)	25 (46–12)	1240 (2360–670)
82/08/28	13:50	T	0	2.8 (3.2–2.4)	5 (9–2)	350 (490–250)
82/10/24	06:52	F	1	2.3 (2.6–2.1)	10 (15–6)	520 (750–370)
82/10/28	19:34	F	8	1.4 (1.6–1.2)	130 (220–75)	7800 ($>$ 9900–4600)
82/11/04	03:30	T	8	2.2 (2.3–2.1)	12 (14–10)	570 (640–510)
83/01/21	21:12	F	8	2.4 (2.6–2.3)	7 (9–5)	400 (460–350)
83/02/10	12:20	T	1	3.0 (3.3–2.8)	3 (5–2)	260 (300–220)

SMM/GRS GAMMA-RAY BURST LIST

DATE	START TIME	IN FOV?	EMAX (MeV)	PL INDEX (95% RANGE)	TS E_{CRIT} (keV) (95% RANGE)	OTTB (keV) (95% RANGE)
83/03/28	08:32	F	0	2.4 (3.0–2.0)	10 (22–4)	610 (1100–350)
83/04/14	01:56	F	0	2.5 (2.9–2.2)	6 (11–3)	400 (550–290)
83/05/02	16:47	F	3	1.6 (2.0–1.3)	62 (120–29)	3400 (6400–1810)
83/05/22	22:47	F	0	2.1 (2.8–1.7)	17 (41–5)	860 (2120–360)
83/05/29	18:23	F	1	2.2 (2.7–1.9)	17 (30–8)	1030 (1700–530)
83/06/07	20:34	F	1	2.2 (2.9–1.8)	8 (21–2)	410 (920–200)
83/08/24	02:21	T	0	2.6 (3.2–2.1)	5 (10–2)	320 (500–210)

LIST OF REFERENCES

Apparao, K. M. V., and Allen, D. 1982, *Astr. Ap.*, **107**, L5. "Infrared Scans of Gamma-Ray Burst Source Regions."

Atteia, J. L., *et al.* 1985, *Conf. Papers 19th ICRC*, **1**, 33. "A Second Catalog of Gamma Ray Bursts: 1978–1980 Localizations from the Interplanetary Network."

Baity, W. A., *et al.* 1981, *Ap. J.*, **244**, 429. "Centaurus A (NGC 5128) at 2 keV–2.3 MeV: HEAO-1 Observations and Implications."

Barat, C., Chambon, G., Hurley, K., Niel, M., Vedrenne, G., Estulin, I. V., Kuznetsov, A. V., and Zenchenko, V. M. 1981, *Ap. Space Sci.*, **75**, 83. "A Review of Recent Results from the Franco-Soviet SIGNE Gamma-Burst Experiments."

Barat, C., Chambon, G., Hurley, K., Niel, M., and Vedrenne, G. 1982, *Astr. Ap.*, **109**, L9. "The Log N-log S Curve of Gamma-ray Bursts Detected by the SIGNE Experiments."

Barat, C., *et al.* 1984a, *Ap. J.*, **280**, 150. "Time History, Energy Spectrum, and Localization of an Unusual Gamma-Ray Burst."

Barat, C., *et al.* 1984b, *Ap. J.*, **285**, 791. "On the Morphology and Spectra of the Short Gamma-Ray Bursts."

Barat, C., *et al.* 1984c, *Ap. J. (Letters)*, **286**, L5. "1979 January 13: An Intense Gamma-Ray Burst with a Possible Associated Optical Transient."

Barat, C., *et al.* 1984d, *Ap. J. (Letters)*, **286**, L11. "Possible Short Annihilation Flashes in the 1978 November 4 Gamma-Ray Burst."

Barat, C., *et al.* 1984e, *Adv. Space Res.*, **3**(10-12), 105. "Fast Spectroscopy of the 4 November 1978 Gamma-Ray Burst."

Barat, C. 1983, in *Positron-Electron Pairs in Astrophysics*, ed. M. L. Burns, A. K. Harding, and R. Ramaty (New York: American Institute of Physics), p. 54. "Fine Time Resolution Spectral Analysis of the 1978 November 4 and 19 Gamma-Ray Bursts."

Berger, M. J., and Seltzer, S. M. 1972, *Nucl. Inst. Meth.*, **104**, 317. "Response Functions for Sodium Iodide Scintillation Detectors."

Bisnovaty-Kogan, G. S., Estulin, I. V., Havenson, N. G., Kurt, V. G., Mersov, G. A., and Novikov, I. D. 1981, *Ap. Space Sci.*, **75**, 219. "The Transformation of the Coordinates of a Gamma Burst Source to a Star Catalogue."

Brown, J. C., Loran, J. M., and MacKinnon, A. L. 1985, *Astr. Ap.*, **147**, L10. "The shortest time scales present in solar hard X-ray bursts."

Bussard, R. W., and Lamb, F. K. 1982, in *Gamma Ray Transients and Related Astrophysical Phenomena*, ed. R. E. Lingenfelter, H. S. Hudson, and D. M. Worrall (New York: American Institute of Physics), p. 189. "The Low Energy Spectra of Gamma-Ray Bursts."

Carrigan, B. J., and Katz, J. I. 1984, *Astron. Express*, **1**, 89. "Fluxes and Distances of Gamma-ray Bursts."

Cavallo, G., and Rees, M. J. 1978, *Mon. Not. R. Astr. Soc.*, **183**, 359. "A qualitative study of cosmic fireballs and gamma-ray bursts."

Chupp, E. L. 1976, *Gamma-Ray Astronomy* (Dordrecht, Holland: D. Reidel).

Cline, T. L., and Desai, U. D. 1975, *Ap. J. (Letters)*, **196**, L43. "Observations of Cosmic Gamma-Ray Bursts with IMP-7: Evidence for a Single Spectrum."

Cline, T. L., Desai, U. D., Klebesadel, R. W., and Strong, I. B. 1973, *Ap. J. (Letters)*, **185**, L1. "Energy Spectra of Cosmic Gamma-Ray Bursts."

Cline, T. L., Desai, U. D., Pizzichini, G., Spizzichino, A., Trainor, J., Klebesadel, R., Ricketts, M., and Helmken, H. 1979a, *Ap. J. (Letters)*, **229**, L47. "Helios 2-Vela-Ariel 5 Gamma-Ray Burst Source Position."

Cline, T. L., Desai, U. D., Pizzichini, G., Spizzichino, A., Trainor, J. H., Klebesadel, R. W., and Helmken, H. 1979b, *Ap. J. (Letters)*, **232**, L1. "Gamma-Ray Burst Observations from Helios 2."

Cline, T. L., *et al.* 1980, *Ap. J.*, **237**, L1. "Detection of a Fast, Intense and Unusual Gamma-Ray Transient."

Cline, T. L., *et al.* 1981, *Ap. J. (Letters)*, **246**, L133. "High-Precision Source Location of the 1978 November 19 Gamma-Ray Burst."

Cline, T. L., *et al.* 1984, *Ap. J. (Letters)*, **286**, L15. "Three Precise Gamma-Ray Burst Source Locations."

Cline, T. L. 1975, *Ann. N. Y. Acad. Sci.*, **262**, 159. "Recent Observations of Cosmic Gamma-Ray Bursts."

Cline, T. L. 1982, in *Gamma Ray Transients and Related Astrophysical Phenomena*, ed. R. E. Lingenfelter, H. S. Hudson, and D. M. Worrall (New York: American Institute of Physics), p. 17. "A Review of the 1979 March 5 Transient."

Colgate, S. A., and Petschek, A. G. 1981, *Ap. J.*, **248**, 771. "Gamma Ray Bursts and Neutron Star Accretion of a Solid Body."

Colgate, S. A., and Petschek, A. G. 1985, in *Numerical Astrophysics*, ed. J. M. Centrella, J. M. LeBlanc, and R. L. Bowers (Boston: Jones and Bartlett), p. 171. "Gamma Bursts."

Daugherty, J. K., and Harding, A. K. 1982, *Ap. J.*, **252**, 337. "Electromagnetic Cascades in Pulsars."

Daugherty, J. K., and Harding, A. K. 1983, *Ap. J.*, **273**, 761. "Pair Production in Superstrong Magnetic Fields."

Daugherty, J. K., and Ventura, J. 1978, *Phys. Rev. D*, **18**, 1053. "Absorption of radiation by electrons in intense magnetic fields."

Dennis, B. R., Frost, K. J., Kiplinger, A. L., Orwig, L. E., Desai, U., and Cline, T. L. 1982, in *Gamma Ray Transients and Related Astrophysical Phenomena*, ed. R. E. Lingenfelter, H. S. Hudson, and D. M. Worrall (New York: American Institute of Physics), p. 153. "Time Variations of an Absorption Feature in the Spectrum of the Gamma-Ray Burst on 1980 April 19."

Dennis, B. R., Frost, K. J., Orwig, L. E., Kiplinger, A., Dennis, H. E., Gibson, B. R., Kennard, G. S., and Tolbert, A. K. 1983, *The Hard X-Ray Burst Spectrometer Event Listing 1980, 1981 and 1982* (NASA TM84998).

Donnelly, R. F., Grubb, R. N., and Cowley, F. C. 1977, *Solar X-Ray Measurements from SMS-1, SMS-2, and GOES-1: Information for Data Users* (NOAA Tech. Mem. ERL SEL-48).

Dunphy, P. P., and Forrest, D. J. 1985, *IEEE Trans. Nucl. Sci.*, **32**, 538. "Photofraction of a 5 cm $\times$ 2 cm BGO Scintillator."

Epstein, R. I. 1985a, Talk given at the Center for Astrophysics, Cambridge, Mass. 1985 March 21.

Epstein, R. I. 1985b, *Ap. J.*, **291**, 822. "Feeding a Gamma-Ray Burster."

Erber, T. 1966, *Rev. Mod. Phys.*, **38**, 626. "High-Energy Electromagnetic Conversion Processes in Intense Magnetic Fields."

Evans, R. D. 1955, *The Atomic Nucleus* (New York: McGraw-Hill).

Evans, W. D., *et al.* 1980, *Ap. J. (Letters)*, **237**, L7. "Location of the Gamma-Ray Transient Event of 1979 March 5."

Fabian, A. C., Icke, V., and Pringle, J. E. 1976, *Ap. Space Sci.*, **42**, 77. "A Neutron Star Crustquake Origin for Gamma-Ray Bursts."

Fenimore, E. E., Klebesadel, R. W., and Laros, J. G. 1983, *Adv. Space Res.*, **3**(4), 207. "Problems in the Analysis of Gamma-Ray Burst Spectra."

Fenimore, E. E., Klebesadel, R. W., and Laros, J. G. 1984, in *High Energy Transients Astrophysics*, ed. S. E. Woosley (New York: American Institute of Physics), p. 590. "Inverse Comptonization vs. Thermal Synchrotron."

Fenimore, E. E., Klebesadel, R. W., Laros, J. G., Stockdale, R. E., and Kane, S. R. 1982a, *Nature*, **297**, 665. "Gamma-ray sources as comptonized X-ray sources."

Fenimore, E. E., Laros, J. G., Klebesadel, R. W., Stockdale, R. E., and Kane, S. R. 1982b, in *Gamma Ray Transients and Related Astrophysical Phenomena,* ed. R. E. Lingenfelter, H. S. Hudson, and D. M. Worrall (New York: American Institute of Physics), p. 201. "On the Interpretation of Gamma-Ray Burst Continua and Possible Cyclotron Absorption Lines."

Fikani, M. M., and Laros, J. G. 1984, *B. A. A. S.,* **16**, 935. "The Frequency of Weak Gamma-Ray Bursts Using Satellite Cross-Correlation."

Fishman, G. J., Duthie, J. G., and Dufour, R. J. 1981, *Ap. Space Sci.*, **75**, 135. "Optical Studies of the Regions of the Gamma-Ray Bursts of 19 November, 1978 and 5 March, 1979."

Fishman, G. J. 1979, *Ap. J.,* **233**, 851. "Galactic Distribution Models of Gamma-Ray Burst Sources."

Forrest, D. J., *et al.* 1980, *Solar Phys.,* **65**, 15. "The Gamma Ray Spectrometer for the Solar Maximum Mission."

Giacconi, R. 1972, *Ap. J. (Letters),* **173**, L79. "On the Use of Long-Base Time-Delay Measurements in the Study of Rapidly Varying X-Ray Stars."

Gilman, D., Metzger, A. E., Parker, R. H., Evans, L. G., and Trombka, J. I. 1980, *Ap. J.,* **236**, 951. "The Distance and Spectrum of the Apollo Gamma-Ray Burst."

Gleske, I. U., and Forrest, D. J. 1980, *IEEE Trans. Nucl. Sci.,* **27**, 313. "A nuclear detector gain stabilizing technique with only one stable gain position."

Golenetskii, S. V., Mazets, E. P., Aptekar, R. L., and Ilyinskii, V. N. 1983, *Nature,* **306**, 451. "Correlation between luminosity and temperature in gamma-ray burst sources."

Gould, R. J. 1981, *Phys. Fluids,* **24**, 102. "Kinetic Theory of Relativistic Plasmas."

Gould, R. J. 1982a, *Ap. J.,* **254**, 755. "Processes in Relativistic Plasmas."

Gould, R. J. 1982b, in *Gamma Ray Transients and Related Astrophysical Phenomena,* ed. R. E. Lingenfelter, H. S. Hudson, and D. M. Worrall (New York: American Institute of Physics), p. 169. "Relativistic Plasmas."

Grindlay, J. E., *et al.* 1982, *Nature,* **300**, 730. "Persistent X-ray emission from a gamma-ray burst source."

Hameury, J. M., Bonazzola, S., Heyvaerts, J., and Lasota, J. P. 1984, *Adv. Space Res.,* **3**(10-12), 297. "Thermonuclear Flashes on Neutron Stars as a Model for Gamma-Ray Bursts."

Hameury, J. M., Lasota, J. P., Bonazzola, S., and Heyvaerts, J. 1985, *Ap. J.,* **293**, 56. "Spectra of Gamma-Ray Bursts."

Helfand, D. J., and Long, K. S. 1979, *Nature,* **282,** 589. "X-ray observations of the 5 March 1979 gamma-ray burst field."

Helfand, D. J., and Vrtilek, S. D. 1983, *Nature,* **304,** 41. "Constraints on gamma-ray bursters from soft X-ray transients."

Herterich, K. 1974, *Nature,* **250,** 311. "Absorption of gamma rays in intense X-ray sources."

Higdon, J. C., and Lingenfelter, R. E. 1985, *Conf. Papers 19th ICRC,* **1,** 37. "Gamma Ray Burst Size-Frequency Distributions: Spectral Selection Effects."

Hjellming, R. M., and Ewald, S. P. 1981, *Ap. J. (Letters),* **246,** L137. "A Search for Radio Emission Associated with the 1978 November 19 Gamma-Ray Burster."

Hueter, G. J. 1984, in *High Energy Transients Astrophysics,* ed. S. E. Woosley (New York: American Institute of Physics), p. 373. "Observation of an Absorption Feature in a Gamma Ray Burst Spectrum."

Hurley, K. 1982, in *Gamma Ray Transients and Related Astrophysical Phenomena,* ed. R. E. Lingenfelter, H. S. Hudson, and D. M. Worrall (New York: American Institute of Physics), p. 85. "Gamma Ray Burst Positions."

Hurley, K. 1983a, *Adv. Space Res.,* **3**(4), 163. "Gamma-Ray Bursts — The Current Status."

Hurley, K. 1983b, *Adv. Space Res.,* **3**(4), 203. "Gamma-Ray Burst Localization with the International Solar Polar Mission."

Imamura, J. N., Epstein, R. I., and Petrosian, V. 1985, *Ap. J.,* **296,** 65. "High-Energy Thermal Synchrotron Emission."

Jacobson, A. S., Ling, J. C., Mahoney, W. A., and Willett, J. B. 1978, in *Gamma Ray Spectroscopy in Astrophysics,* ed. T. L. Cline and R. Ramaty (NASA TM 79619), p. 228. "Observational Evidence for Extraterrestrial Gamma-Ray Line Sources."

Jennings, M. C. 1982, in *Gamma Ray Transients and Related Astrophysical Phenomena,* ed. R. E. Lingenfelter, H. S. Hudson, and D. M. Worrall (New York: American Institute of Physics), p. 107. "The Observational Consequences of an Intrinsic Burst Luminosity Distribution."

Jennings, M. C. 1984, in *High Energy Transients Astrophysics,* ed. S. E. Woosley (New York: American Institute of Physics), p. 412. "The Gamma-Ray Burst Spatial Distribution Log N(>S) *vs* Log S and N(>S, l^{II}, b^{II}) *vs* S."

Jennings, M. C. 1985, *Ap. J.,* **295,** 51. "Gamma-Ray Burst Statistics: Guidance or Deception?"

Kafka, P., and Meyer, F. 1984, in *High Energy Transients Astrophysics,* ed. S. E. Woosley (New York: American Institute of Physics), p. 578. "Gamma-Ray Bursts—The Roundabout Way?"

Katoh, M., Murakami, T., Nishimura, J., Yamagami, T., Fujii, M., and Itoh, M. 1984, in *High Energy Transients Astrophysics,* ed. S. E. Woosley (New York: American Institute of Physics), p. 390. "Observation of a Cosmic Gamma-Ray Burst on Hakucho."

Katz, J. I. 1982, *Ap. J.,* **260**, 371. "Physical Processes in Gamma-Ray Bursts."

Katz, J. I. 1983, in *Positron-Electron Pairs in Astrophysics,* ed. M. L. Burns, A. K. Harding, and R. Ramaty (New York: American Institute of Physics), p. 65. "Theories of Gamma-Ray Bursts."

Kiplinger, A. L., Dennis, B. R., Emslie, A. G., Frost, K. J., and Orwig, L. E. 1983, *Ap. J. (Letters),* **265**, L99. "Millisecond Time Variations in Hard X-Ray Solar Flares."

Klebesadel, R. W., Strong, I. B., and Olson, R. A. 1973, *Ap. J. (Letters),* **182**, L85. "Observations of Gamma-Ray Bursts of Cosmic Origin."

Klebesadel, R. W., and Strong, I. B. 1976, *Ap. Space Sci.,* **42**, 3. "Observations of Cosmic Gamma-Ray Bursts."

Klebesadel, R., *et al.* 1982, *Ap. J. (Letters),* **259**, L51. "A Catalog of Gamma-Ray Bursts with Earth Crossing Times."

Klebesadel, R. W., Fenimore, E. E., and Laros, J. G. 1984, in *High Energy Transients Astrophysics,* ed. S. E. Woosley (New York: American Institute of Physics), p. 429. "Log N-Log S is Inconclusive."

Knight, F. K., Matteson, J. L., and Peterson, L. E. 1981, *Ap. Space Sci.,* **75**, 21. "The Spectra and Light Curves of Two Gamma-Ray Bursts."

Lamb, D. Q., Lamb, F. K., and Pines, D. 1973, *Nat. Phys. Sci.,* **246**, 52. "Soft Gamma-ray Bursts from Accreting Compact Objects."

Lamb, D. Q. 1982, in *Gamma Ray Transients and Related Astrophysical Phenomena,* ed. R. E. Lingenfelter, H. S. Hudson, and D. M. Worrall (New York: American Institute of Physics), p. 249. "Surface and Magnetospheric Physics of Neutron Stars and Gamma-Ray Bursts."

Lamb, D. Q. 1984a, *Ann. N. Y. Acad. Sci.,* **422**, 237. "Physics of Gamma-Ray Bursts."

Lamb, D. Q. 1984b, in *High Energy Transients Astrophysics,* ed. S. E. Woosley (New York: American Institute of Physics), p. 512. "Physics of Gamma-Ray Burst Spectra."

Lang, K. R. 1980, *Astrophysical Formulae* (Berlin: Springer-Verlag).

Laros, J. G., *et al.* 1981, *Ap. J. (Letters),* **245**, L63. "Location of the 1979 April 6 Gamma-Ray Burst."

Laros, J. G., Evans, W. D., Fenimore, E. E., and Klebesadel, R. W. 1982, *Ap. Space Sci.,* **88**, 243. "Comments on the Gamma-Ray Burst Catalog of Mazets et al. (1981a)."

Laros, J. G., Evans, W. D., Fenimore, E. E., and Klebesadel, R. W. 1983, *Ap. Space Sci.,* **99**, 213. "Further Comments on the KONUS Catalog."

Laros, J. G., Evans, W. D., Fenimore, E. E., Klebesadel, R. W., Schulman, S., and Fritz, G. 1984, *Ap. J.,* **286**, 681. "3 keV to 2 MeV Observations of Four Gamma-Ray Bursts."

Laros, J. G., *et al.* 1985a, *Ap. J.,* **290**, 728. "Locations and Time Histories of Five 1979 Gamma-Ray Bursts."

Laros, J. G., Fenimore, E. E., Fikani, M. M., Klebesadel, R. W., van der Klis, M., and Gottwald, M. 1985b, *Nature,* **318**, 448. "GB841215, the fastest gamma-ray burst?"

Lasota, J. P., and Belli, B. M. 1983, *Nature,* **304**, 139. "Non-absorption dips in spectra of gamma-ray bursts."

Liang, E. P., Jernigan, T. E., and Rodrigues, R. 1983, *Ap. J.,* **271**, 766. "Analysis of the Konus Catalog of Gamma-Ray Bursts with the Thermal Synchrotron Model."

Liang, E. P., and Antiochos, S. K. 1984, *Nature,* **310**, 121. "Magnetic flare model of gamma-ray bursts."

Liang, E. P. T. 1981, *Nature,* **292**, 319. "Inverse comptonization and the nature of the March 1979 gamma-ray burst event."

Liang, E. P. 1982, *Nature,* **299**, 321. "Emission mechanism and source distances of gamma-ray bursts."

Liang, E. P. 1983, *Ap. J. (Letters),* **268**, L89. "On the Nature of Two Gamma Bursts with Spectral Evolution Observed by the KONUS Experiment."

Liang, E. P. 1984, in *High Energy Transients Astrophysics,* ed. S. E. Woosley (New York: American Institute of Physics), p. 597. "Physics of the Synchrotron Model of Cosmic Gamma Ray Bursts."

Ling, J. C., Mahoney, W. A., Willett, J. B., and Jacobson, A. S. 1982, in *Gamma Ray Transients and Related Astrophysical Phenomena,* ed. R. E. Lingenfelter, H. S. Hudson, and D. M. Worrall (New York: American Institute of Physics), p. 143. "10 June 1974 Transient."

Mandrou, P., Niel, M., Vedrenne, G., and Dupont, A. 1977, *Ap. J.,* **212**, 704. "A Low-Energy Gamma-Ray Observation of the Crab Nebula."

Matz, S. M., Chupp, E. L., Forrest, D. J., Share, G. H., Nolan, P. L., and Rieger, E. 1984, in *High Energy Transients Astrophysics,* ed. S. E. Woosley (New York: American Institute of Physics), p. 403. "Are There Nuclear Contributions to Gamma-Ray Burst Spectra?"

Matz, S. M., Forrest, D. J., Vestrand, W. T., Chupp, E. L., Share, G. H., and Rieger, E. 1985, *Ap. J. (Letters),* **288**, L37. "High-Energy Emission in Gamma-Ray Bursts."

Mazets, E. P., and Golenetskii, S. V. 1981, *Ap. Space Sci.,* **75**, 47. "Recent Results from the Gamma-Ray Burst Studies in the KONUS Experiment."

Mazets, E. P., and Golenetskii, S. V. 1982, *Ap. Space Sci.,* **88**, 247. "A Reply to 'Comments on the Gamma-Ray Catalog' of Laros et al."

Mazets, E. P., Golenetskii, S. V., Il'inskii, V. N., Aptekar', R. L., and Guryan, Yu. A. 1979, *Nature,* **282**, 587. "Observations of a flaring X-ray pulsar in Dorado."

Mazets, E. P., Golenetskii, S. V., Aptekar', R. L., Gur'yan, Y. A., and Il'inskii, V. N. 1980, *Sov. Astr. Lett.,* **6**, 372. "Lines in the energy spectra of gamma-ray bursts."

Mazets, E. P., *et al.* 1981a, *Ap. Space Sci.,* **80**, 3. "Catalog of Cosmic Gamma-Ray Bursts from the KONUS Experiment Data: Parts I and II."

Mazets, E. P., *et al.* 1981b, *Ap. Space Sci.,* **80**, 85. "Catalog of Cosmic Gamma-Ray Bursts from the KONUS Experiment Data: Part III."

Mazets, E. P., *et al.* 1981c, *Ap. Space Sci.,* **80**, 119. "Catalog of Cosmic Gamma-Ray Bursts from the KONUS Experiment Data: Part IV."

Mazets, E. P., Golenetskii, S. V., Aptekar', R. L., Gur'yan, Y. A., and Il'inskii, V. N. 1981d, *Nature,* **290**, 378. "Cyclotron and annihilation lines in gamma-ray bursts."

Mazets, E. P., *et al.* 1982a, *Ap. Space Sci.,* **82**, 261. "Cosmic Gamma-Ray Burst Spectroscopy."

Mazets, E. P., Golenetskii, S. V., Guryan, Yu. A., and Ilyinskii, V. N. 1982b, *Ap. Space Sci.,* **84**, 173. "The 5 March 1979 Event and the Distinct Class of Short Gamma Bursts: Are They of the Same Origin?"

Mazets, E. P., Golenetskii, S. V., Guryan, Yu. A., Aptekar, R. L., Ilyinskii, V. N., and Panov, V. N. 1983, in *Positron-Electron Pairs in Astrophysics,* ed. M. L. Burns, A. K. Harding, and R. Ramaty (New York: American Institute of Physics), p. 36. "Energy Spectra of the Cosmic Gamma-Ray Bursts."

Meegan, C. A., Fishman, G. J., and Wilson, R. B. 1984, in *High Energy Transients Astrophysics,* ed. S. E. Woosley (New York: American Institute of Physics), p. 422. "Measurement of the Rate of Weak Gamma-Ray Bursts."

Michel, F. C. 1985, *Ap. J.*, **290**, 721. "Gamma-Ray Bursts from Remnant Neutron Star Disks."

Mills, B. Y. 1952, *Austral. J. Sci. Res.*, **5A**, 266. "The distribution of the discrete sources of cosmic radio radiation."

Minkowski, R. 1975, in *Galaxies and the Universe (Stars and Stellar Systems, vol.IX)* , ed. A. Sandage, M. Sandage, and J. Kristian (Chicago: Univ. of Chicago Press), p. 177. "The Identification of Radio Sources."

Mitrofanov, I. G., Dolidze, V. S., Barat, C., Vedrenne, G., Niel, M. and Hurley, K. 1984, *Sov. Astron.*, **28**, 547. "Rapid spectral variability of cosmic gamma-ray bursts."

Newman, M. J., and Cox, A. N. 1980, *Ap. J.*, **242**, 319. "Collisions of Asteroids on Neutron Stars as a Cause of Cosmic Gamma-Ray Bursts."

Nolan, P. L., Share, G. H., Forrest, D. J., Chupp, E. L., Matz, S., and Rieger, E. 1983, in *Positron-Electron Pairs in Astrophysics,* ed. M. L. Burns, A. K. Harding, and R. Ramaty (New York: American Institute of Physics), p. 59. "Upper Limits on Narrow Annihilation Lines in Gamma-Ray Bursts."

Nolan, P. L., Share, G. H., Chupp, E. L., Forrest, D. J., and Matz, S. M. 1984a, *Nature,* **311**, 360. "Spectral feature of 31 December 1981 gamma-ray burst not confirmed."

Nolan, P. L., Share, G. H., Matz, S., Chupp, E. L., Forrest, D. J., and Rieger, E. 1984b, in *High Energy Transients Astrophysics,* ed. S. E. Woosley (New York: American Institute of Physics), p. 399. "High-Energy Emission from Gamma-Ray Bursts."

Norris, J. P., Cline, T. L., Desai, U. D., and Teegarden, B. J. 1984, *Nature,* **308**, 434. "Frequency of fast, narrow gamma-ray bursts."

Norris, J. P., Share, G. H., Messina, D. C., Cline, T. L., Desai, U. D., Dennis, B. R., Matz, S. M., and Chupp, E. L. 1986, *Ap. J.*, **301**, 213. "Spectral Evolution of Pulse Structures in Gamma-Ray Bursts."

Norris, J. P. 1983, Ph. D. thesis, University of Maryland (NASA TM 85031). "A Study of the Temporal and Spectral Characteristics of Gamma Ray Bursts."

Õgelman, H., Ayasli, S. and Hacinliyan, A. 1977, in *The Structure and Content of the Galaxy and Galactic Gamma Rays,* ed. C. E. Fichtel and F. W. Stecker (NASA CP-002), p. 109. "Gamma-Ray Pulsars."

Orwig, L. E., Frost, K. J., and Dennis, B. R. 1980, *Solar Phys.*, **65**, 25. "The Hard X-Ray Burst Spectrometer on the Solar Maximum Mission."

Pedersen, H., Motch, C., Tarenghi, M., Danziger, J., Pizzichini, G., and Lewin, W. H. G. 1983, *Ap. J. (Letters),* **270**, L43. "Optical Candidates for the 1978 November 19 Gamma-Ray Burst Source."

Petrosian, V. 1981, *Ap. J.*, **251**, 727. "Synchrotron Emission from Mildly Relativistic Particles."

Pizzichini, G., *et al.* 1981, *Space Sci. Rev.*, **30**, 467. "X-Ray and Optical Observations of the November 19, 1978 Gamma-Ray Burst Source Region."

Pizzichini, G. 1982, in *Gamma Ray Transients and Related Astrophysical Phenomena*, ed. R. E. Lingenfelter, H. S. Hudson, and D. M. Worrall (New York: American Institute of Physics), p. 101. "Statistical Study of Gamma-Ray Burst Source Locations."

Ramaty, R., Bonazzola, S., Cline, T. L., Kazanas, D., Meszaros, P., and Lingenfelter, R. E. 1980, *Nature*, **287**, 122. "Origin of the 5 March 1979 gamma-ray transient: a vibrating neutron star."

Ramaty, R., Lingenfelter, R. E., and Bussard, R. W. 1981, *Ap. Space Sci.*, **75**, 193. "Synchrotron Cooling and Annihilation of an e^+e^- Plasma: The Radiation Mechanism for the 5 March, 1979 Transient."

Rothschild, R. E., Mushotsky, R. F., Baity, W. A., Gruber, D. E., Matteson, J. L., and Peterson, L. E. 1983, *Ap. J.*, **269**, 423. "2–165 keV Observations of Active Galaxies and the Diffuse Background."

Ruderman, M. 1975, *Ann. N. Y. Acad. Sci.*, **262**, 164. "Theories of Gamma-Ray Bursts."

Schaefer, B. E. 1981, *Nature*, **294**, 722. "Possible optical counterpart of a gamma-ray burster."

Schaefer, B. E., Seitzer, P., and Bradt, H. V. 1983, *Ap. J. (Letters)*, **270**, L49. "Candidates for a Gamma-Ray Burster Optical Counterpart."

Schaefer, B. E., and Cline, T. L. 1985a, *Ap. J.*, **289**, 490. "Gamma-Ray Burster Recurrence Time Scales."

Schaefer, B. E., and Cline, T. L. 1985b, *Conf. Papers 19th ICRC*, **1**, 27. "Search for Infrared Counterparts of Gamma-Ray Bursters."

Schaefer, B. E., and Ricker, G. R. 1983, *Nature*, **302**, 43. "Size of a gamma-ray burster optical emitting region."

Schaefer, B. E., *et al.* 1984, *Ap. J. (Letters)*, **286**, L1. "Two Probable Optical Flashes from Gamma-Ray Bursters."

Schmidt, W. K. H. 1978, *Nature*, **271**, 525. "Distance limit for a class of model gamma-ray burst sources."

Schwartz, R. A., Ling, J. C., Mahoney, W. A., Wheaton, W. A., and Jacobson, A. S. 1985, *Conf. Papers 19th ICRC*, **1**, 51. "Gamma-Ray Burst Variability Above 4 MeV."

Shklovsky, I. S. 1960, *Cosmic Radio Waves* (Cambridge, Mass.: Harvard Univ. Press).

Strong, I. B., and Klebesadel, R. W. 1976, *Sci. American,* **235**(4), 66. "Cosmic Gamma-Ray Bursts."

Sturrock, P. A. 1971, *Ap. J.,* **164,** 529. "A Model of Pulsars."

Teegarden, B. J., and Cline, T. L. 1980, *Ap. J. (Letters),* **236,** L67. "High-Resolution Spectroscopy of Two Gamma-Ray Bursts in 1978 November."

Teegarden, B. J. 1982, in *Gamma Ray Transients and Related Astrophysical Phenomena,* ed. R. E. Lingenfelter, H. S. Hudson, and D. M. Worrall (New York: American Institute of Physics), p. 123. "Gamma-Ray Burst Spectra."

Teegarden, B. J. 1984, in *High Energy Transients Astrophysics,* ed. S. E. Woosley (New York: American Institute of Physics), p. 352. "The Spectral Properties of Gamma-Ray Bursts: A Review of Recent Developments."

Trombka, J. I., Dyer, C. S., Evans, L. G., Bielefeld, M. J., Seltzer, S. M., and Metzger, A. E. 1977, *Ap. J.,* **212,** 925. "Reanalysis of the Apollo Cosmic Gamma-Ray Spectrum in the 0.3 to 10 MeV Energy Region."

Tsai, W., and Erber, T. 1974, *Phys Rev D,* **10,** 492. "Photon pair creation in intense magnetic fields."

Tucker, W. H. 1975, *Radiation Processes in Astrophysics* (MIT Press:Cambridge).

Vedrenne, G. 1981, *Phil. Trans. R. Soc. Lond. A,* **301,** 645. "Cosmic gamma-ray bursts."

Vedrenne, G. 1984, *Adv. Space Res.,* **3**(10-12), 97. "Gamma-Ray Burst Observations: The Present Situation."

Ventura, J. 1983, *Adv. Space Res.,* **3**(4), 185. "Nature of Gamma-Ray Burst Sources."

Wheaton, W. A., Ulmer, M. P., Baity, W. A., Datlowe, D. W., Elcan, M. J., Peterson, L. E., Klebesadel, R. W., Strong, I. B., Cline, T. L., and Desai, U. D. 1973, *Ap. J. (Letters),* **185,** L57. "The Direction and Spectral Variability of a Cosmic Gamma-Ray Burst."

Woosley, S. E., and Wallace, R. K. 1982, *Ap. J.,* **258,** 716. "The Thermonuclear Model for Gamma-Ray Bursts."

Woosley, S. E. 1984, in *High Energy Transients Astrophysics,* ed. S. E. Woosley (New York: American Institute of Physics), p. 485. "The Theory of Gamma-Ray Bursts."

Yamagami, T., and Nishimura, J. 1985, *Ap. Space Sci.,* submitted. "Selection Effects on the Size and Frequency Distribution of Cosmic Gamma-Ray Bursts."

Yoshimori, M. 1978, *Aust. J. Phys.*, **31**, 189. "Interpretation of the Size Spectrum of Cosmic Gamma-ray Bursts in terms of an Idealized Galactic Distribution of Sources."

Yoshimori, M., Okudaira, K., Hirasima, Y., and Kondo, I. 1984, *Ap. Space Sci.*, **105**, 379. "Gamma-Ray Bursts Observed from the Hinotori Satellite."